

Distinct behavioural and neuronal signatures  
in delayed response and working memory tasks  
of mice and man

Victoria Hohendorf



Graduate School of  
Systemic Neurosciences  
LMU Munich

Dissertation at the  
Graduate School of Systemic Neurosciences  
Ludwig-Maximilians-Universität München

27<sup>th</sup> May 2024

First reviewer and  
supervisor:

Prof. Dr. Simon Jacob  
Department of Neurosurgery  
Technical University of Munich

Second reviewer:  
External reviewer:

Prof. Dr. Mark Hübener  
Dr. Sevil Duvarci

Date of submission:  
Date of defence:

27<sup>th</sup> May 2024  
18<sup>th</sup> October 2024

# Table of Content

<b>Abstract</b>	7
<b>Introduction</b>	
A definition for working memory	9
Delayed response vs. working memory	10
Working memory research	13
Technological progress advancing neuroscientific research	15
The present study	17
<b>Materials and Methods</b>	
Housing and husbandry	21
Behavioural training	21
Neuronal recordings	26
Data analysis	30
Human task design and analysis	34
<b>Results</b>	
Behavioural signatures of mice and man	38
A visual working memory task in mice	38
Faster reactions in humans when stimulus location is predictable	39
Microsaccades are affected by task type	41
Mice learn a non-matching to location task	44
Animal trajectories become more efficient throughout learning	47
Preplanning in DR task is observable in movement trajectories	49
Mice change their strategy to adapt to working memory conditions	50
Neuronal signatures	54
<i>In vivo</i> one-photon calcium imaging	54
Individual prefrontal units are tuned to task parameters	56
Fraction of units tuned to sample location is affected by task type	60
Neuronal populations maintain information about task variables	63
Single unit tuning throughout the trial	66
Prefrontal encoding of sample location and choice in individual units	70
Temporal dynamics of population coding	72

<b>Discussion</b>	
Summary of the study	78
Behavioural & neuronal signatures of delayed response and working memory	81
Limitations	83
Updating the definition of working memory	85
Outlook	86
Conclusion	89
<b>References</b>	90
<b>Acknowledgments</b>	106
<b>Affidavit</b>	107

“These creatures you call mice, you see, they are not quite as they appear.”

Douglas Adams,  
A Hitchhiker’s Guide to the Galaxy



## Abstract

Short-term storage of sensory information in working memory (WM) is an important function of the prefrontal cortex (PFC) and the foundation of intelligent behaviour. Working memory tasks differ from delayed response (DR) tasks, in which sensory information does not need to be maintained online for manipulation and instead the motor output can be readily planned. I therefore hypothesised that in WM, but not DR tasks, memory traces of the to-be-remembered sample would be actively maintained throughout the delay, whereas in DR information about the animals' upcoming choice would dominate. To investigate this hypothesis, I trained freely moving mice on a touchscreen-based spatial non-match-to-location task. Importantly, training proceeded in two steps. I first trained on a DR task, in which the animals could use the sample stimulus location to fully predict the location of the correct test stimulus. I then trained on a WM task, in which the animals had to memorise the sample location without being able to predict the test location and prepare an action. Mice met criterion performance in both task types but showed faster learning and higher performance in DR compared to WM conditions. Locomotion analysis showed that the animals displayed idiosyncratic strategies to meet the tasks' different behavioural demands, which had to be adapted when progressing from DR to WM. During expert sessions of the respective tasks, I imaged medial PFC pyramidal neurons expressing GCaMP6f using single-photon head-mounted miniature microscopes ( $n = 1319$  neurons from 6 mice). I found individual neurons significantly tuned to sample location, choice and trial outcome, exhibiting monotonic and labelled line tuning patterns. Importantly, during the sensory epoch the fraction of sample-selective units increased earlier and more strongly in the WM task than in the DR task (25% and 14% at peak, respectively) and remained higher throughout the delay epoch (17% and 8%, respectively). This pattern was reflected in the strength of sample coding in single neurons. Sample location during the sensory epoch and choice location during the test epoch were encoded by sparse, non-overlapping populations with only few mixed-selectivity units. In summary, I find evidence for distinct behavioural and neuronal signatures associated with delayed response and working memory tasks, illuminating a crucial difference in their respective cognitive requirements.



## Introduction

Short-term storage of sensory information in working memory is an essential function of the prefrontal cortex (PFC) and the foundation of intelligent behaviour. As defined by Baddeley (1987), working memory is a short-term storage space for information that needs to be kept cognitively available for a behavioural output. This ability is critical in many instances of daily behaviour, such as writing down a recently heard phone number or multiplying numbers in one's head. Working memory is impaired in several psychiatric disorders, such as schizophrenia (Gold et al., 2019), ADHD (Kofler et al., 2018) and autism-spectrum disorders (Steele et al., 2007), and it overlaps with many other cognitive functions, such as attention, perception, and intelligence. The prefrontal cortex has been shown to be essential for working memory function. Regardless, the neuronal basis of how sensory information is temporarily stored and manipulated is still an active area of research (Fuster, 2015). Various behavioural tasks probing working memory have been developed and adapted for a diverse set of experimental animals, allowing researchers to record directly from neurons in the brain. However, varying results and difficulty translating these back to humans pose the question of whether the underlying behavioural paradigms are truly equivalent and measure the same cognitive functions.

### **A definition for working memory**

Observational studies in humans indicated early on that there could be different systems for long-term and short-term information storage in the brain. These included studies of amnesic patients, specifically patients with Korsakoff syndrome whose performance in simple recall tests was unaffected; however, their long-term memory was greatly disturbed (Zangwill, 1946). In addition, the now famous patient HM could solve crossword puzzles and remember newly learned information over short periods. However, the next day, he would have forgotten that he had solved the crossword puzzle as he could not retain information over long periods and form new long-term memories (Scoville, 1968). Conversely, Shallice and Warrington (1970) observed a patient with damage to the parieto-occipital region after a motorbike accident who had

## Introduction

impaired short-term memory function, which they assessed using word and number sequence repeating tasks. However, he was able to perform normally on long-term memory tests. These patient studies indicated early on that there are different mechanisms involved in long-term memory storage and short-term memory information retention, which led to the development of several models on how these memory systems work and interact in the human brain. Atkinson and Shiffrin (1968) described, based on a combination of observations and simple behavioural studies of short-term memory in humans, a “short-term store”, which received input from a “sensory register” and interacted bidirectionally with a “long-term store”, where memories were held indefinitely. Based on this, Baddeley and Hitch (1974) proposed the multi-modal model of working memory, including a “central executive”, “visuo-spatial sketch pad”, and “phonological loop”. The central executive was proposed to regulate cognitive processes by controlling selective attention to external cues and interacting with the visuo-spatial sketch pad and the phonological loop. The visuo-spatial sketch pad and phonological loop were described as subsystems to the central executive acting as short-term storage for visuo-spatial and verbal information, respectively. The phonological loop depends on the human ability to use language; therefore, parts of the model are not applicable to non-human animals. Nevertheless, the definition of working memory as a short-term storage space for information needed for a prospective behavioural output based on these models is still used in research today.

## Working memory research

A plethora of tests, for example, repeating different word or number sequences (Warrington and Shallice, 1969), were developed to assess working memory function in humans to test cognitive functions of patients with brain injuries. These tests take advantage of the human ability to use language; however, tests using visual stimuli, such as icons, images or photographs also exist, for example, the touchscreen-based Cambridge Neuropsychological Test Automated Battery (CANTAB, Sandberg, 2011). Studies in non-human animals allow researchers to precisely manipulate areas of interest in the brain and determine their function in observed behaviours. However, adapting a working memory task to non-human animals posed the difficulty of finding

a task design that fulfils the requirements of keeping sample information online and being solvable by non-human animals. The apparent difficulty being that language cannot be used to explain the task design beforehand.

Hunter (1913) was among the first to show that rats, racoons, dogs and children could solve a delayed response task. Here, information about a choice had to be remembered over a short delay. Throughout the second half of the 20<sup>th</sup> century, many different working memory tasks were developed and tested across various species.

Operant condition chambers containing levers or buttons, which, when pressed correctly, released a food or water reward, were used on various species. Honig and Wasserman (1981) showed that these could be used to train pigeons in delayed response and working memory tasks, where the specific combination of two visual stimuli, colour and line orientation, either presented simultaneously or temporally separated, indicated reward. This study showed behavioural differences between delayed response and working memory tasks in pigeons and argued for a distinction of the two task types.

The development of variations of small mazes, for example, radial arm mazes (Olton and Samuelson, 1976) or t-mazes (Tolman, 1925), allowed to efficiently train rodents in a spatial delayed response task, capitalising on their innate alternation and novelty-seeking behaviour. In addition, operant chambers using delayed response tasks in rodents were developed. However, many delayed response tasks were criticised, as they allowed the animal to use mediating strategies, such as turning and facing the correct response lever in an operant chamber during the delay epoch (Chudasama and Muir, 1997), essentially removing the need to keep any sensory information actively maintained in the brain. Technological advances, such as visual projected stimuli (Andrews and Janssen, 1996), enabled the development of working memory tasks in rodents. For example, Nakagawa (1993) used an automatic t-maze, where rats were shown a sample stimulus and had to match or non-match it to two test stimuli shown immediately or after a 2 s delay. Further technological advances, specifically the development of touchscreens, allowed the development of more advanced automated behavioural setups and task designs where mediating strategies could be prevented by, for example, increasing the number of response windows (Talpos et al. 2010). Touchscreen boxes also allowed the development of working memory tasks in mice, such as spatial non-matching to location tasks (Oomen et al., 2013; Kim et al., 2015).

## Introduction

Delayed response paradigms were also developed early on for monkeys (Fuster and Alexander, 1971; Funahashi et al., 1989). Fuster and Alexander (1971) used a box where the monkey had to remember the location of a fruit reward after a delay. Here, as well, advances in and availability of technology, such as computer screens and eye tracking, allowed researchers to develop more complex task designs using abstract rules and stimuli with multiple dimensions, such as colour, shape or category, which lead to the development of delayed (non-)match to sample tasks to investigate working memory (Miller and Desimone, 1994).

These tasks allowed researchers to investigate the neuronal basis of working memory in more detail, as they were no longer bound to human individuals with brain injuries or disorders. Early on, lesion studies were used to determine the central role of the prefrontal cortex in delayed response and working memory tasks (Alexander and Fuster, 1973; Bauer and Fuster, 1976; Goldman-Rakic, 1995). More specifically, the dorsolateral PFC proved crucial for sensory processing and decision-making (Meyer et al., 2011; Riley et al., 2016; Carlén, 2017; Le Merre, 2024). Fuster and Alexander (1971) were the first to use microelectrodes to detect action potentials of single neurons in the dorsolateral prefrontal cortex of macaque monkeys performing the delayed response task described above. The researchers reported that most neurons discharged in the transition from cue to delay, i.e. during the end of the sensory period. They further described neurons with an increase in delay period activity, with some neurons showing persistent firing that declined slowly and irregularly towards the end of the delay. Increased delay period activity has been observed in many delayed response (Funahashi et al., 1989; Takeda and Funahashi, 2002) and working memory tasks (Hussar and Pasternak, 2012) and can be related to task performance (Bolkan et al., 2017; Liu et al., 2017). Notably, the delay period activity in working memory studies was found to encode information about the sample stimulus. For example, Miller et al. (1996) showed increased activity during delay periods in the prefrontal cortex of two rhesus monkeys memorising complex visual stimuli. In contrast, Vogel et al. (2022) showed that the information encoded during the delay period of a t-maze in mice encoded task parameters, such as linear location, direction, and task phase, most strongly during the delay.

Furthermore, whether the activity of single units is persistent throughout the delay or if single neurons fire sparsely to dynamically encode sample information is still under debate (Constantinidis et al., 2018; Lundqvist et al., 2018). It has been argued that

persistent neuronal activity is an artefact from trial-averaging of individual neurons and that the activity is more dynamic, with multiple units covering the delay period sequentially, where every unit only fires sparsely (Lundqvist et al., 2018; Shafi et al., 2007; Quintana et al., 1988). However, so far proponents of the persistent activity theory have been arguing that persistent activation could be found in both delayed response-, as well as working memory tasks and opponents have described dynamic delay epoch activation in those same studies (Constantinidis et al., 2018; Lundqvist et al., 2018).

The advent of computational modelling allowed more advanced theories of how neuronal networks integrate and maintain information in the absence of sensory inputs. Different ways in which single neurons encode sensory information have been described. Neurons with monotonically ramping activity to a specific location have been found; for example, in monkeys, the closer a to-be-remembered item was to a particular location, the higher the firing rate of a specific unit would be (Funahashi et al., 1989, Takeda et al., 2002). Furthermore, units in the prefrontal cortex of monkeys showed so-called “labelled-line tuning” to different numerosities. Their firing rate peaked at a specific numerosity; however, the response to immediately neighbouring numerosities was reduced significantly, leading to a unit specifically responsive to one numerosity (Nieder and Merten, 2007). In addition, many neurons in higher-order brain areas, such as the PFC, exhibit complex firing responses. For example, neurons tuned to multiple task parameters, such as colour, shape and motor output. Neurons in the prefrontal cortex with non-linear mixed selectivity have been proposed to pose a significant computational advantage in processing and integrating information (Rigotti et al., 2013). Nevertheless, the underlying single-unit responses of working memory are still not fully understood.

### **Delayed response vs. working memory**

Working memory was initially defined in humans but, for research purposes, adapted to model organisms such as mice, rats, pigeons, and monkeys. Baddeley and Hitch’s (1976) definition described working memory maintenance and the manipulation of information; however, it has been proposed that “the maintenance of information” is too ambiguously defined. Pontecorvo et al. (1995) point out that there is a difference

## Introduction

in tasks where the animal is given all information during the sensory epoch, allowing it to preplan the behavioural output throughout the delay, and tasks where some information is presented as a sample, but the animal has to wait until the test phase because only the sample and test stimuli in combination can determine the correct behavioural output. They define these two task types as delayed response and delayed comparison tasks. The behavioural difference between the two task types has been proposed in several studies and reviews across multiple animals, such as pigeons (Honig and Dodd, 1983; Honig and Wasserman, 1981), mice (Bennett et al., 2022), rats (Pontecorvo et al. 1996), and monkeys (Quintana et al., 1988). Problematically, the definitions for the two differing task types are not universally agreed upon, and each study proposes different terminology, i.e. delayed response vs delayed comparison (Honig and Dodd, 1983) or retrospective working memory vs prospective working memory (Bennett et al. 2022). The consensus is that information must be kept available, but in one task type, this information is related to behavioural output, and in the other, it is related to sensory information. However, frequently in working memory research, this distinction is not made, leading to confusion when studies with differing behavioural paradigms or species need to be compared. Furthermore, it has become increasingly clear that distinct neuronal activity patterns reflect these behavioural differences. While strong delay activity encoding of the sample stimulus during the delay is frequently found in working memory tasks (Miller et al., 1996), this becomes less pronounced during the delay epoch of delayed response tasks, where other task parameters, such as the location of the animal or the time passed are more easily decoded from delay period activity (Vogel et al., 2022). Here, I propose that a differentiation of delayed response and working memory might be appropriate to explain behavioural and neuronal findings and translate them across species.

In the interest of clarity, I will use the following definitions for the rest of this thesis:

*Delayed response (DR) task:*

*Delayed response tasks will be defined as tasks where the sensory stimulus can be used to preplan the motor output of the task. These tasks can be solved by preplanning the motor behaviour during the delay epoch or, alternatively, by remembering the sample information and comparing it to the test stimuli. A variety of delayed response*

*tasks are used across many species, for example, forced alternation t-mazes in mice (Spellman et al., 2015; Vogel et al., 2022; Duvarci et al., 2018), delayed alternation tasks in operant boxes in rats (Horst and Laubach, 2012), oculo-motor delayed response tasks using saccades in monkeys (Takeda and Funhashi, 2002) or delayed response task using button-presses in humans (Verin et al. 1993).*

*Working memory (WM) tasks:*

*Working memory tasks will be defined as tasks where the sample information must be maintained throughout the delay period, and only the sample and test stimuli in combination will determine the behavioural output. These tasks can only be solved correctly by remembering the sample information and integrating this information with the test stimulus to determine the motor output. There is also a large variety of working memory tasks used across species, for example, olfactory delayed non-match to sample task in mice (Liu et al. 2014), cue-guided attention task with multiple sensory dimensions in mice (Rikhye et al., 2018), delayed match and non-match to sample tasks with visual stimuli in rats (Nakagawa, 1993; Andrew and Jansen, 1996), and colour change localisation task in primates (Buschman et al. 2011).*

## **Technological progress advancing neuroscientific research**

Neuroscientific research methodologies have progressed from simple behavioural observations and acute single-neuron measurements to advanced tracking software and chronic imaging of individual cell activity over days up to months and years. The foundation of these advances was made by humanity's general technological progress throughout the last decades, namely, an increase in data storage capacity and computational power. Increases in storage capacity have allowed us to acquire more extensive data sets of higher quality, for example, higher resolution behavioural videos or neuronal data from chronically implanted multi-electrode arrays. In addition, computational power has steadily increased over the last few years, enabling us to process and analyse larger amounts of data, which has multiple advantages. For example, in the field of behavioural neuroethology, free software packages like DeepLabCut (Mathis et al. 2018) enable the tracking of animal parts reliably and autonomously once a network is trained (Wiltschko et al. 2015). Automation reduces

## Introduction

the time scientists spend on tracking animals by hand. In addition, the classification of single behaviours, for example, determining freezing behaviours in an open field task, can vary widely between individuals and even within one individual throughout a long day of behavioural classification. Software packages, such as Keypoint-MoSeq (Weinreb et al., 2023, preprint), are now freely available and can classify behavioural motifs of tracked animals unsupervised and determine behavioural dynamics without human bias (von Ziegler et al. 2020; Wiltschko et al. 2015).

Furthermore, neuronal recording techniques have improved vastly over the last decades, from single-unit electrophysiological recordings, as used in the famous studies by Hubel and Wiesel (1962), who showed the responsiveness of single neurons to specific visual stimuli in the cat's visual cortex, towards meso-scale calcium recordings of the entire dorsal cortex of the mouse brain, allowing researchers to determine functionally connected brain areas and relate them to behavioural observations, as seen for example in MacDowell et al. (2024).

Calcium imaging has become popular in the last two decades, as it allows tracking of multiple neurons within and across sessions. This technological advance has become possible with the synthetic generation of genetically encoded calcium sensors, such as early examples generated by Miyawaki et al. (1997), as well as the popular GCaMP sensors first synthesised by Nakai et al. (2001). These sensors fluoresce in response to the dynamically changing calcium levels in the neuron during an action potential. However, the calcium sensor dynamics are slow taking about 1 s to rise and fall (Chen et al., 2013). In contrast, action potentials last only a few milliseconds, which can be recorded with much greater temporal resolution using electrophysiology. Electrophysiological recordings, however, have much worse spatial resolution, and tracking specific neurons over multiple recording sessions is challenging. Here, calcium imaging poses the advantage of improved spatial resolution. Videos of the fluorescence changes of the calcium sensor can be aligned with the appropriate software, and single units can be detected across several sessions. Tracking individual units over a long time becomes immensely useful when comparing neural activation patterns in cognitively challenging tasks, where it can take months to train the animal. Further advantages of calcium imaging are that they are easily deliverable via a viral vector or endogenously expressed via transgenic breeding, which allows the expression in specific subpopulations of neurons. Subpopulation can be a particular class of neurons, for example, expression in pyramidal neurons using the CamKII

promotor or neurons receiving input from a particular area, such as prefrontal neurons receiving direct input from the medio-dorsal thalamus.

Technological advances enable us to study neuroscientific problems in greater detail than ever before, as well as decrease the time spent on tedious, repetitive tasks and reduce human biases. It also allows us to process and analyse data from experiments that contain higher numbers of variables, which aids research into variable behaviour with less reduced experimental setups. Here, these advances enabled me to use state-of-the-art behavioural touchscreen setups to train mice in a non-matching to location task and analyse their individual behavioural strategies in detail, as well as use calcium imaging to determine the underlying neuronal patterns *in vivo*.

### **The present study**

Here, I argue that behavioural differences between delayed response and working memory tasks are reflected in differences in neuronal activity during the delay epoch. I further hypothesise that the sensory information does not need to be maintained in delayed response tasks and is, therefore, not reflected in the neuronal activation during the delay epoch. In contrast, the sample information must be neuronally maintained during the delay in working memory tasks.

In this study, I trained humans and mice on a non-matching to location task, which, notably, proceeded from a delayed response task, where they could predict the correct test stimulus location from the sample location, to a working memory task, where they could not make this prediction from the sample location alone. Crucially, the human and mouse tasks were kept as similar as possible to facilitate comparisons of behavioural differences across species. In most studies with direct comparisons between rodents and humans, the tasks, although testing for the same cognitive ability, e.g. working memory, are adapted to the species (Böhner et al., 2015; Jackson et al., 2024; Nithianantharajah et al., 2015; Nithianantharajah et al., 2013). However, specifically in the case of working memory, this may lead to equating a delayed response in mice, e.g. forced alternation in a t-maze, with a working memory task, such as a change detection task in humans, where only the sample and test stimuli together allow the detection of a change, e.g. in colour, and determine the behavioural output. Both tasks are classified as working memory; however, one allows

## Introduction

the mouse to preplan its behavioural output during sample presentation, while in the other, the human cannot preplan, as only the presentation of the test stimuli determines behavioural output.

Nevertheless, finding a task that is not too hard to learn for mice and scientifically feasible, nor too easy for humans to be behaviourally relevant, can pose some difficulty. The non-matching to location task has the additional advantage that mice were trained on a delayed response task first and then progressed to a working memory task without changing the general trial structure. Few studies compare these two task types directly in the same animals. Nevertheless, it has been shown in monkeys (Quintana et al., 1988), pigeons (Honig and Dodd, 1983; Honig and Wasserman, 1981) and mice (Bennett et al., 2022) that performance and learning can be distinctive in the two task types. However, only very few studies measured the underlying neuronal signatures and found differences between the number of units responsive to the sample and the choice in two monkeys (Quintana et al., 1988).

In addition, the touchscreen setup used in this study allows the mice to freely progress throughout the trials and exhibit a multitude of natural behaviours. In combination with infrared cameras and modern markerless pose estimation tools, i.e. DeepLabCut (Mathis et al. 2018), enables the investigation of idiosyncratic behavioural strategies and their adaption during the progression from delayed response to working memory tasks.

The tremendous advantage of mouse models is the richness of available methodologies measuring neuronal signals. One-photon calcium imaging was used to determine neuronal activation patterns throughout the task, as it allows single unit responses to be determined and tracked across sessions. The main difference between delayed response and working memory tasks is the maintenance of the sample information. Thus, I hypothesise that in the delayed response task, the sample location is neurally represented in the sensory period but decays throughout the delay, where the focus can already be shifted towards the behavioural choice (**Fig. 1a/b**). In contrast, in the WM task, the sample location information needs to be kept mentally available throughout the delay, which may also cause the encoding of the sample to be stronger in the sensory epoch. It is further to be investigated if the sample information is encoded by the same neural population in the sensory and delay epochs or if it is encoded and maintained by two distinct populations (**Fig. 1c/d**).

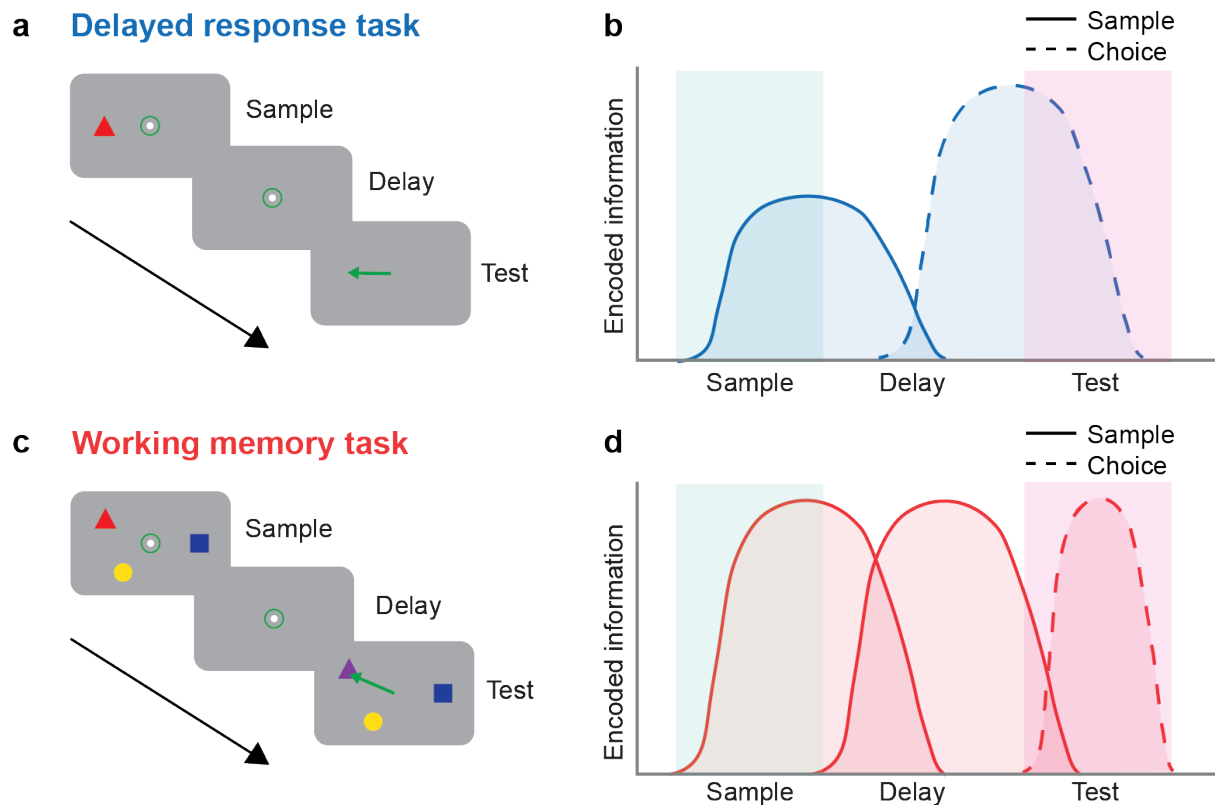


**Figure 1 | Proposed difference between delayed response and working memory tasks**

**a** Diagram illustrating a delayed response task. The subject has to memorise the location of the item (red triangle) and then saccade to its location during the test epoch. As soon as the item is presented, the motor output to correctly solve the task is known and, thus, can be planned. The described task design was inspired by Funahashi et al. (1989) **b** Sample information in the delayed response task does not need to be maintained throughout the delay period, as the correct choice can be predicted from sample stimulus. **c** Diagram illustrating a working memory task, where three items (circle, square and triangle) must be kept in mind during the delay epoch. After the delay epoch the subject has to saccade to the item that changed colour. Therefore, the sample information must be kept in mind to compare it to the test stimuli, and the motor output can only be planned after the delay. The described task design was inspired by Buschman et al. (2011). **d** The sample information in a working memory task must be remembered to determine the correct choice after the delay, thus it is maintained throughout the delay epoch. The neuronal population maintaining the information about the sample may be different from the population encoding the sample information.

## Introduction

In summary, the aim of the present study was to determine differences in behaviour between delayed response and working memory tasks in mice and man, specifically if individual strategies for each task type could be discovered using state-of-the-art analysis techniques. Furthermore, it was investigated if these behavioural differences were reflected by distinct neuronal activation patterns in the prefrontal cortex, specifically if the information about the sample location is maintained during the delay epoch in working memory tasks but not delayed response tasks.

# Materials and Methods

## Housing and husbandry

Wildtype male mice (C57Bl/6J and C57Bl/6N, Charles River) were kept in a reversed 12 h-light/dark cycle in an environment controlled for temperature and humidity. They had access to food (Altromin, 1324, standard diet) *ad libitum*. Water access in the home cage was restricted during experimental procedures, with mice receiving a minimum of 1 ml of water during behavioural experiments. Mice were examined daily to monitor their health status. All animal experiments were authorised by the local authorities (Regierung von Oberbayern). Mice were aged 8-10 weeks at the start of the experiments.

## Behavioural training

### *Behavioural setup*

A touchscreen chamber (80614A, Campden Instruments) was controlled by a custom PC. The chamber contained a trapezoidal behavioural arena with a touchscreen on one side (**Fig. 2**). A mask (CI.80614-M4, Campden Instruments) was used to focus the animal's responses towards five windows (3x3cm) on the touchscreen. On the side opposite the touchscreen, a reward trough delivered 10  $\mu$ l water rewards. In addition, the chamber contained three infrared (IR) beams (in the reward trough and the front and back of the arena), a white LED light in the reward trough (reward light) and above the arena (house light) and speakers (**Fig. 2a**). The IR-beam in the reward trough was used to trigger stimulus presentation. LED lights and sounds were used to signal the trial structure to the animal. The house light signalled the inter-trial interval, the reward trough light signalled that the mouse had to enter the reward trough and the sounds were used as a signal for initiation (3 kHz), correct choice (5 kHz), and incorrect choice (white noise). An infrared camera (FLIR, Chameleon®3 USB3 Camera) was placed above the arena to record behavioural videos (**Fig. 2b**). The recording frame rate was 30 Hz with 640x512 pixels resolution. A commutator allowed animals wearing

## Materials & Methods

miniscopes to move as freely as possible and avoid tangling and damage to the coaxial cable. Custom MonkeyLogic (Hwang et al., 2019) scripts were used to trigger trial events and collect behavioural data. The miniscope was attached to a second PC via a coax cable during imaging sessions. The calcium signal recording was initiated by the MonkeyLogic script, and the imaging data were transferred and saved on the second PC.

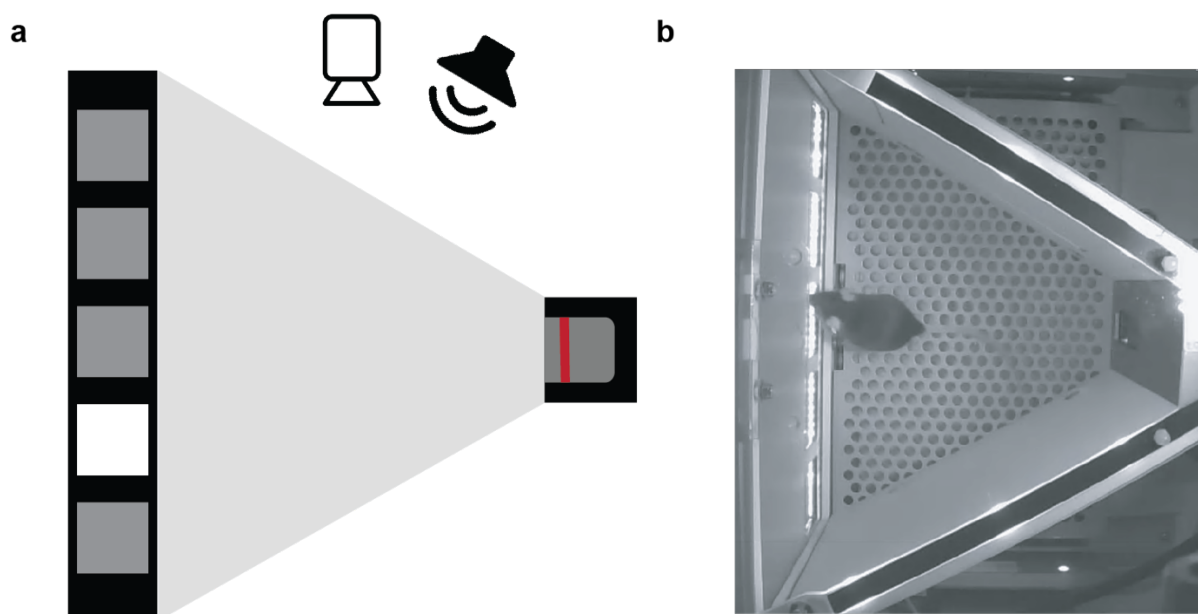


**Figure 2 | Behavioural touchscreen setup**

**a** Diagram of the behavioural chamber, indicating the location of the five response windows (one window lit, as seen during sample presentation), reward trough with infrared beam (red), infrared camera and loudspeaker. **b** Photograph of a mouse during the behavioural training in the touchscreen chamber

### *Pretraining*

The stimuli were white squares (3x3 cm) presented on a black screen, that appeared behind the windows of the mask. The animals were habituated to the chamber and taught the basic task structure during the pretraining (adapted from Oomen et al., 2013). During the first two days, the animals were habituated to the setup for 30-40 minutes daily with free access to 1.5 ml water in the reward trough. During the following sessions, all five windows were lit continuously, and the animal received 30  $\mu$ l whenever it touched any of the five windows. The session ended after 1 hour or if the

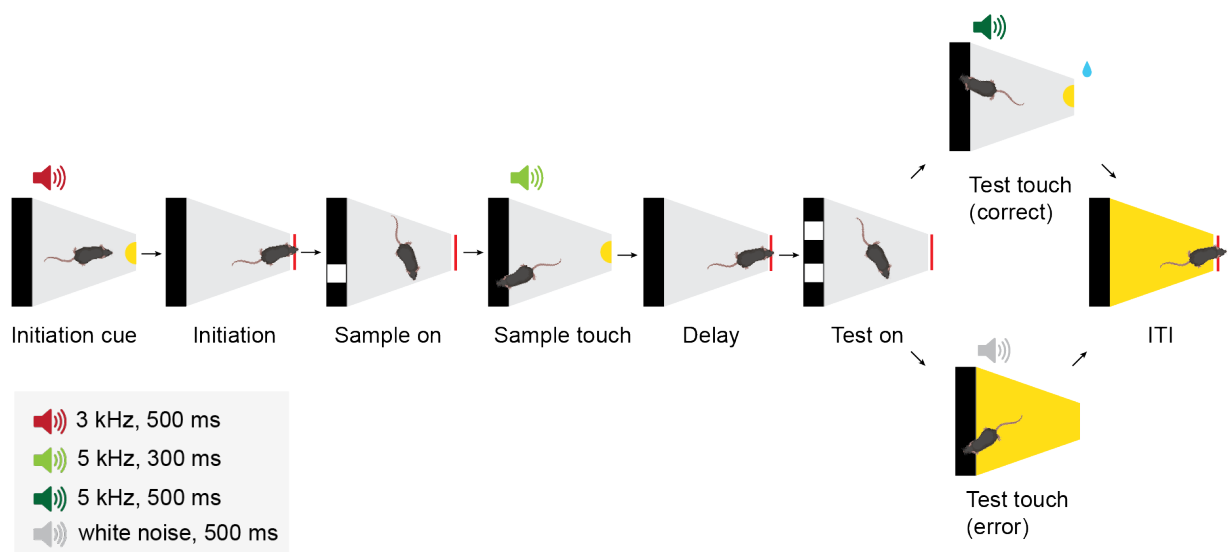
animal reached a total of 1.5 ml water consumed. Additionally, when touching the stimulus, a 5 kHz sound cue was given for 500 ms, and the reward light lit up to signify success and water availability. The reward light was turned off when the mouse broke the IR beam in the reward trough. After two days, the reward for touching the screen was reduced to 10  $\mu$ l for two sessions. Then, the number of lit windows was reduced to three, and eventually one, with the animal only receiving a reward when a lit window was touched. After that, an initiation cue was introduced to signal the beginning of the trial with a sound (3 kHz, 500 ms) and the reward trough light being turned on. The animal had to break the IR beam in the reward trough to trigger the stimulus presentation on the touchscreen and turn off the reward light. The trial then proceeded as before. Lastly, a timeout was introduced if the animals touched an unlit window. The timeout was signified by the houselight and 500 ms of white noise. During all task types, trials were separated by a 5 s intertrial interval (ITI), which was signalled to the mouse by the houselight. Animals were advanced when they reached 1-1.5 ml reward consumption within an hour over two consecutive days. After progression through all pretraining stages, the animals were moved on to the behavioural training of the non-matching to location task.

### *Behavioural task*

The protocol for the non-matching to location task was adapted from Oomen et al. (2013). An individual trial (**Fig. 3**) proceeded as follows: The initiation cue (3k Hz, 500 ms) and the reward trough light turned on, signalling the start of the trial. The animal could then poke the head in the reward trough, breaking the IR beam, which turned off the reward trough light. Removing its head from the reward trough triggered the presentation of the sample stimulus, i.e. one of the five windows lighting up. The animal had to touch the lit window, which triggered a reward sound cue (5 kHz, 300 ms) and the reward trough light turning on. The animal had to return to the reward trough and poke its head in again, which triggered the reward trough light to turn off. When removing its head from the reward trough, the test stimuli were presented on the touchscreen. The test stimuli consisted of a lit window in the same location as the sample stimulus (match) and one in a different location (non-match). The mouse had to touch the window in the non-matching location to trigger a reward

## Materials & Methods

of 10  $\mu$ l water, accompanied by the reward sound cue (5k Hz, 500 ms). After the mouse broke the reward trough IR beam to consume the water reward, the intertrial interval (ITI) was triggered, which consisted of a 5s timeout, which was signalled by the house light turning on. If the mouse touched the test stimulus in the matching location or a non-lit window during the sample or test epoch, a 5 s timeout was triggered. If the animals chose incorrectly, the trial was repeated later in the session to ensure that the mice did not just learn easier conditions to receive sufficient water reward in one session.



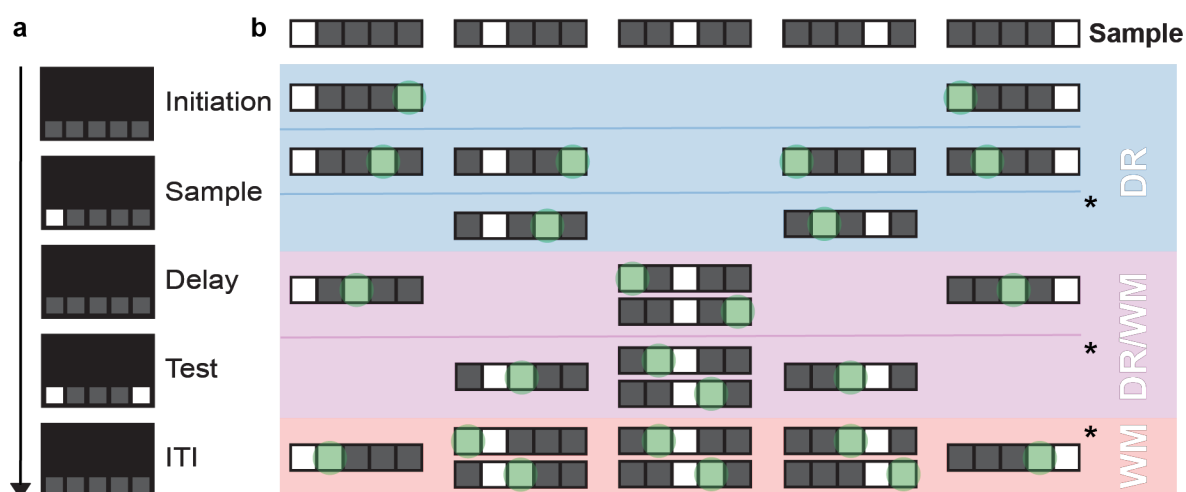
**Figure 3 | Trial progression of the non-matching to location task**

Diagram of one example trial, indicating important trial events, such as the sample onset, sample touch, test onset and test touch. Light in the reward trough is indicated as the yellow semicircle on the right of the arena. Houselight is shown as yellow background. Different auditory cues are signified with the speaker icon. Mice could decide freely when to progress through the trial. (Mouse image from BioRender.com)

The possible locations of the sample and test stimuli (**Fig. 4a**) advanced through the behavioural training to increase difficulty. In the beginning, only the two corner windows were used. When the mice reached over 70% performance on two consecutive days (criterion), they were moved to the next training phase (**Fig. 4b**). The separation of the windows decreased throughout the training phases. In the first phase, all stimuli were shown in the outer windows (window locations: left, middle left, middle right and right), excluding the middle window. The sample stimuli always

occurred on one side of the touchscreen, e.g. the right, which meant that the correct test stimulus would be on the other side, i.e. left, or vice versa. Thus, the location of the correct stimulus was predictable from the sample stimulus, which meant that the information about the sample stimulus was not needed to solve the task. These phases will be defined as delayed response (DR) conditions (**Fig. 4b, blue**). During the first sessions of the DR task, one-third of the samples were randomly chosen to be rewarded with 5  $\mu$ l water, which is necessary for the mice to learn the complete trial structure. The sample reward was removed once the mice reached over 70% performance on two consecutive days of the smallest separation level of the DR tasks. After the mice successfully reached criterion performance, they were moved to a 50:50 mixture of DR and WM conditions. In half of the conditions, the correct test location was still predictable from the sample location. However, in the other half, the sample stimulus appeared in the middle window and the mice could not know from the sample alone if the correct test stimulus would be to the right or the left. This phase will be referred to as delayed response/working memory task (DR/WM) (**Fig 4b, purple**). When the mice reached over 70% performance on two consecutive days and above 60% performance in all individual conditions, the window separation was again reduced. Finally, in the last task type of the behavioural training, 75% of the correct test locations were non-predictable, and only the conditions where the sample appeared in the corner windows, i.e. the left or right, could be solved before the test stimuli presentation. This task will be referred to as working memory (WM) task (**Fig. 4b, red**).

## Materials & Methods



**Figure 4 | Trial structure and training progression for the non-matching to location task**

**a** Trial structure with example sample and test locations. **b** Training progression overview. The sample could appear in one of five locations (top row). Training started with the two conditions in the second row only (right and left corner windows). The animals were progressed to the next task (row) when they reached criterion overall performance, as well as sufficient performance in all individual conditions. Tasks were divided in DR (all correct test locations could be predicted, blue), DR/WM (50/50 mixture of predictable and non-predictable trial conditions, purple) and WM (75% of the test location could be predicted, red). Neuronal imaging sessions were conducted in an expert session at the end of each task type (\*).

## Neuronal recordings

### *Lens implantation surgery*

AAV1.CamKII.GCamp6f.WPRE.SV40 (100834-AAV1, Addgene) was mixed with silk fibroin solution (5154, Sigma Aldrich) at a ratio of 1:1. A nanoinjector (Neurostar NanoW) was then used to slowly drop approximately 50 nl of the virus-silk mixture on a cleaned 0.5 mm  $\varnothing$  gradient index microlens (Inscopix). After the drop had dried, the next drop was applied to the lens surface until a minimum of 300 nl was reached. The lens was left to dry for at least an hour and kept in a cool and dry place until implantation (Jackman et al., 2018).

The animal was anaesthetised using 5% isoflurane before being transferred to a stereotaxic frame (Neurostar). Body temperature was maintained at 37 °C using a heating pad. Breathing rate and body temperature were monitored during the entire surgery to ensure the animal's well-being. Analgesia (Metamizol, 0.1 ml/30 g

animal weight) was injected subcutaneously. The anaesthesia was maintained at 0.8-1.5% isoflurane throughout the surgery and adjusted if the animal showed any signs of abnormal breathing. The fur on the head was removed using a shaver (Grundig, MT 5531) and hair removal cream (Balea, Enthaarungscrème). The skin was disinfected using 70% ethanol, and a local anaesthetic (2% Lidocaine solution) was injected subcutaneously before the incision to expose the skull. The skull was then cleaned thoroughly with 0.9% sodium chloride solution and lightly scored with forceps to improve adherence to the dental cement later. A small hole (drill size 008) was drilled above the prefrontal cortex (AP 1.96, ML +/-0.42, DV 1.62). The lens was inserted virus-side down into the brain to the desired depth of 1.62 mm. The lens was then glued to the skull using an approximately 1:1 mixture of superglue (UHU, Sekundenkleber) and Paladur powder (Kulzer). The open skull was then sealed with Paladur coloured black with eyeshadow (Eyestudio Lasting Drama Gel Eyeliner, Black) to prevent excess light from entering the lens. The lens was then covered with silicone adhesive (KwikSil, World Precision Instruments) and a plastic cover to protect it from mechanical impact. The mouse was injected subcutaneously with meloxicam (Boehringer Ingelheim, 0.1 ml/30 g animal weight) as an analgesic and returned to its cage, which was placed on a heating pad. The mouse was given meloxicam injections daily for 3 days post-surgery. After full recovery from the surgery, mice started behavioural pretraining.

#### *Baseplate adhesion*

The mice were anaesthetised with 5% isoflurane and transferred to the stereotactic setup to maintain and monitor body temperature and breathing rate. The animal was kept under 0.8-1.5% isoflurane anaesthesia. The silicon and plastic cover were carefully removed. The baseplate was attached to the Miniscope (Version 3, UCLA) and positioned above the implanted lens so that the fluorescence signal was visible and in focus. The baseplate was then attached to the hardened Paladur on the skull with more Paladur coloured black with eyeshadow. All gaps between the baseplate and the skull were covered with Paladur to reduce excess light entering the lens. The mouse was transferred back to its home cage, and training was continued after full recovery from the procedure.

## Materials & Methods

### *Histology and anatomy*

After the last imaging session, the animals were perfused transcardially with 4% paraformaldehyde. The brains were fixed in paraformaldehyde overnight and then washed in phosphate-buffered saline (PBS) before being sectioned coronally using a vibratome (Leica VT1000S). The slices were then covered with a mounting medium containing DAPI (VectaShield) and fixed with a coverslip. They were then imaged at 358 nm and 395 nm using a confocal microscope (Leica SP8) with a 10x objective to verify lens location and calcium sensor expression. The images were then registered to a mouse brain atlas (QuickNII) to confirm the implantation locations.

### *Calcium imaging*

Light microscopy, which traditionally uses big instruments, has recently been adapted to allow brain imaging in freely behaving animals (Ghosh et al., 2011). These take advantage of small but bright light-emitting diodes (LEDs) and complementary metal-oxide semiconductor (CMOS) image sensors with fine pixel sizes and high sensitivity. All components are contained in a small plastic housing, only weighing about 3 g (Miniscope V3.2) and can, therefore, be carried by a mouse on its head. The Miniscope works as follows: The LED emits light, which is collected by a drum lens, filtered through an excitation filter and deflected by a dichroic mirror. The light then enters the imaging pathway through the objective and a gradient refractive index (GRIN) lens, which focuses on the sample, e.g. the neurons in the brain. The fluorescence emitted from the sample returns through the objective, passing through the dichroic mirror, an emission filter and an achromatic doublet lens, which focusses the image on the CMOS image sensor (Ghosh et al., 2011). The acquired image data are then transferred to a PC via a coaxial cable and the data acquisition system and saved locally. Since then, Miniscopes have been adapted to be lighter and image larger fields of view (Guo et al., 2021).

Here, I used Miniscopes (V3, LabMaker) to record one-photon calcium signals of pyramidal neurons in the prefrontal cortex (**Fig. 5a/b**). The calcium sensor GCaMP6f was expressed under the CaMKII promotor (**Fig. 5c/d**). After the baseplate was

attached, the animals were habituated to wearing a Miniscope for 20-30 minutes over two days in their home cage. They were then trained on the last pretraining stage with the Miniscope until they reached 70% performance again. The coaxial cable of the Miniscope was attached to a commutator (FL-6-C-MICRO, Dragonfly) to allow the animal to move freely in the behavioural arena. Neural data were acquired in four imaging sessions: one at the end of the pretraining phase and one expert session of each behavioural task type (DR, DR/WM and WM). Animals were trained to wear a dummy Miniscope on all non-imaging sessions to keep the animal habituated to the weight and, thus, the behaviour consistent on imaging days. Miniscope acquisition software (Miniscope-DAQ-QT-Software) was used to collect the calcium signal data at 30 frames per second for each trial.

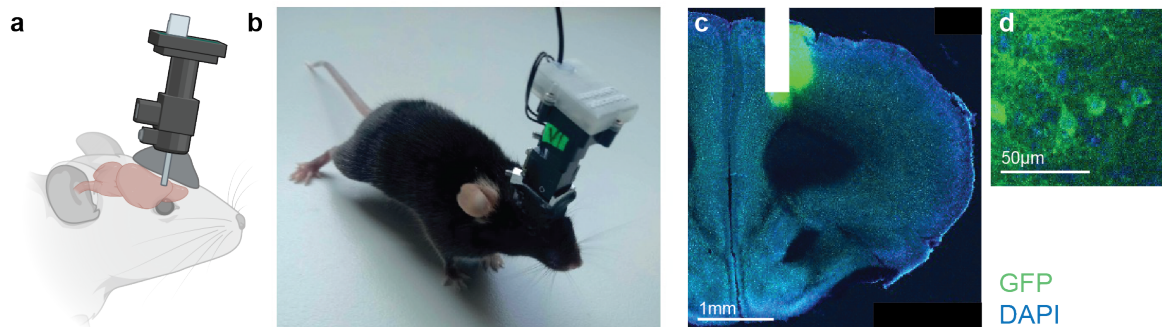


**Figure 5 | Chronic microendoscopic calcium imaging in the prefrontal cortex**

**a** Diagram of a mouse with a GRIN lens implanted in the prefrontal cortex and a miniscope attached (created with BioRender.com). **b** Photograph of a C57BLG mouse with a miniscope (UCLA, V3). **c** Coronal brain section of an example mouse, showing lens location and GCaMP6f expression (GFP fused to calcium sensor), neuronal nuclei are counterstained with DAPI (blue). **d** Single pyramidal neurons expressing the GCaMP6f calcium sensor.

### *Preprocessing and quality control*

The acquired calcium signals were then preprocessed using the Calcium Imaging data Analysis (CalmAn) Python toolbox programmed in Python and run in the caiman virtual environment (Giovannucci et al., 2019), which uses the CNMF-E algorithm (Pnevmatikakis et al., 2016). Due to variability in imaging quality, the CalmAn parameter “gSig”, defined as the expected half-size of neurons in pixels, was adjusted

## Materials & Methods

for individual imaging sessions to maximise signal-to-noise separation. The change in expected half-size was due to focus issues, which moved the neurons slightly in or out of the focal plane, minimally changing the visual size. The CalmAn pipeline determines several quality measures for each unit. For each session the mean and standard deviation of the spatial footprint consistency (“rval”) over all units was determined. The spatial footprint consistency was established by comparing the spatial footprint of the component in the frames where it is active, removing other components' signals from these frames and correlating the resulting raw data against the spatial component (Giovannucci et al., 2019). In addition, the mean and the standard deviation of the natural logarithm of the overall signal-to-noise ratio (SNR) of all identified units was calculated. Individual units with rval and  $\ln(\text{SNR})$  smaller than one standard deviation below the mean across all units were considered noise and excluded from further analyses. Secondly, each unit was manually assessed for signal consistency, footprint shape and footprint location and removed if they did not meet the following criteria. The spatial footprint criterion excluded units whose spatial footprint was not a roundish shape, e.g. a shape resembling the number “8”, indicating two neighbouring or overlapping units being processed as one. Further units detected outside of the visible edge of the lens were excluded based on unit location.

### **Data analysis**

Task performance and locomotion path were analysed using custom-written MATLAB scripts (The MathWorks Inc., R2023a). The neuronal data were analysed using custom-written Python code, using the packages NumPy (Harris et al., 2020), Matplotlib (Hunter, 2007) and Scikit-Learn (Pedregosa et al., 2011).

#### *Task performance*

Performance was defined as the number of correct trials divided by the number of completed trials per session. Trials in which the mouse touched a non-lit window during the sample or test phase, leading to premature termination of the trial (miss), were excluded from further analyses.

*Locomotion path analysis*

DeepLabCut (Mathis et al., 2018) was used to train two separate neural networks to label mice without and with miniscopes, as the labels on the head, specifically the nose and miniscope marker, differed between groups (**Fig. 6a/b**). Single coordinate pairs were removed if the distance to the preceding coordinate pair exceeded 150 pixels, which is far above the physiologically possible movement of the mouse. The average distance between two coordinate pairs across all mice was 4.68 pixels. Custom-written MATLAB scripts were then used to visualise the movement of the mouse by plotting the progression of the head marker throughout the test epoch of the trial, which was defined as the time point when the mouse pulled its head out of the reward trough, triggering the presentation of the test stimuli, until touching the correct (non-matching) test stimulus (**Fig. 6c**). The average normalised path length (NPL) was calculated by dividing the trajectory length during the test epoch with the Euclidean distance (ED) from the midpoint of the reward trough to the closest corner of the choice window (**Fig. 6d**). It was calculated for each trial and then averaged across sessions or conditions:

$$NPL = \frac{\sum(x_{trajectory}/ED_{trajectory})}{n}$$

The Fréchet distance (FD), which describes the similarity of two curves by comparing the direct distance between each consecutive point on the two curves going forward (**Fig. 7e**), was calculated for the test epoch of each trial within and between different conditions as described in Mosberger et al. (2024) using the “DiscreteFrechetDist” MATLAB function (Danziger, 2024).

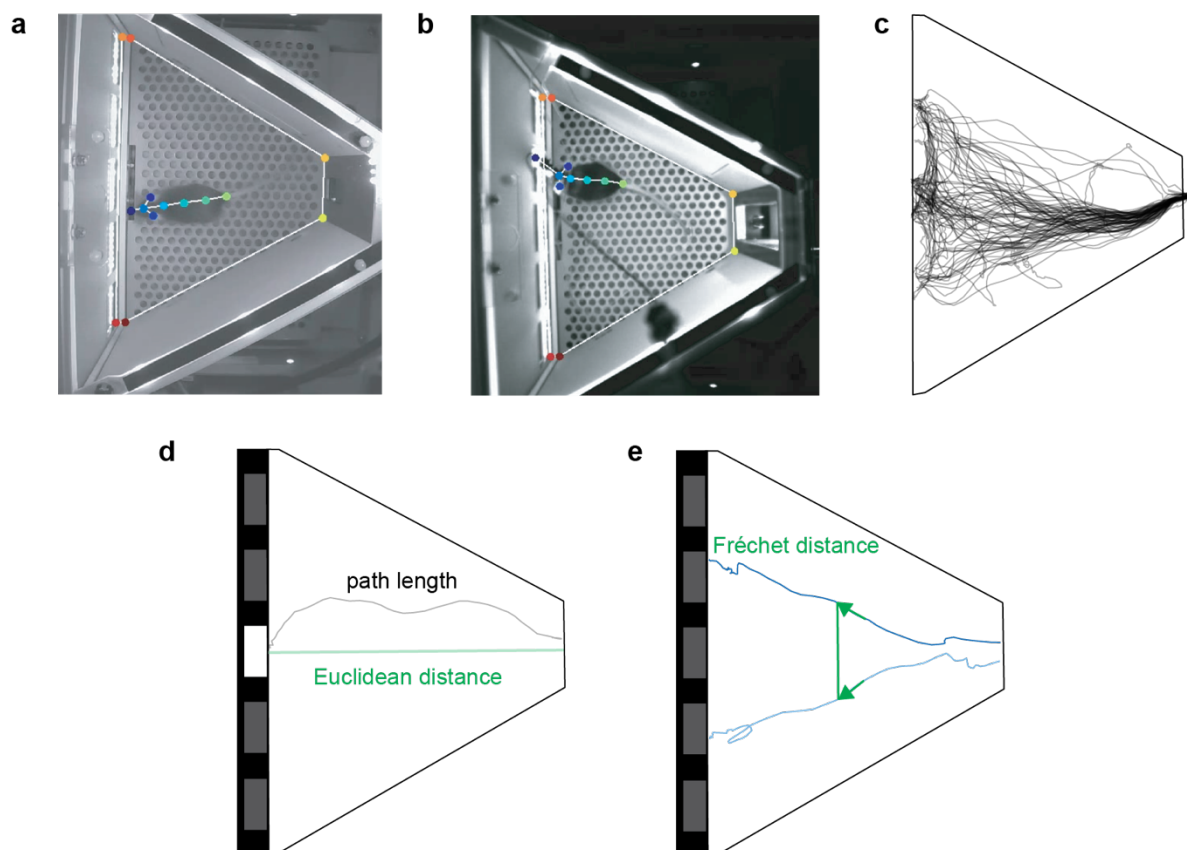


**Figure 6 | Locomotion path analyses during the test epoch**

**a/b** Example images of two animals with and without miniscope showing marker locations. DeepLabCut was used to track the mice throughout the task, each mouse was labelled with eight markers (nose or miniscope, head, ears, spine and tailbase), in addition to the corners of the arena. **c** Example paths of each trial from test onset to test touch (test epoch) for one session of the mouse (only correct trials shown). **d** Normalised path length (NPL) was calculated by dividing the path length by the Euclidean distance between the reward trough midpoint and the closest point of the correct window. **e** The Fréchet distance was calculated by progressively comparing the distance of each pair of points of the two curves, adapted from Mosberger et al. (2024).

### *Neuronal analysis*

The progression of the mouse through the trial was not enforced, allowing it to proceed at its chosen speed and exhibit idiosyncratic behaviours and strategies. The free progression, however, led to task events never co-occurring at the same time in a trial, which made the alignment of trials to multiple events at the same time impossible. Therefore, calcium traces were aligned to four different task events of interest, i.e. sample onset, sample touch, test onset and test touch. The z-score of the raw

fluorescence signal was then calculated for each accepted unit by subtracting the session mean of the trace and then dividing by the session standard deviation:

$$z = \frac{x - \mu}{\sigma}$$

A one-way ANOVA was used to determine significant tuning to the sample location, choice side (left or right) or trial outcome (correct or error) for individual units, which was used to determine the fraction of accepted units significantly tuned to a task parameter, for time windows of 400 ms, moved by a 200 ms step, 2 s before and after each aligned event.

Furthermore, the percentage explained variance ( $\omega^2$ ) was used to quantify the information about the sample location, choice side or trial outcome carried by a unit's calcium signal. The same 400 ms moving window with a step size of 200 ms was used as in the one-way ANOVA described above. It was calculated as follows:

$$\omega^2 = \frac{SS_{Groups} - df * MSE}{SS_{Total} + MSE}$$

Where the individual terms were derived from a one-way categorical ANOVA:  $SS_{Groups}$  is the sum-of-squares between the groups (sample location, choice site and trial outcome),  $SS_{Total}$  is the total sum-of-squares,  $df$  is the degrees of freedom and  $MSE$  the mean squared error (Jacob and Nieder, 2014). The number of trials in each condition was balanced using a random subset of trials from each condition. The condition with the smallest number of trials determined the number of trials in the subsets. The overall statistic was then taken as the mean of the  $\omega^2$  calculation repeated 25 times. For every unit and window, the significance level was calculated by randomly shuffling the labels of the trials and repeating the process 1000 times for single unit plots and 100 times for population averages. The significance level was then determined to be the 99<sup>th</sup> percentile of the shuffle.

A trial-averaged principal component analysis (PCA) was performed by averaging the z-score of each trial type, i.e. for each of the five windows (sample location), the correct test stimulus being the left or the right lit window (choice side) or correct and error (trial outcome) at each alignment event across all accepted units for that session. Error

## Materials & Methods

trials were only included in the analysis of trial outcome. The trial averages were then concatenated separately for each task parameter, and the PCA was applied using the Python toolbox Scikit-Learn (Pedregosa et al., 2011), which maintains the time dimension of the trials. PCAs were run separately for each task parameter and alignment.

### Human task design

#### *Subjects and setup*

The task was tested on two healthy individuals (one female), naïve to the task design and research question. An eye tracker (EyeLink 1000 plus, tower mount) was used to monitor eye movements. Participants sat at a viewing distance of 57 cm from a screen (Samsung S24E650, screen diagonal 59.8 cm) and were instructed to rest their head on a chin rest throughout the task.

#### *Behavioural task*

The non-matching to location task described above for mice was adapted for human subjects to test the translatability of the behavioural results. The task design was adapted from a touchscreen-based approach to be controlled with eye movements. Furthermore, the number of windows was increased from five to nine to better visualise the behavioural effects in humans. Custom MonkeyLogic scripts were used to trigger task events and record behavioural data (Hwang et al., 2019). Individual trials were structured as follows: The subjects had to fixate on a central fixation dot (colour: #000000) for 500 ms. The fixation window was a circle with a radius of 1.5 ° with the fixation dot at its centre. Nine dark grey squares (colour: #5C6062) were centred on a horizontal line 6.8 ° below the fixation dot, with 0.4 ° between squares. During the sample presentation, one square changed its colour to light grey (colour: #D3D2D2) for 500 ms. Then, briefly, all nine squares changed to light grey (colour: #D3D2D2) for 100 ms to reduce the afterimage effect (mask). All squares were dark grey again during the delay (1000 ms). After the delay, the fixation dot

disappeared, and two squares turned light grey, one in the same location as the sample and one in a different location. The subject had to saccade to the non-matching location for a correct trial. Visual, in the form of a green or red corona around the chosen square, and auditory feedback, in the form of two distinctive correct and error sounds, were given to the subject before proceeding to the intertrial interval (ITI) for 2000 ms (**Fig. 7a**).

Testing proceeded in three blocks. In the first block, the sample and correct test location were always on opposite sides of the screen. For example, if the sample was in the square to the very right, the correct test was on the left side of the screen, thus making the approximate location of the correct choice predictable and allowing motor preparation, which will be referred to as the DR block (**Fig. 7b, blue**). The DR block proceeded in three subblocks, starting with the four outermost sample locations and then slowly moving the locations closer together, equivalent to the mouse task. In the second block, two conditions for each sample location were used, one with the correct test stimulus location on the right of the sample and one where it was on the left, thus removing predictability. This block will be referred to as the WM block (**Fig. 7b, red**). Lastly, all possible conditions were mixed in one block (**Fig. 7b, purple**). This block was used as a control to rule out effects of sample location, i.e. longer reaction times due to the sample being further away from the fixation dot. Blocks were run until each used condition was chosen correctly approximately five times.

## Materials & Methods

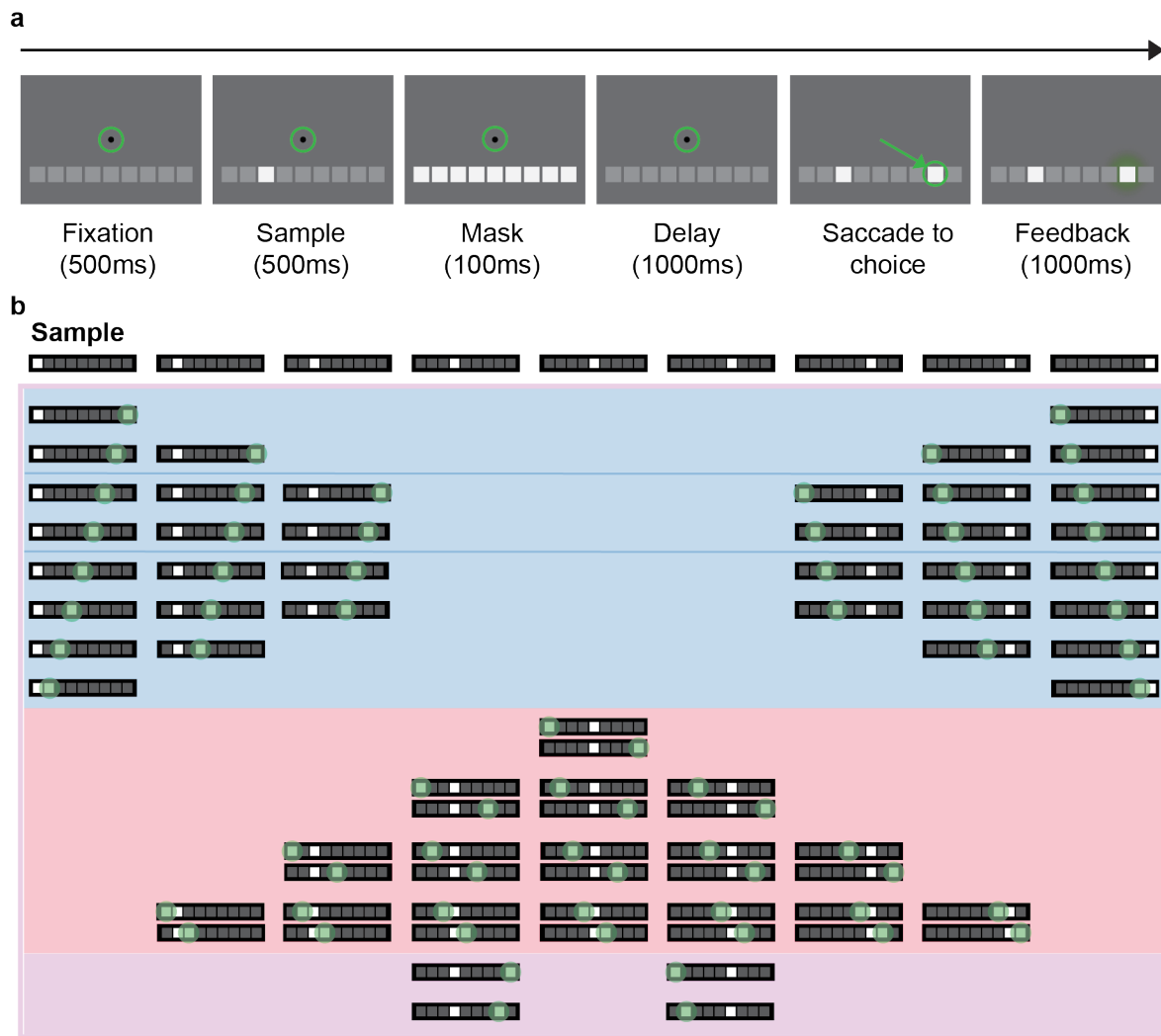


**Figure 7 | Delayed non-matching to location task for humans**

**a** Trial structure with example sample and test locations. Participants had to fixate on the fixation dot during fixation, sample, mask and delay epoch (green circle). When the test stimuli were presented, the fixation dot disappeared, and the participant had to saccade to their chosen square. Visual and auditory feedback was then given. **b** The sample could appear in one of nine possible sample locations (squares in the top row). The colours and lines show the block design of the task progression. In the first block the sample only appeared in the four outermost locations and the correct test stimuli on the other side of the screen (rows 1-2). The task was progressed to the next block when a sufficient number of correct trials within each condition was reached. The first three DR blocks (blue) contained only conditions where the correct test stimulus was in the other half of the screen (left versus right). In the fourth block the correct test location could not be predicted from the sample (WM, red). The last block contained all shown 72 conditions (DR/WM, purple).

### *Behavioural analysis*

Custom MATLAB scripts (The MathWorks Inc., R2023a) were used to analyse the behavioural data. Performance was defined as correct trials divided by the sum of correct and error trials per session, excluding missed trials, where the subject broke the fixation by leaving the 1.5 ° circle surrounding the fixation dot or failed to initiate fixation within 10 seconds after the beginning of the trial. The reaction time was defined as the time from test stimuli presentation to the choice registration after 500 ms fixation on the chosen target. Differences between the reaction times for each block were tested for significance using a Kruskal-Wallis test (significance level:  $p < 0.05$ ).

### *Microsaccades*

Microsaccades, i.e. eye movement below an amplitude of one visual degree, have been associated with visual working memory (Liu et al., 2022; Hafed et al., 2002; Engbert et al., 2003; Lowet et al., 2018). Here, microsaccades were detected during the delay epoch, where subjects had to maintain sample location information or plan motor output. Microsaccade detection was based on the criteria described in Liu et al. (2022). In brief, the x-coordinates of the eye movements were converted to velocity by taking the first derivative. The absolute velocity was then smoothed with a Gaussian kernel with a window size of 14 pixels. If the trace exceeded the threshold set at three times the median of the trace for more than 10 ms, the eye movement was classified as a microsaccade. The analysis of the delay epoch of the trial did not include the macrosaccade to make the choice and if the fixation was broken, the trial was aborted. Direction, amplitude, and frequency were determined for each microsaccade in all the task blocks. Differences between microsaccade amplitudes in DR and WM blocks were tested for significance using a Kruskal-Wallis test (significance level:  $p < 0.05$ )

# Results

## Behavioural signatures of mice and man

### *A visual working memory task in mice*

DR and WM tasks using matching or non-matching icons have been developed for a variety of species, such as pigeons (Honig and Wasserman, 1981), rats (Nakagawa, 1993; Andrew and Janssen, 1996) and primates (Miller and Desimone, 1994). However, a delayed (non-)match to sample paradigm using visual icons has yet to be developed in mice. As the touchscreen setup used in the present study allows easy implementation of behavioural paradigms, three mice were trained on a non-matching to sample task using two icons, spider and plane (**Fig. 8a**). The performance level across approximately 50 training sessions stayed at the chance level of 50% (**Fig. 8b**). In comparison, Nakagawa (1993) found that rats could learn such a task in on average 59.6 session (with a standard deviation of 18 sessions). There are only a few non-spatial working memory tasks published in mice, one using multiple modalities, i.e. giving an auditory cue indicating if the mouse should attend to visual or auditory rules (Rikhye et al. 2018), another being a delayed non-match to sample task using olfactory cues (Liu et al. 2014). Importantly, mice had learned the olfactory non-match to location task to a stable high performance at 50 training sessions. Although it must be noted that these animals were head-fixed, the licking rates were compared, and the cues were olfactory, all of which may influence the learning rate of the task. Therefore, this study used a spatial non-matching to location task. The task was adapted from the trial-unique non-matching to location (TUNL) task for mice in touchscreen setups (Talpos et al., 2010; Bussey et al., 2012; Oomen et al., 2013; Kim et al., 2015), which shows reproducible behavioural performance across different laboratories (Nakamura et al., 2021; Sokolenko et al., 2020; Dexter et al., 2022).

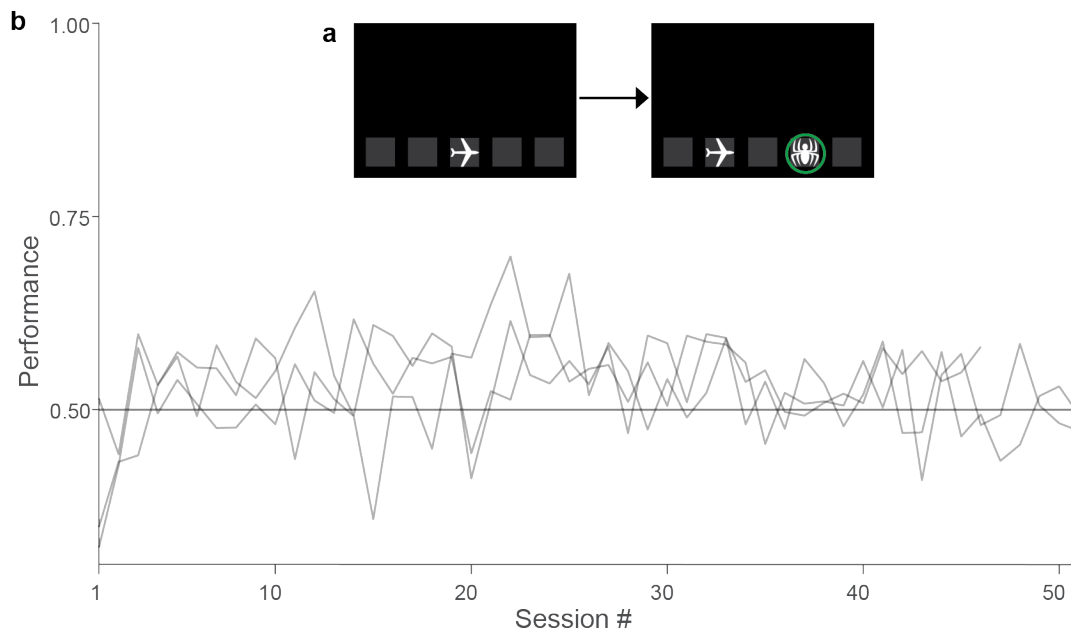


**Figure 8 | Mouse performance in a non-match to sample task using icons**

**a** Task diagram of the non-match to sample task using icons. Mice were shown one icon (spider or plane) in the middle window. They had to touch the icon and were then presented with two icons (spider and plane) in the windows to the right and left of the middle window. Importantly, not in the same location as the sample. The mice then had to touch the non-matching test icon (green circle). **b** Performance for individual mice ( $n = 3$ ) over 50 sessions. Chance level is at 0.5.

### *Faster reactions in humans when test stimulus location is predictable*

The difference between DR and WM tasks has been shown in several species (Honig and Dodd, 1983; Honig and Wasserman, 1981; Pontecorvo et al., 1996; Bennett et al., 2023; Quintana et al., 1988).

With the aim to determine if there are behavioural differences between DR and WM tasks in humans, a mouse working memory task, i.e. the trial-unique non-matching to location (TUNL) task (Talpos et al., 2010; Bussey et al., 2012; Oomen et al., 2013; Kim et al., 2015) was adapted by substituting the touchscreen- with a saccade-controlled task design. The stimuli, i.e. white squares, and task structure were kept as similar as possible to the mouse task. However, the number of prospective sample and test locations was increased from five to nine (**Fig. 4b** and **Fig. 7b**). Two human subjects, who were naïve to the task design and research question, were instructed to fixate on the fixation dot, observe the changes in the row of squares below and choose one of the squares as soon as the fixation dot disappeared. Both subjects learned the task

## Behavioural results

and the task rule, i.e. to select the non-matching location, within the first two trials. Notably, both choose the matching stimulus first. The performance remained at ceiling level with only a few error trials in both DR, WM and the mixed DR/WM block (**Fig. 9a/b**). When asked about the task design and the different blocks at the end of the session, only one participant reported correctly that in the first block, it was possible to predict the test location to be on the other side of the screen as the sample location, suggesting that human subjects learn this task by abstracting the rule, “choose the non-matching location”.

Looking more in-depth at the reaction time, which was defined as the time epoch from test presentation until the end of the saccade to the chosen square, showed significant differences between the DR and WM blocks, with the reaction time in the predictable DR block being faster (**Fig. 9c/d**, Kruskal-Wallis-Test, human subject #1 (c): median<sub>DR</sub> = 0.36 s, median<sub>WM</sub> = 0.42 s,  $p = 3 \cdot 10^{-6}$ , human subject #2 (d): median<sub>DR</sub> = 0.36 s, median<sub>WM</sub> = 0.48 s,  $p = 1 \cdot 10^{-8}$ ). This difference was not due to other confounding factors, such as the sample or test stimuli being further away from the fixation dot or the separation level of the two test stimuli, because the effect disappeared in the mixed DR/WM block (**Fig. 9c/d**, Kruskal-Wallis-Test, human subject #1 (c): median<sub>DR/WM</sub> = 0.39 s, median<sub>DR/WM</sub> = 0.42 s,  $p = 0.223$ , human subject #2 (d): median<sub>DR/WM</sub> = 0.42 s, median<sub>DR/WM</sub> = 0.42 s,  $p = 0.720$ ). These results illustrate that differences between DR and WM blocks can be detected in simple behavioural measurements in humans in a task directly adapted from a mouse paradigm.

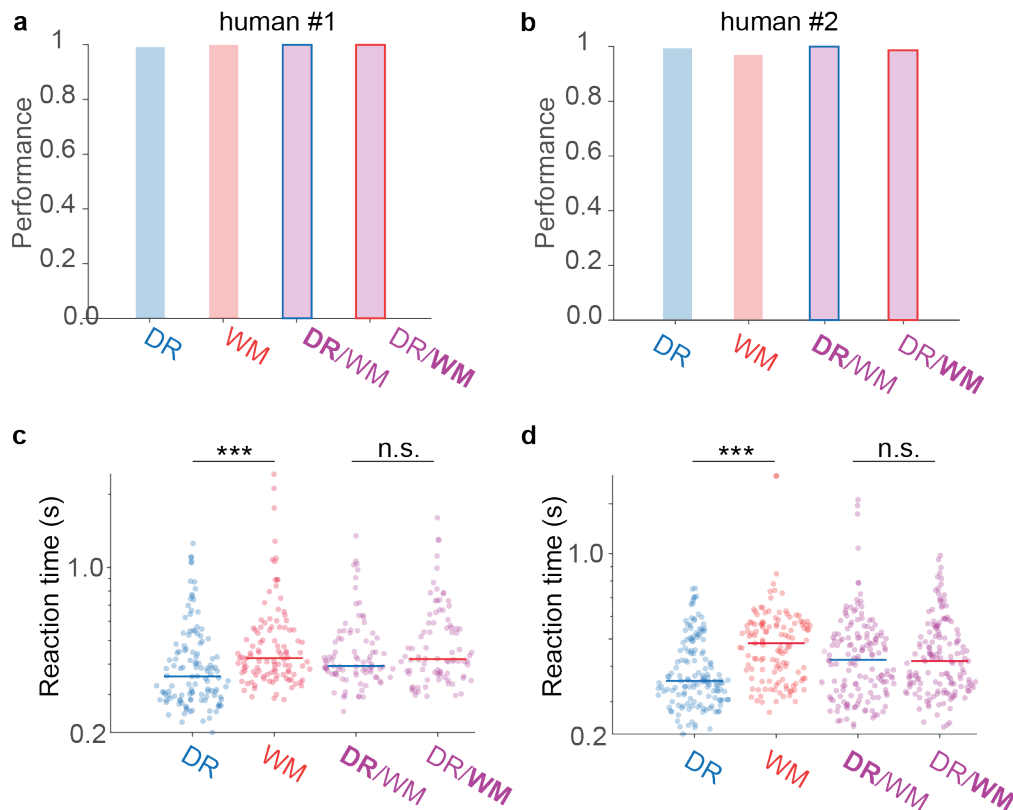


**Figure 9 | Effect of task type on performance and reaction time in humans**

**a/b** Performance, i.e. number of correct trials divided by the sum of correct and error trials, of two human participants (a and b) in each task type. The DR/WM block (purple) was divided into DR and WM trials. **c/d** Reaction time of the two participants (c and d) from test presentation to fixate on the chosen test stimulus, for each task type, again, the DR/WM block was divided by trial type. Horizontal lines indicate median reaction time. Kruskal-Wallis test. \*\*\* $p > 0.001$ .

### *Microsaccades are affected by task type*

The adapted saccade-controlled task design offered the additional advantage of allowing a more in-depth characterisation of the eye movements (**Fig. 10a**). Specifically, microsaccades, i.e. eye movements below an amplitude of one visual degree (**Fig. 10b**), have been commonly observed during gaze fixation and seem to be associated with spatial attention and visual working memory (Liu et al., 2022; Gaunt and Bridgeman, 2012; Lowet et al., 2018; Engbert et al., 2003; Hafd et al., 2002). Here, microsaccades were analysed during the delay epoch to contrast microsaccade direction, amplitude, and frequency between the DR and WM tasks and illustrate potential differences due to diverging cognitive demands. Both

## Behavioural results

participants exhibited more microsaccades in the DR block compared to the WM block. However, they also exhibited more microsaccades in the DR conditions compared to the WM conditions in the mixed block (**Fig. 10c/d**), which indicates that the locations towards the sides, i.e. further away from the fixation dot, led to a higher number of microsaccades compared to the locations in the middle of the screen. Notably, there was a similar amount of microsaccades towards the sample versus the correct test location in the delay epoch (Fig.). In addition, the microsaccade frequency throughout the trial was determined. There was an initial decrease in microsaccades when the subjects had to fixate before the sample presentation (**Fig. 10e/f**). The microsaccade frequency increased during the sample presentation and into the beginning of the delay epoch. In the second half of the delay epoch, the frequency of microsaccades decreased again, possibly in preparation for the test presentation and choice macrosaccade. These results align with past studies investigating the frequency of microsaccades in visuo-spatial working memory tasks (Gaunt and Bridgeman, 2012). Additionally, Liu et al. (2023) showed that the microsaccade frequency shifts from microsaccades towards the sample location, when it must be maintained, to microsaccades toward the correct test location once it is cued. In the future, separating the frequency of microsaccades towards the sample and the correct test stimuli could reveal a similar shift in the DR block.

Investigating the features of individual microsaccades revealed that the amplitudes differed significantly between the DR and the WM block in both individuals (**Fig. 10g/h**, Kruskal-Wallis-Test, human subject #1 (e):  $\text{mean}_{\text{DR}} = 23.44$  min,  $\text{mean}_{\text{WM}} = 20.14$  min,  $p = 0.013$ , human subject #2 (f):  $\text{mean}_{\text{DR}} = 15.98$  min,  $\text{mean}_{\text{WM}} = 13.29$  min,  $p = 0.023$ ), while this effect was, again, lost when all conditions were mixed (**Fig. 10g/h**, Kruskal-Wallis-Test, human subject #1 (e):  $\text{mean}_{\text{DR/WM}} = 22.75$  min,  $\text{mean}_{\text{DR/WM}} = 23.03$  min,  $p = 0.856$ , human subject #2 (f):  $\text{mean}_{\text{DR/WM}} = 17.25$  min,  $\text{mean}_{\text{DR/WM}} = 17.30$  min,  $p = 0.955$ ). These results may indicate that the correct test location's predictability might influence the microsaccades' amplitude, leading to larger microsaccades, potentially in preparation for the choice macrosaccade.

## Behavioural results

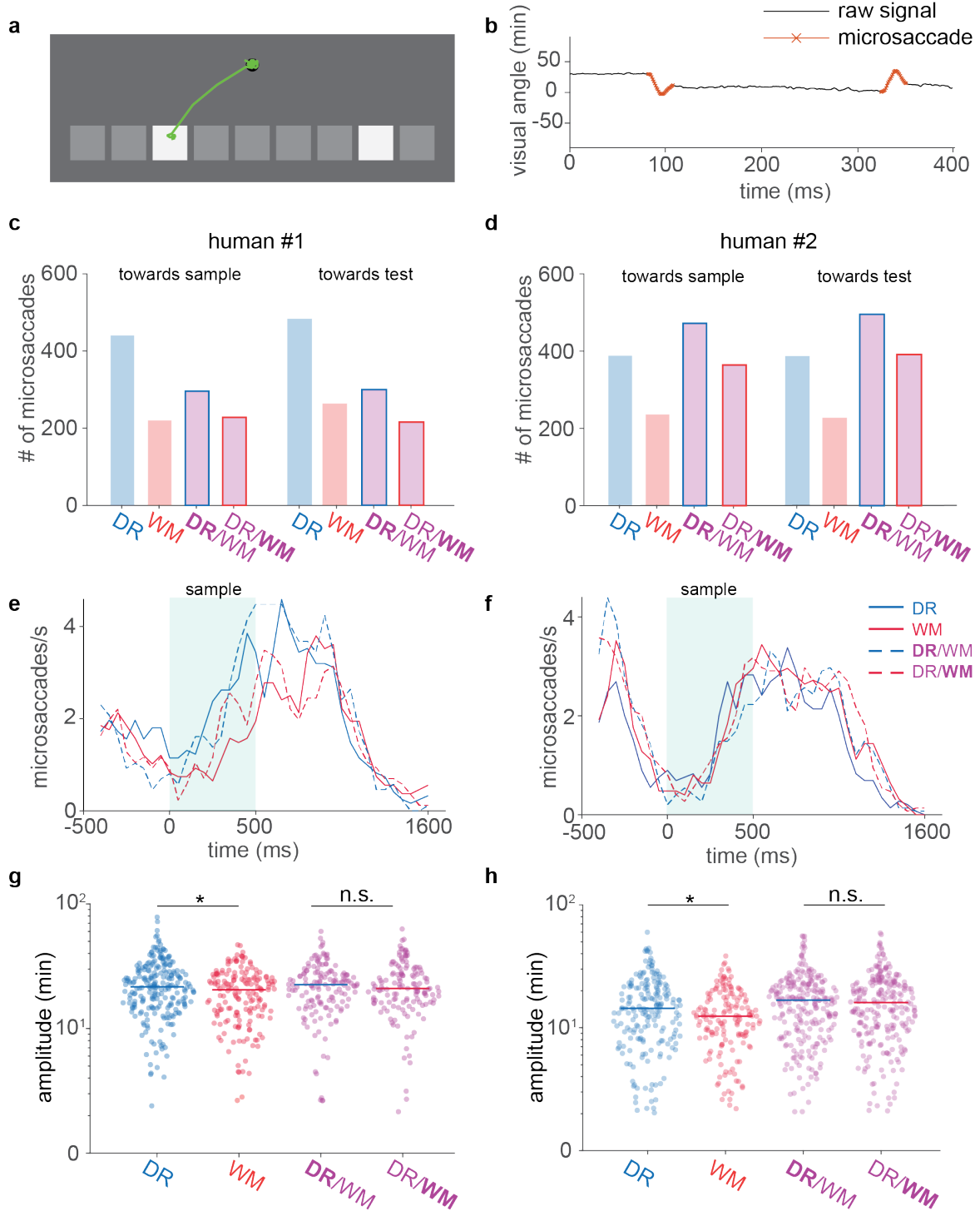


**Figure 10 | Microsaccades during the delay epoch are affected by task type**

**a** Eye movement (green) throughout an entire example trial, including the macrosaccade to the test stimulus. **b** Examples of microsaccades during the delay epoch, showing the raw signal (x-coordinates) of the eye movement against time (black) and detected microsaccades (red). **c/d** Number of microsaccades of both participants for each task type, the DR/WM block is divided into DR and WM trials. **e/f** Microsaccade frequency for each block, calculated for a 100ms window with 50ms step size throughout the entire trial, sample presentation is shaded turquoise. **g/h** Microsaccade amplitude in

## Behavioural results

visual minutes for each block, for both participants. Horizontal lines indicate mean amplitude. Kruskal-Wallis test. \* $p < 0.05$ .

Taken together, even though this task is very simple for humans, and a ceiling performance was observed in both subjects, significant behavioural differences between the two task types could be determined, suggesting that even though the human subjects might not be consciously aware of the difference between the blocks, our brains deal with these two tasks distinctly.

### *Mice can learn a non-matching to location task*

Mice were trained on the same, although simplified, non-matching to location task to investigate if they portray comparable behavioural characteristics and if these are reflected in differentiated neuronal activity. Learning a non-spatial WM task, where mice must retain the sample information without being able to plan a motor output, has only been shown in a few studies (Rikhye et al., 2018; Liu et al., 2014). Most working memory studies using mice are spatial DR paradigms, such as mazes (Spellman et al., 2015; Vogel et al., 2022; Duvarci et al., 2018). Here, a spatial WM paradigm, modelled on the trial-unique non-matching to location (TUNL) task was used in a touchscreen setup (Talpos et al., 2010; Bussey et al., 2012; Oomen et al., 2013; Kim et al., 2015). Briefly, the mice had to initiate the trial by poking their head into the reward trough, then touch one out of five windows that lit up on the touchscreen (sample stimulus), return to the reward trough and poke their head in again to trigger the presentation of the test stimuli. The animals had to choose one of two lit-up windows, one shown in the same location as the sample (match) and one in a different location (non-match). The non-matching location was the correct choice, and touching it led to dispensing a water reward in the reward trough (**Fig. 3**). During the first training sessions, only the corner locations were used to display the sample and test stimuli. Thus, the mouse could predict that if the sample was shown in the right corner window, the correct test stimulus would be in the left corner window. The mouse, therefore, did not need to keep the sample location in mind and could already plan its delayed response (DR). When the mice reached criteria, i.e. an overall performance  $>70\%$  on two consecutive days, the test stimuli locations were moved

closer together. In the following, all three separation levels of the DR task are described together (**Fig. 4b**).

Mice learned the first separation level of the DR task within 2-9 days, with the four fastest animals reaching above 70% performance in the first session. The fastest mice progressed through all three separation levels in 6 days. Progression through all separation levels of the DR task took mice on average  $9.28 \pm 0.60$  (mean and SEM,  $n = 18$ ) training sessions (**Fig. 11a/b, blue**). The performance and learning progression of wild-type mice observed here is comparable to t-maze tasks (Duvarci et al., 2018). After successfully learning the DR task, animals progressed to the DR/WM phase. Here, WM conditions were introduced where the mice could no longer predict the correct test stimulus location from the sample stimulus location (**Fig. 4b, purple, middle column**). The overall performance dropped initially and then recovered after  $10.67 \pm 2.05$  (mean and SEM,  $n = 18$ ) days of training. The separation level was then further reduced to neighbouring squares to increase difficulty, which led to another small drop in performance, which was recovered after  $18 \pm 2.41$  (mean and SEM,  $n = 16$ ) days of training (**Figure 11a/b, purple**). This initial drop in performance when decreasing the separation level, as shown before (Nakamura et al., 2021; Kim et al., 2015), could be due to the animal having to memorise the location more precisely, i.e. a specific window instead of the left side of the behavioural arena. Notably, the overall performance did not drop to the chance level of 50%. However, if the performance for DR and WM conditions was separated, it became clear that the drop in overall performance was mainly due to the newly introduced WM conditions. In contrast, the performance in the DR conditions stayed relatively stable (**Figure 11c, middle**). Performance in WM conditions slowly recovered during training but was generally lower than in DR conditions.

Finally, mice were moved to the WM task. Overall, the performance was also lower than in the preceding phases (**Fig. 11a/b, red**). Therefore, the criterion was relaxed to an overall performance above 65% and more than 60% correct trials in more than half of the individual conditions on two consecutive days. The initial drop was also steeper, with the mean performance of all animals being at chance level (**Fig. 11a/b, red**). Mice took on average of  $16.38 \pm 2.64$  (mean and SEM,  $n = 15$ ) days to criterion. Again, animals did less well in WM conditions than in DR conditions throughout the task, even though WM condition performance recovered after the initial drop (**Fig. 11c, right**).

## Behavioural results

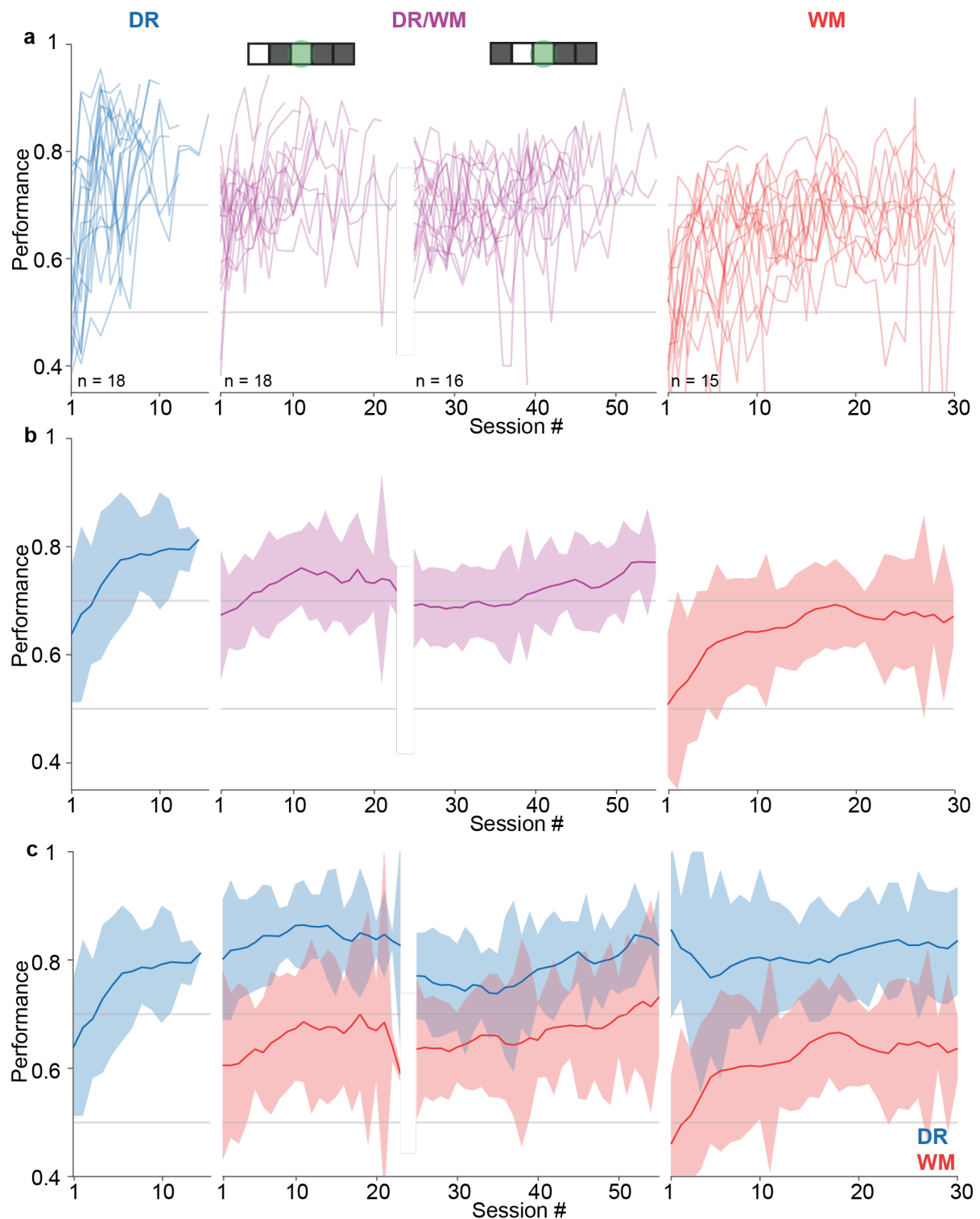


**Figure 11 | Mice learn behavioural task, but performance is affected by trial type**

**a** Overall performance of individual mice in the three task types, with DR in blue, DR/WM in purple and WM in red. Chance level was at 0.5. The DR/WM task is divided into the two separation levels, as indicated above. **b** Moved mean and standard error of the mean (SEM) of the individual performance curves (**a**) for each task type. **c** Moved mean and SEM of the performance curves split by trial types, showing DR trials in blue and WM trials in red.

Differing performance and learning rates suggest distinct approaches to solving the two task types. The difference in performance in three task types has been described in the same task before and attributed to the differing task demands (Bennett et al., 2023; Nakamura et al., 2021). In addition, it shows the importance of separating the performance of condition types, as especially in the DR/WM mixed task type, the overall performance only had a small initial drop and recovered to >70% within a few days, whilst the performance in WM trials was still low (**Fig. 11b/c, middle**).

#### *Animal trajectories become more efficient throughout learning*

Using a touchscreen setup for the WM task offers the advantage of allowing the animal to behave freely and exhibit a large variety of idiosyncratic behaviours. In addition, trial progression was not enforced, so the mice could proceed throughout the trial as fast or slow as they decided to and exhibit various behaviours, for example, exploring different behavioural strategies to solve the task. This freedom of movement allows a more detailed description of animal behaviour within the task compared to head-fixed task types. DeepLabCut (Mathis et al., 2018) tracked the mice throughout the task. In addition, the corner points of the arena were labelled to determine the relative location of the mouse within the arena, which is especially important if the location of the camera moved slightly throughout the four months of behavioural training (**Fig. 6a/b**). Recording the mice through the trials for each behavioural session and detecting their movement trajectories generated a large dataset rich in behavioural variation.

The following analysis is focused on the test epoch, defined as the time from test presentation to test touch, as the behaviour was expected to differ the most in the epoch where the decision of the animal became behaviourally relevant. Specifically, here, the first and last session of each trial type for each mouse is analysed, to determine the effect of the behavioural training. The test epoch was analysed by plotting the marker on the centre of the head of the animals relative to the arena markers (**Fig. 6c**).

Four mice were excluded from path analyses due to technical issues with the dental cement of the miniscope implant loosening, which strongly affected the behaviour and

## Behavioural results

led to the early termination of the experiment for these mice. Comparing the mean normalised path length, defined as the actual path length of each trial divided by the Euclidean distance from the reward trough to the closest point of the chosen window (**Fig. 6d**), of the first and last session of each task type showed that animals ( $n_{DR} = 15$ ,  $n_{DR/WM} = 15$ ,  $n_{WM} = 14$ ) decreased the average NPL from  $1.62 \pm 0.06$  to  $1.51 \pm 0.01$  (mean and SEM) in DR, from  $1.77 \pm 0.08$  to  $1.33 \pm 0.04$  (mean and SEM) in DR/WM and from  $1.45 \pm 0.04$  to  $1.36 \pm 0.05$  (mean and SEM) in the WM task type and became significantly more targeted in their response (**Fig. 12**,  $p_{DR} = 0.021$ ,  $p_{DR/WM} = 0.021$ ,  $p_{WM} = 0.026$ , Wilcoxon rank test). There was also a significant increase in normalised path length in the first session of the DR/WM task compared to the last session of the DR task ( $p = 0.010$ , Wilcoxon rank test) and in the first session of the WM task compared to the last session of the DR/WM task ( $p = 0.013$ , Wilcoxon rank test), mirroring the drop in performance level and illustrating the increased difficulty of the task. These results reflect the prior analyses of the task performance, showing that animals learn the task and that introducing WM conditions affects the behaviour significantly, suggesting a difference in the task demands to the animals.

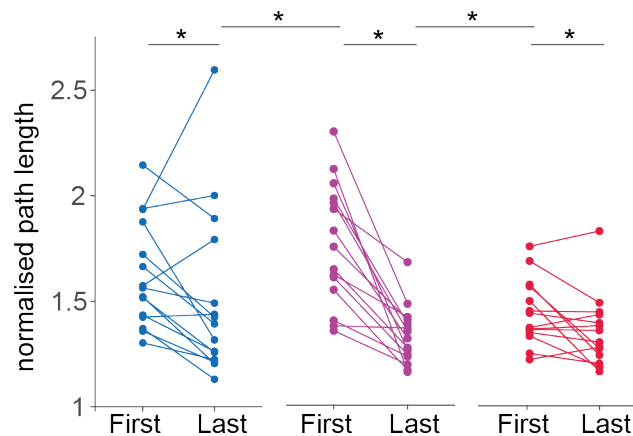


**Figure 12 | Mouse trajectories become more efficient throughout learning**

Mean normalised path length for each animal in the first and last session of each task type, with the DR task in blue, the DR/WM task in purple and the WM task in red. Wilcoxon signed rank test,  $*p > 0.05$ , ( $n_{DR} = 15$ ,  $n_{DR/WM} = 15$ ,  $n_{WM} = 14$ ).

*Preplanning in DR task is observable in movement trajectories*

The trajectories were analysed further to determine individual strategies and potential changes from DR to WM. The individual trajectories of mice throughout the test epoch can give details about the mice's strategy to solve the task. Here, the paths of the mice were plotted to visualise individual differences and the Fréchet distance (FD) was used to quantify these behavioural strategies. The FD describes the similarity of two curves by comparing the shortest distance between each point moving forward in time (**Fig. 6e**). It was used to compare each possible trial pair within and between conditions, inspired by Mosberger et al. (2024). When visualising the movement trajectories of mice during the DR task, 16 out of 18 mice already turned towards the smallest possible path in the direction of the correct test location after they pulled their head out of the reward trough (**Fig. 13a, mouse #1, traces**). Therefore, there is a large separation of the trajectories between the two DR conditions, with the difference between the FD between conditions and within conditions being 88.71 pixels (**Fig. 13a, mouse #1, heatmap**). This preplanning is only possible if the mouse has already planned its behavioural output before it saw the locations of the test stimuli. Interestingly, two mice solved the task by turning in the same direction in almost all trials (**Fig. 13b, mouse #2, traces**). These mice turned around first, and then, whilst being able to see the test locations, they either went toward the stimulus on the left or the right. Therefore, paths for the two different conditions diverged only a third through the arena, leading to a smaller separation of the trajectories in the two conditions. This effect was quantified using the difference between the FD between conditions and within conditions, which was only 48.55 pixels (**Fig. 13b, mouse #2, heatmap**).

The FD within the two DR conditions was consistently lower in all animals (mean: 71.72 pixels, SEM: 4.00 pixels), indicating that within a condition, the trajectories were conserved for each condition, and the animals optimised their path. In comparison, the FD difference between conditions was higher (mean: 132.71 pixels, SEM: 3.67 pixels), indicating the difference between the conditions. This effect was consistent and significant across all animals (**Fig. 13c**,  $p = 3.01 \cdot 10^{-7}$ ).

Visualising the movement trajectories in the test epoch in the DR further demonstrates that most animals pre-planned their choice before seeing the correct test location. They predicted the side of the correct test location, which indicates a shift from

## Behavioural results

maintaining the sample location information to planning the choice side. This is in line with general criticisms of DR tasks in operant chambers where animals were observed to use mediating behaviours, i.e. already turning towards the correct lever, and so minimising the energy needed to solve the task (Chudasama and Muir, 1997).

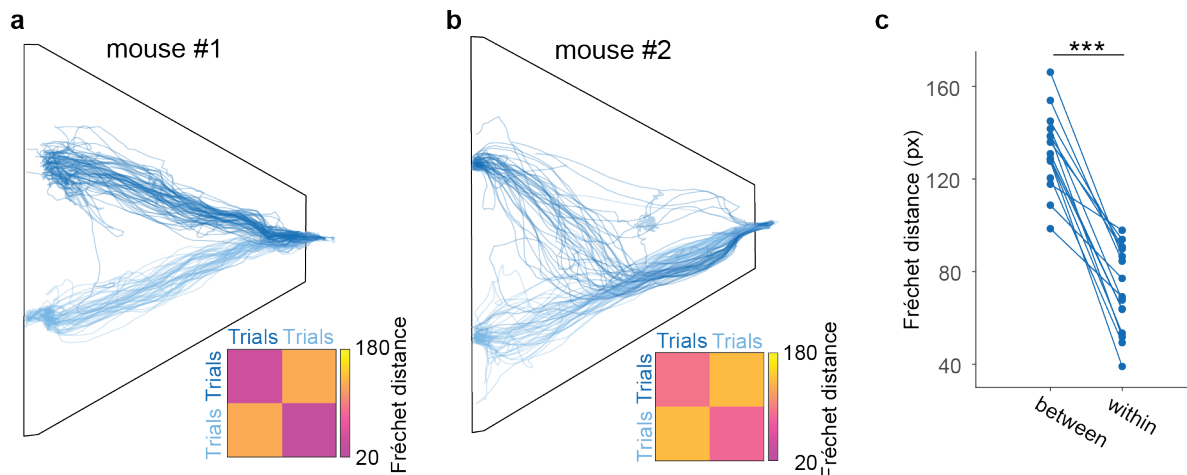


**Figure 13 | Mice preplan motor output to solve delayed response task**

**a/b** Example traces from test onset to test touch (test epoch) for two mice during the DR task. Shades of blue indicate trials with different sample locations, i.e. different conditions. Heatmap matrices show the Fréchet distances (FD) for within and between different conditions. **c** Mean FD for each animal on the last day of the DR task between and within conditions. Kruskal-Wallis test, \*\*\* $p < 0.001$ .

### *Mice change their strategy to adapt to working memory conditions*

In the DR/WM task, mice were confronted with two WM conditions, where they could not predict the correct test location from the sample stimulus location alone. In addition, two DR conditions were added to balance the sample and test locations and keep the animals motivated. The two DR conditions had the same window (middle) as the correct test location. This resulted in the difference between the FD within and between trials being very low in expert animals, e.g. 5.33 pixels for the animal shown in **Figure 14a (left)**. Across all animals, the average FD between DR conditions was  $67.78 \pm 3.35$  pixels (mean and SEM) and the average FD distance within conditions was  $57.97 \pm 2.95$  pixels (mean and SEM). Regardless, there was a small, albeit significant, difference of the FD between and within conditions (**Fig. 14b**,  $p = 0.044$ ). Visualising the trajectories of the WM conditions for an example expert animal

(**Fig. 14a, right**) shows that the animal turned the same way for both WM conditions, and only once it could see which windows were lit up, the paths diverged, comparable to the strategy of mouse #2 in the DR condition (**Fig. 13b**). This is also shown in the significantly bigger difference in the average FD between (115.64±3.63 pixels) and within (55.11±3.05 pixels) WM conditions (**Fig. 14c**,  $p = 3.01 \cdot 10^{-6}$ , Kruskal-Wallis test), indicating a divergence of the paths in the second half of the test epoch. However, this path divergence in the DR/WM task (**Fig. 14c**, average FD distance: 115.64±3.63 pixels) is smaller compared to the divergence of the conditions in the DR task (**Fig. 13c**, average FD distance: 132.71±3.67 pixels), and this effect is significant (**Fig. 14d**,  $p = 0.021$ , Kruskal-Wallis test). These results indicate that animals have to shift their strategy from using the most efficient path by already turning toward the correct test location, leading to a larger average FD distance between conditions, towards a strategy where they turn in the same direction in all conditions, leading to a smaller FD between the two WM conditions.

## Behavioural results

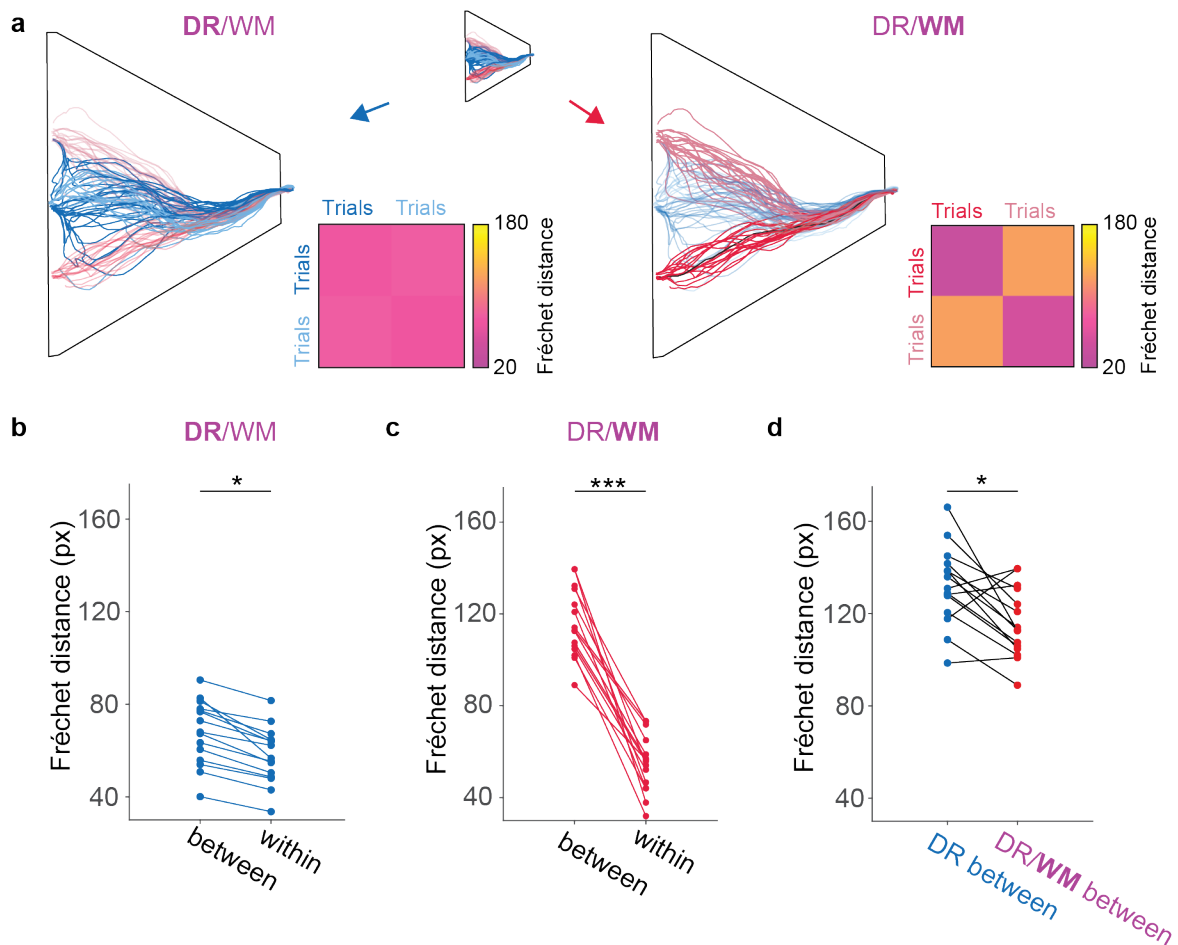


**Figure 14 | Mice change their strategy to adapt to WM trials**

**a** Example traces from test onset to test touch for one mouse during the DR/WM task, split by DR (blue shades) and WM (red shades) conditions. Heatmap matrices show the Fréchet distance (FD) within and between conditions for each trial type. **b/c** Mean FD between and within conditions for DR (b) and WM conditions (c).  $n = 15$ . **d** Mean FD during the DR task between conditions and the DR/WM task between WM conditions. Kruskal-Wallis, \* $p < 0.05$ , \*\*\* $p < 0.001$ .

In addition, the investigation of the FD distance throughout the test epoch (average across all animals in 400 ms non-overlapping windows aligned to the test presentation) showed that in the DR task, the curves of the two conditions diverge much earlier and stronger, compared to the WM conditions in the DR/WM task, even though the test locations (mid-right and mid-left) are the same (**Fig. 15**). Moreover, the divergence of the trajectories between DR and WM conditions in the DR/WM task can be seen in the second half of the test epoch (**Fig. 15**).

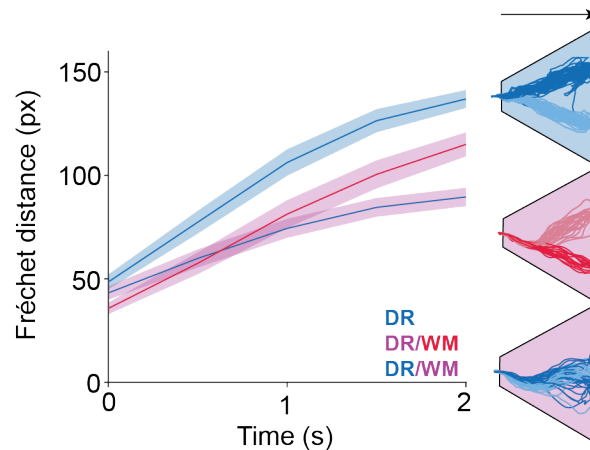


**Figure 15 | Fréchet distance throughout the test epoch of different task types**

Mean Fréchet distance and standard error of the mean calculated for each non-overlapping 400 ms window. Task and condition type are indicated by colour with the DR task in blue and the DR/WM task in purple. In the DR/WM task, DR and WM conditions can be differentiated by the colour of the line, with DR conditions in blue and WM conditions in red. Trials are aligned to test presentation (time = 0).  $n_{DR} = 13$ ,  $n_{DR/WM} = 15$ . Right: Traces for the epoch of one example mouse in DR (blue) and DR/WM (purple). The DR/WM task is split into DR (blue) and WM (red) conditions. The arrow indicated the direction of the movement of the example mouse through the arena, from timepoint 0 s (test presentation) until touching the touchscreen.

In summary, the in-depth analysis of the movement trajectories indicates that animals used different strategies to solve these two task types. Most mice were observed to use a preplanning strategy to solve the DR task, which can be compared to mediating strategies observed in operant boxes, where animals already turn toward the correct response location during the delay epoch (Chudasama and Muir, 1997). They shifted their strategy in response to WM conditions, where they could not predict the location of the correct test stimulus. The data demonstrate a behavioural difference between DR and WM tasks, as observed in the human subjects, suggesting an underlying difference in neuronal activity.

## Neuronal signatures

### *In vivo one-photon calcium imaging*

Chronic microendoscopic calcium imaging was used to investigate the hypothesised differences in neuronal activity between DR and WM tasks in pyramidal neurons of the prefrontal cortex. Neuronal signals were recorded four times throughout the training: Once immediately preceding the training protocol and once in an expert session of each task type. The calcium activity was then preprocessed using the CalmAn pipeline (Giovannucci et al., 2019) to determine the spatial footprint and activity of each potential unit throughout the session (**Fig. 16a**). Units could be detected in all analysed sessions ( $n_{\text{animals}} = 6$ ,  $n_{\text{sessions}} = 24$ ). However, units could not be registered across sessions satisfactorily, as the focal plane between sessions shifted slightly (**Fig. 16b**). This was due to the dental cement used during the adhesion of the baseplate changing its volume when fully dried and, thus, moving the baseplate slightly out of focus. Manually readjusting the focus back was not possible due to the small scale and inability to headfix the animal. Therefore, the following analysis considers the three expert sessions of the three task types individually. The signal-to-noise ratio and the spatial footprint consistency for all units were consistent across animals in each task type and across task types (**Fig. 16c/d**). The quality assessment of each potential unit was achieved by removing units where the natural logarithm of the signal-to-noise ratio was lower than the mean subtracted by the standard deviation (**Fig. 16c**), as well as units with a spatial footprint consistency lower than the mean subtracted by the standard deviation (**Fig. 16d**). In addition, all units were manually inspected, for spatial footprint shape, location and firing consistency and units not meeting set criteria were removed. In the end, a similar number of units was removed from each task type, indicating consistent data quality throughout all imaging sessions. In total, there were 450 accepted units in the DR task, 423 in the DR/WM task and 446 accepted units in the WM task. These populations were used for the following analysis below.

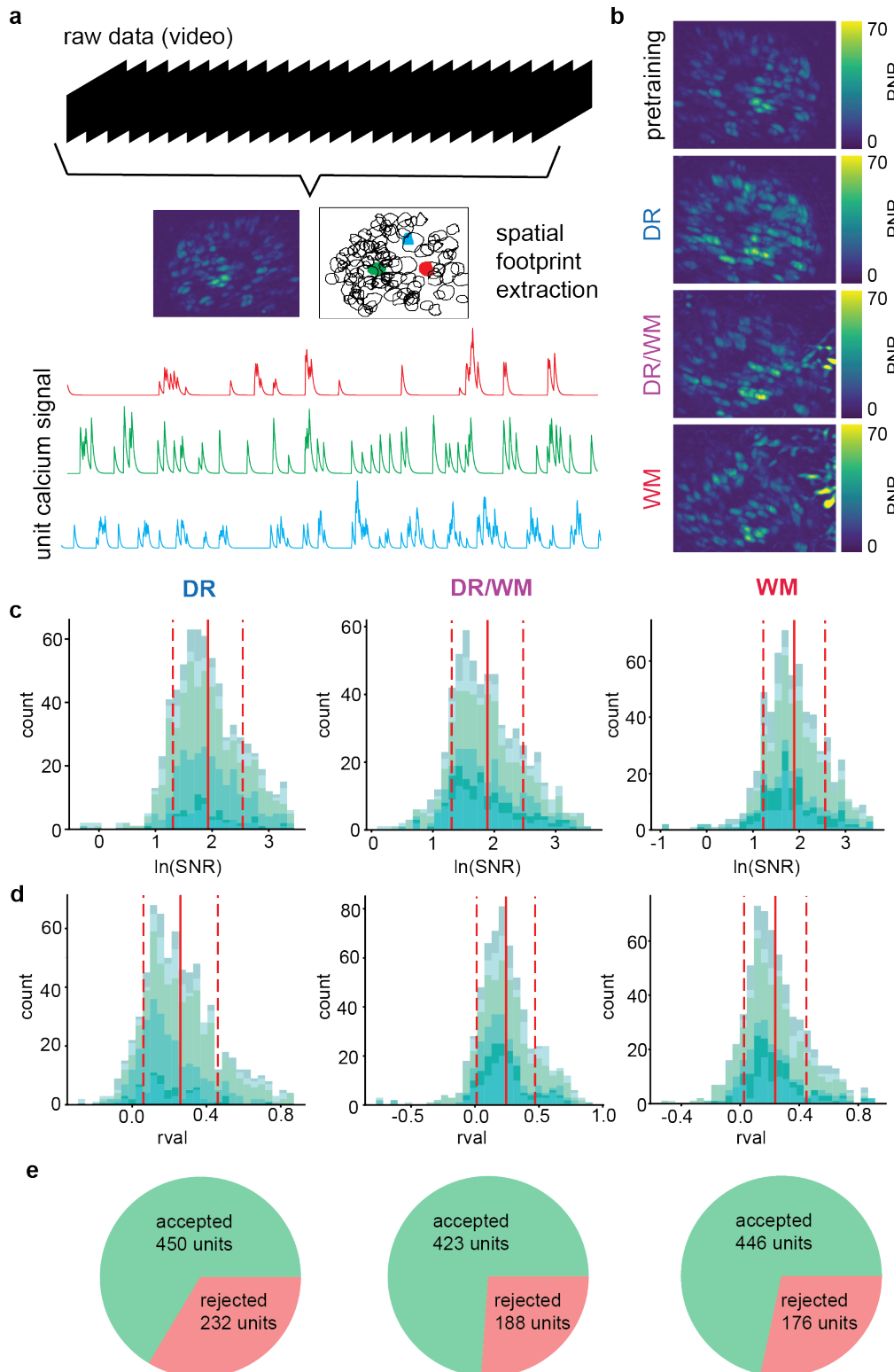


**Figure 16 | Preprocessing and quality assessment of recorded calcium signals**

**a** Signal extraction using the calcium imaging analysis pipeline (CalMan). Figure adapted from Giovannucci et al. (2019). **b** Peak signal-to-noise ratio of the four different imaging sessions in the same example animal. **c** Natural logarithm of the signal-to-noise ratio distribution of all detected units split by task types. Lines indicate the mean (full line)  $\pm$  one standard deviation (dotted lines). Different shades indicate different mice ( $n = 6$ ). **d** Spatial footprint consistency (rval) of all detected units split by task

## Neuronal results

type. Lines show the mean (full line)  $\pm$  one standard deviation (dotted lines). Different shades indicate different animals ( $n = 6$ ). **e** Percentage and absolute numbers of units rejected after  $\ln(\text{SNR})$  and  $r_{\text{val}}$  cutoff and manual quality assessment split by task type.

### *Individual prefrontal units are tuned to task parameters*

The behavioural task did not enforce trial progression so mice could move through the task structure at their own pace. As a consequence, trial epochs differed between individual trials. Therefore, each trial was separately aligned to the four key task events, namely: sample onset, sample touch, test onset and test touch (**Fig. 3**). Units were analysed based on their tuning to the sample locations, i.e. one of the five windows, the choice side, i.e. if the correct test stimulus was the right or left of the two shown test stimuli, and the trial outcome, i.e. correct and error trials.

Units with a clear separation of activity for different sample locations could be found in the sensory epoch, i.e. when the sample stimulus was present, but the mouse had not touched it yet, of all three task types (**Fig. 17a, d and g**). These units showed significant differences in normalised (z-scored) fluorescence between trials with differing sample locations (**Fig. 17b**:  $p = 2.33 * 10^{-43}$ , **e**:  $p = 1.98 * 10^{-20}$ , **h**:  $p = 3.09 * 10^{-94}$ , one-way ANOVA,  $*p < 0.01$ ). Therefore, the information about the sample location increased in these units above the significance level during the sensory epoch (**Fig. 17c, f and i**). In addition, examples of monotonic or summation coding with increased firing from left to right or vice-versa were found (**Fig. 17d/e**). Monotonic stimulus encoding has been described in prefrontal neurons before, for example, in monkeys comparing the vibration stimuli with different frequencies (Romo et al., 1999). Furthermore, examples for labelled-line coding, with peaked activity and preferentially encoding of one sample location (**Fig. 17g/h**). These labelled-line codes have also been shown for sample locations (Funahashi et al., 1989; Takeda et al., 2002) or numerosities (Nieder and Merten, 2007) in the prefrontal cortex of monkeys.

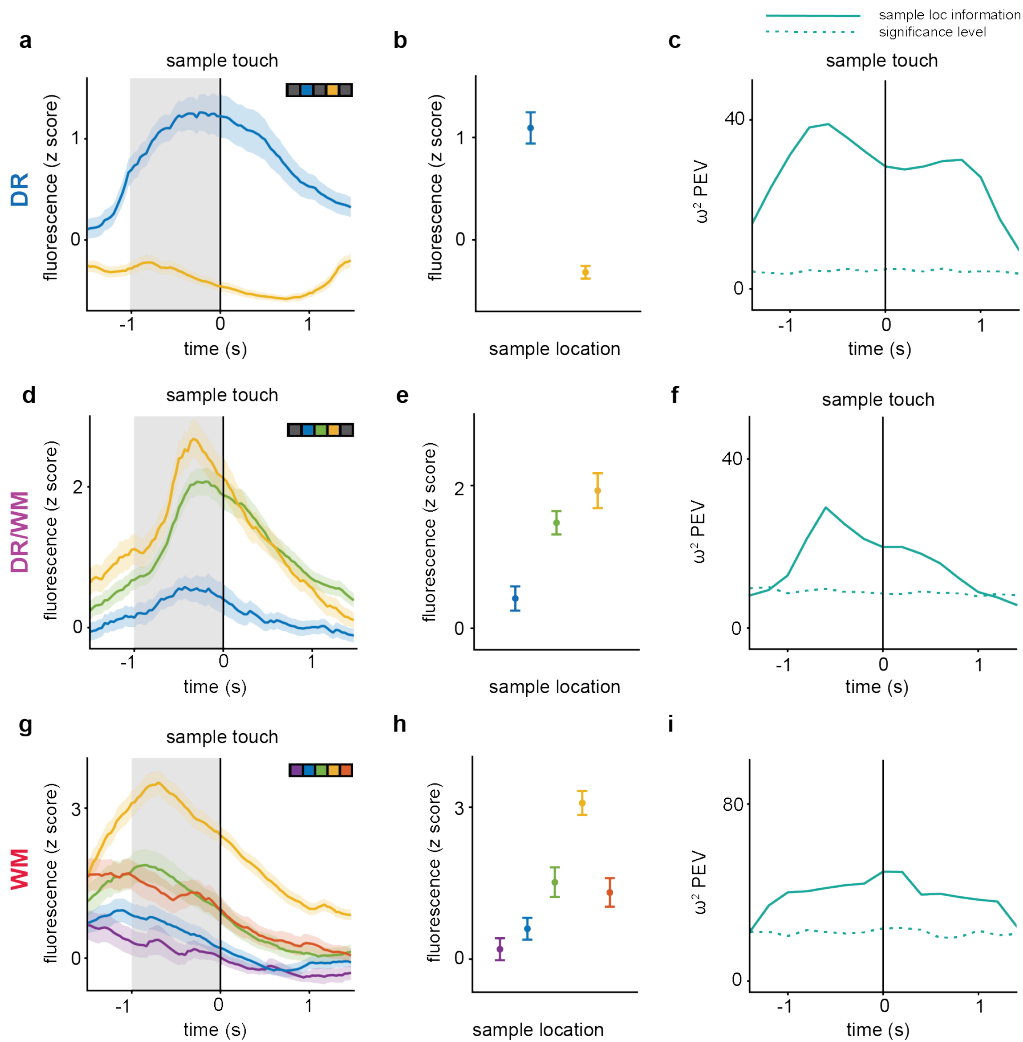


**Figure 17 | Sample location tuning in the sensory epoch of different task types**

**a** Average z scores and standard error of the mean (SEM) from one example unit in the sensory epoch (aligned to sample touch) of the DR task. Trials are split into groups by sample location. **b** Average z score and SEM (error bars) for the 1 s time window before sample touch (shaded area in **a**). **c** Percentage explained variance ( $\omega^2$ ) for traces in **a**. The significance level is the 99<sup>th</sup> percentile of the data shuffled 1000 times. **d-f** The same layout as in **a-c** for a different example unit in the DR/WM task. **g-i** The same layout as in **a-c** for a different unit in the WM task.

Units with a clear separation of activity for each sample location were also found in the delay epoch, i.e. after sample touch and before test presentation, of all three task types (**Fig. 18a, d and g**). These units had a significant difference in neural activity between the trials with differing sample locations (**Fig. 18b**:  $p = 2.69 \cdot 10^{-23}$ , **e**:  $p = 2.37 \cdot 10^{-62}$ , **h**:  $p = 1.70 \cdot 10^{-103}$ , one-way ANOVA,  $*p < 0.01$ ). This difference is also reflected in the amount of information about the sample present being above the significance level in these units (**Fig. 18c, f and i**). The percentage explained variance (PEV) also

## Neuronal results

illustrates the variability of the timepoint of peak sample location information present in the different units, with the information in one unit increasing toward the test stimuli presentation and peaking shortly after (Fig. 18c), peaking before the test presentation and decreasing toward test stimuli presentation (Fig. 18f) and the information about the sample location being present throughout the delay into the test epoch (Fig. 18i).

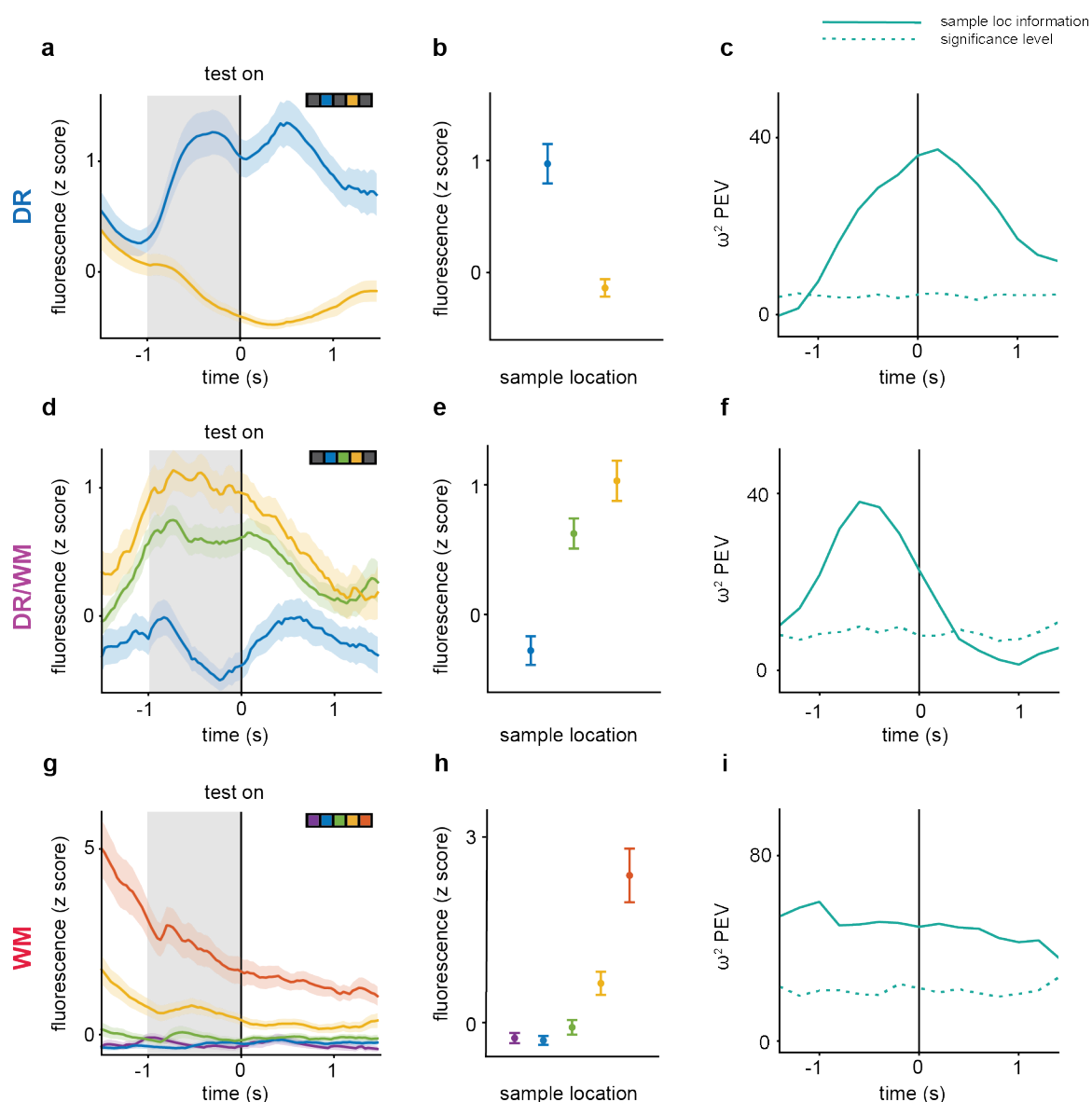


**Figure 18 | Sample location tuning in the delay epoch of different task types**

**a** Average z scores and standard error of the mean (SEM) from one example unit in the delay epoch (aligned to test onset) of the DR task. Trials are split by sample location. **b** Average z score and SEM (error bars) for the 1 s window before test on (shaded area in **a**). **c** Percentage explained variance ( $\omega^2$ ) for traces in **a**. The significance level is the 99<sup>th</sup> percentile of the data shuffled 1000 times. **d-f** The same layout as in **a-c** for a different example unit in the DR/WM task. **g-i** The same layout as in **a-c** for a different unit in the WM task.

Neurons in the prefrontal cortex respond to various different parameters, such as sensory input, rules, behavioural output, or a combination of these (Rigotti et al., 2013). Here, units with responses to sample location and choice side were also found. For example, units which were significantly responsive to one side of the touchscreen (**Fig. 19a/b**:  $p = 7.14 * 10^{-41}$ , one-way ANOVA), encoding some information about the sample location, although not the exact response window (**Fig. 19c**). In addition, units with mixed selectivity encoding of the sample location and the choice side conjunctively were found (**Fig. 19d/e**:  $p = 1.16 * 10^{-35}$ ). Mixed selectivity units have been described in the PFC before, and it has been proposed that these units pose a significant computational advantage by representing information about all task-relevant parameters and their combinations and simplifying local networks, compared to units with a pure-selective response (Rigotti et al., 2013). Here, the alignment to test presentation for a unit with mixed selectivity was shown. The unit's activity was higher in trials where the correct test stimulus is the right one compared to trials where the correct test stimulus was the left one. In addition, the unit's activity increased the further the correct test stimulus was to the right of the touchscreen, thus encoding the choice side in combination with stimulus location (**Fig. 19e**). Accordingly, the information about the choice side was high after the test presentation (**Fig. 19f**). Interestingly, the increase of information about the choice side increased before the test stimulus onset, even though the mouse cannot predict where the correct test location will be.

In summary, units tuned to sample location, choice, and a combination of both were found. Units also showed various tuning patterns, ranging from monotonic tuning towards a side of the touchscreen, over labelled-line coding for specific windows, to units showing mixed selectivity tuning patterns, encoding a combination of sample location and choice side.

## Neuronal results

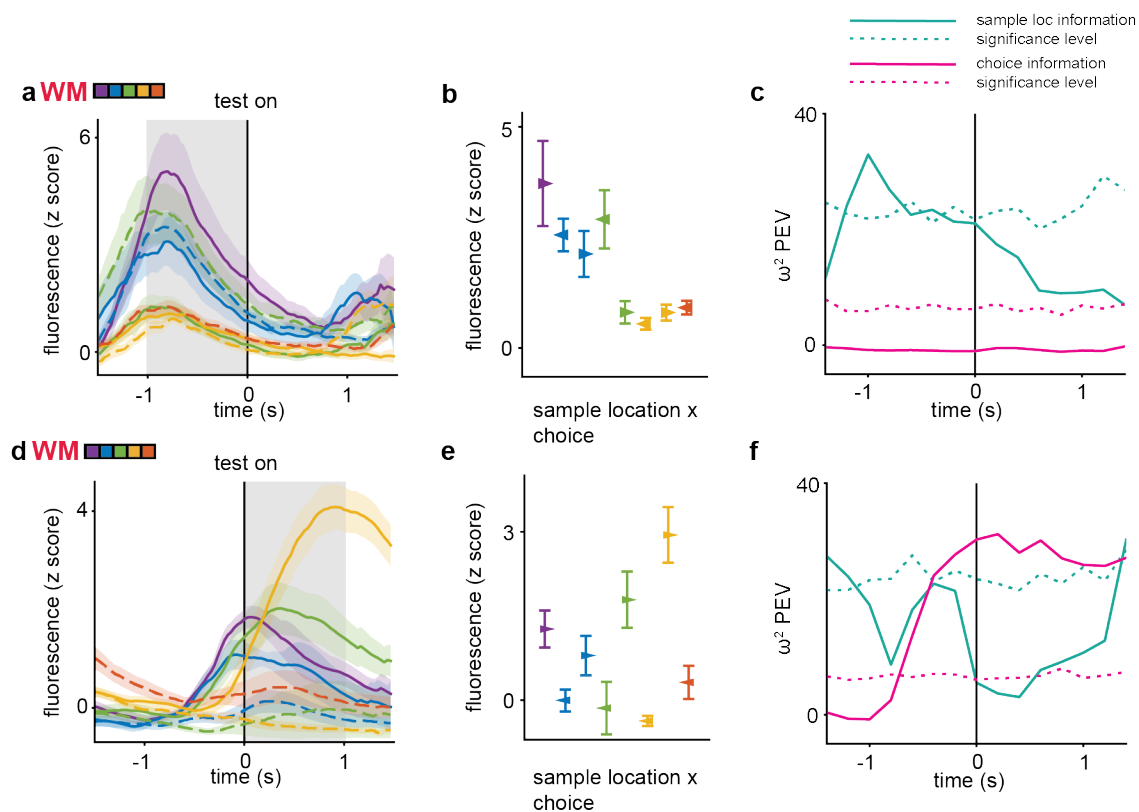


**Figure 19 | Monotonic coding and mixed selectivity in the mouse PFC**

**a** Average z score and standard error of the mean (SEM) from one example unit in the WM task aligned to test onset. Trials are split by sample location (colour) and choice side (left – dotted lines, right – solid lines). **b** Average z scores and SEM for the time window 1 s before the test onset (shaded pink area in **a**). **c** Percentage explained variance ( $\omega^2$ ) by sample location (turquoise) and choice side (pink). The significance level is the 99<sup>th</sup> percentile of the data shuffled 1000 times. **d-f** The same layout as in **a-c** for a different example unit in the WM task.

### *Fraction of units tuned to sample location is affected by task type*

DR and WM tasks have diverging cognitive demands and, thus, should show differences in neuronal activity (**Fig. 1b and d**). The number of units significantly tuned to sample location, choice side and trial outcome was quantified (one-way ANOVA,  $p < 0.01$ ) for a sliding window of 400ms length, moved in 200ms steps for all four alignments. The number of significantly tuned units increased during the sample presentation for all three task types. However, the largest and steepest increase was seen in the WM task, with the peak at 25%, compared to the peak in the DR task at 14% (**Fig. 20a**). The number of units significantly tuned was maintained throughout the delay again with a larger number in the WM task compared to the DR task (17%

and 8%, respectively, **Fig. 20a**). Notably, the number of significantly tuned units in the DR task increased sharply before the end of the delay and presentation of the test stimuli (**Fig. 20a**). This could indicate that the mice recall the sample location in preparation of the behavioural choice. However, due to the task design, in the expert sessions of the smallest separation level of the DR task, only two different conditions were used (**Fig. 4b**, third row), which meant that separating trials by sample location produced the same groups as separating them by choice side, which makes it impossible to differentiate between units tuned to sample location or choice side (see below, **Fig. 22**). Therefore, the increase can also be interpreted as an increase in units tuned to the choice side, pre-planning the behavioural output. During the test epoch, the fraction of units tuned to sample location decreased in all three task types (**Fig. 20a**). Notably, these results are comparable to studies in rats in an operant spatial delayed alternation task, where the number of neurons in the mPFC responsive to choice was found to be comparable with below 10% of responsive neurons during the delay and over 20% just before the choice became available (Horst and Laubach, 2012).

The fraction of units significantly tuned to the choice side also increased only slightly in the sensory epoch for all three task types (DR: 14%, DR/WM: 6%, WM: 6%, **Fig. 20b**). Importantly, the DR curve, which showed a peak at 14%, is the same curve for fraction tuned units for sample location and choice side. During the delay epoch, with about 8% of units being tuned in the DR and DR/WM task and about 5% in the WM task, the fraction of units stayed relatively stable for all three task types (**Fig. 20b**). The fraction of tuned units then increased for all three task types prior to test stimuli presentation. This effect was the strongest in DR and decreased in DR/WM and WM (peaks at 28%, 18%, and 13%, respectively), possibly due to the animal making a prediction or the additional DR conditions present in all three task types. Finally, error trials were analysed in search of units that were significantly selective for trial outcome (correct vs. error). The fraction of units selective for trial outcome increased strongly after the test presentation and peaked at 30% (DR), 43% (DR/WM) and 41% (WM) shortly after touching the test stimulus (**Fig. 20c**). Unexpectedly, selectivity increased *before* the mice touched the test stimuli. This result could be due to the neuronal representation of choice being disrupted in error trials, leading to the mice making the wrong choice. It also illustrates that the selectivity is not due to the presence or absence of the water reward.

## Neuronal results

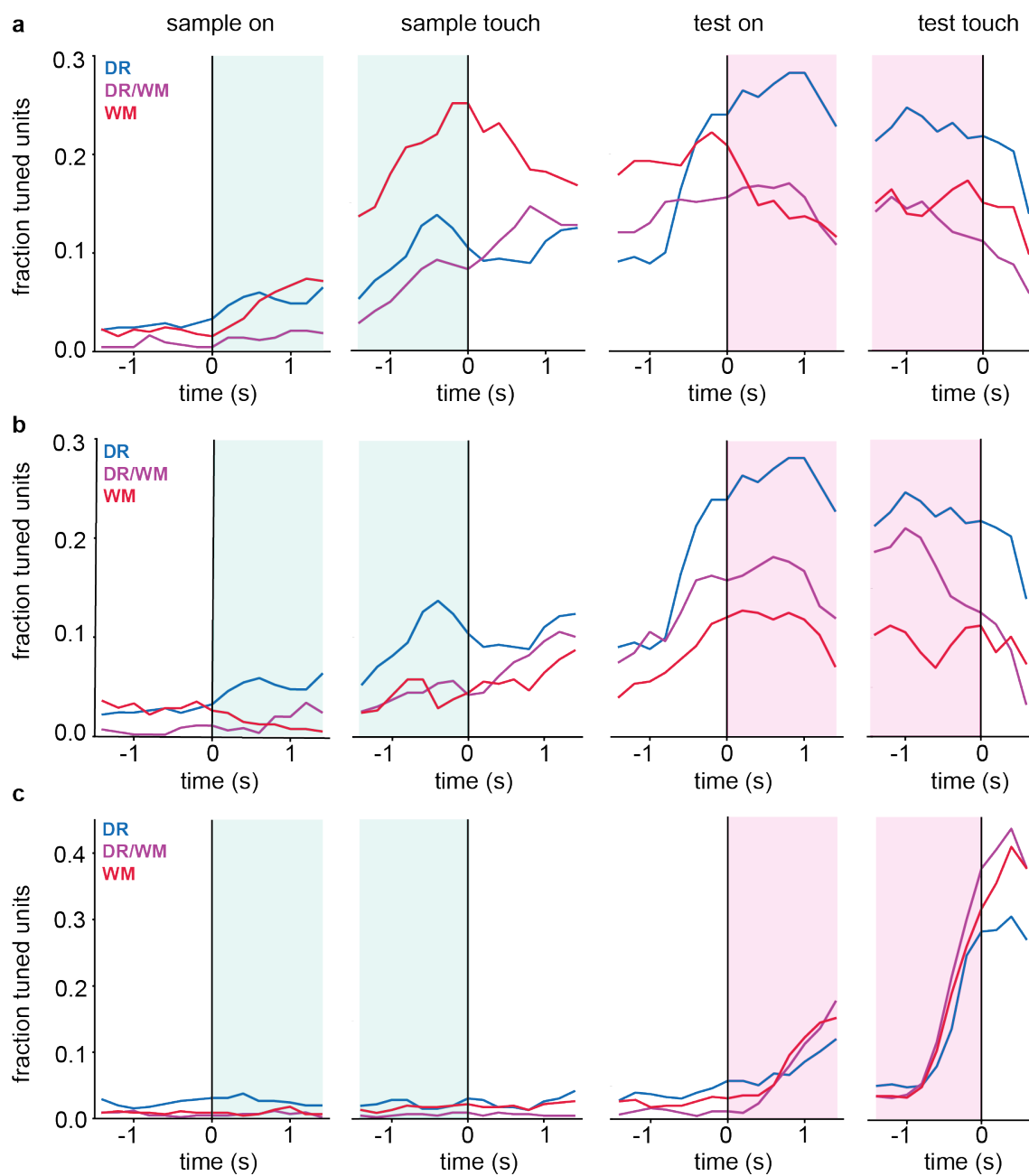


**Figure 20 | Fraction of units tuned to sample location and choice side depends on task type**

**a** Fraction of units significantly tuned to sample location at the four trial alignments of the three task types. **b** The same layout as in **a**, but with units significantly tuned to the choice side of the correct test stimulus, i.e. right or left. **c** The same layout as in **a**, but with units significantly tuned to the trial outcome, i.e. correct or error. Shading indicates time epochs where sample and test stimuli are visible. Moving window ANOVA,  $p < 0.01$ , window size 400 ms, step size 200 ms. Number of units for each task type in all plots: DR:  $n_{\text{units}} = 450$ , DR/WM:  $n_{\text{units}} = 423$ , WM:  $n_{\text{units}} = 446$ .

*Neuronal populations maintain information about task variables*

Not all neurons encoded the information about the sample location, choice side or trial outcome equally strongly. Therefore, the average percentage explained variance (PEV,  $\omega^2$ ) was calculated across all accepted units (**Fig. 21**). The information about the sample location increased earlier and more strongly during the sensory epoch in the WM task compared to the two other task types (**Fig. 21a**). It was maintained at levels more than twice as high compared to either the DR or DR/WM task during the delay, with average ( $\pm$ SEM) PEV in the 1 s window before sample touch being  $6.07 \pm 0.50$  in the WM task compared to  $1.71 \pm 0.19$  in the DR task and  $1.52 \pm 0.20$  in the DR/WM task. In the DR task, the information about the sample location showed a similar low peak in the sensory epoch and a higher peak in the test epoch after the test presentation (**Fig. 21a**). Notably, the peak in the WM task was before test presentation, while in the DR task it only peaks afterwards. This shift could be due to the decoding of sample location from WM in preparation for comparison with the test stimuli, while in the DR task, it could also be the planning of the motor output. This re-emergence of information before the test has been described before, for example, in monkeys, where the information about the sample increases in neurons before the distractor presentation, when the monkey must make a comparison (Nieder and Jacob, 2014).

The information about the choice side stayed relatively low until just before the test stimulus presentation in the DR/WM and WM tasks (**Fig. 23b**), with the average ( $\pm$ SEM) PEV in the 1 s window after the sample touch being  $1.31 \pm 0.17$  in the DR task,  $0.82 \pm 0.13$  in the DR/WM task and  $0.75 \pm 0.13$  in the WM task. However, there was an increase in choice information in the units during the sensory epoch, most likely since sample location and choice side are not separable in DR. Choice was most strongly encoded during the test epoch in the DR task, followed by the DR/WM task and finally the WM task (**Fig. 23b**), with the average ( $\pm$ SEM) PEV in the 1 s window after test presentation being  $4.10 \pm 0.37$  in the DR,  $2.48 \pm 0.27$  in the DR/WM and  $1.62 \pm 0.21$  in the WM task.

Finally, information about the trial outcome only rose after the test presentation equally in all three task types (**Fig. 23c**), with the average ( $\pm$ SEM) in the 1 s window before the test touch being  $2.53 \pm 0.31$  in the DR task,  $3.41 \pm 0.40$  in the DR/WM task and

## Neuronal results

2.62±0.31 in the WM task. These increases showed a difference in neural activity between correct and error trials about 1 second after the test presentation when the mouse likely had already touched the chosen test stimulus. In summary, this analysis confirms a difference in information about task variables in the different task types, as hypothesised. Notably, the DR/WM task seems to be an intermediate state between DR and WM tasks, which reflects the fraction of DR and WM conditions in the task types.

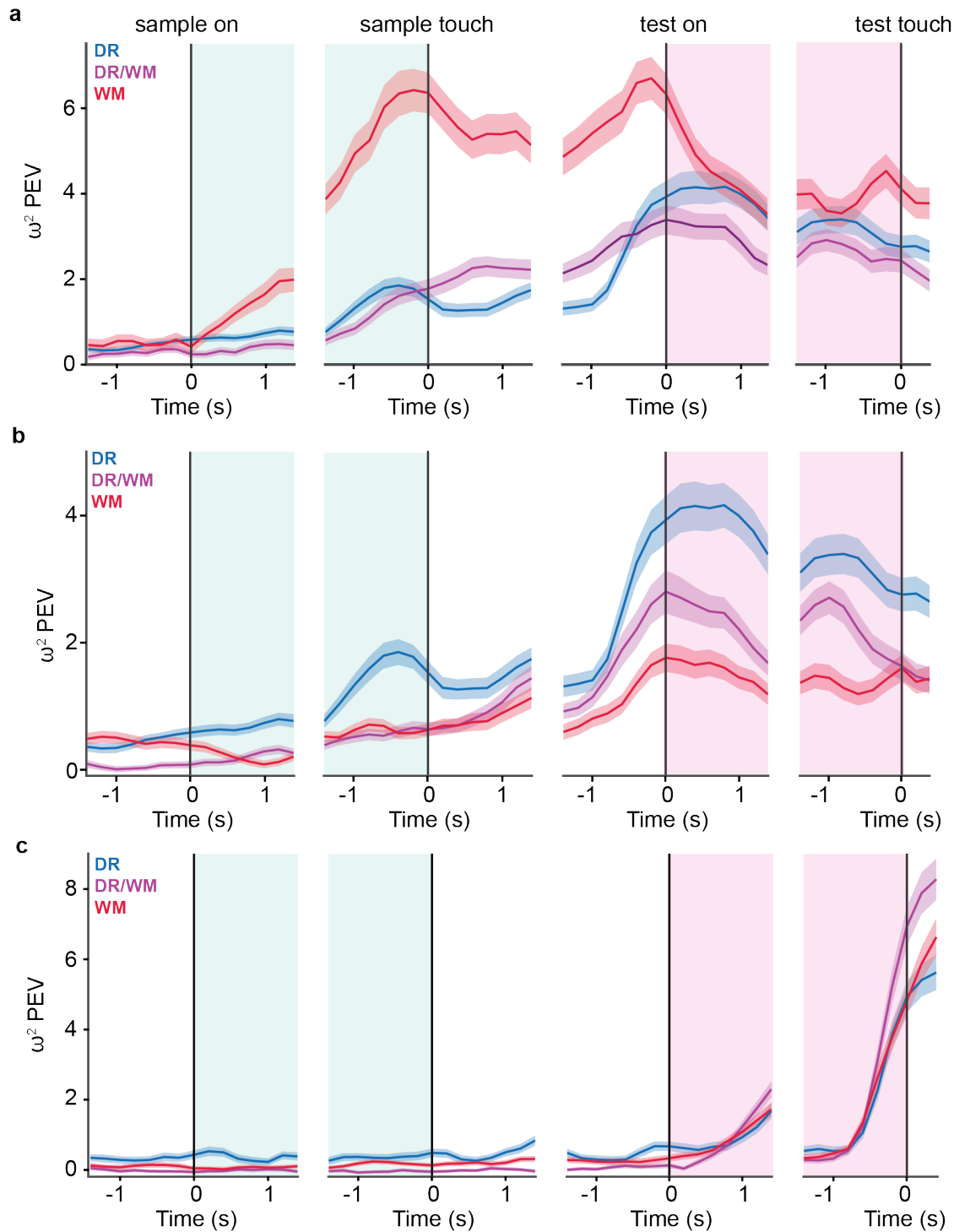


**Figure 21 | Sample location information is encoded earlier and at a higher level in WM**

**a** Average percentage explained variance ( $\omega^2$ ) and standard error of the mean (SEM) for all units for sample location at the four trial alignments of the three task types calculated for a moving window of 400 ms, with a step size of 200 ms. Shaded area indicates trial epochs where the sample or test stimuli were visible. **b** The same layout as in **a**, but for choice side of the correct test stimulus, i.e. right or left. **c** The same layout as in **a**, but for trial outcome, i.e. correct or error trials. Number of units for each task type in all plots: DR:  $n_{\text{units}} = 450$ , DR/WM:  $n_{\text{units}} = 423$ , WM:  $n_{\text{units}} = 446$ .

## Neuronal results

### *Single unit tuning throughout the trial*

As described above, the task design of the DR task prohibited the separation of units tuned to sample location and choice side, as they would be divided into the same groups of trials. Therefore, the firing patterns of single units throughout the trial were examined in more detail, specifically for units tuned in the sensory and the test epoch. An example unit tuned to the mid-left window (**Fig. 22d, green outline**) is shown. The unit fired during the sensory epoch of the trial, where the correct sample location is mid-left (blue), but not in the test epoch. Additionally, the unit fired when the mouse touched the mid-left touchscreen window during the test epoch, i.e. trials with the sample location in the mid-right touchscreen window (yellow), but not in the sensory epoch of these trials (**Fig. 22c/d**). This pattern could indicate that the second peak in tuned units before the test presentation is not due to units tuned to the sample location reactivating. The information about the sample location increased during the sensory epoch and was maintained throughout the beginning of the delay epoch but then decreased. It only increased again after the test stimulus onset (**Fig. 22e**). Quantifying the number of tuned units in these DR task epochs showed that more than twice as many units were significantly tuned to the test epoch only compared to the sample epoch only or both epochs (test epoch only: 71 units, sample epoch only: 27 units, both epochs: 33 units, **Fig. 22a**). As the mouse can predict the correct test location from the sample location alone, both are known after the presentation of the sample location and cannot be differentiated in units that only fired in the sample or the test epoch. However, units that fired in both epochs can be further differentiated. Importantly, they can be separated into four groups based on which touchscreen window they are tuned to (left or right) in which epoch (sample or test). More units were tuned to the same touchscreen window in the sample and test epoch (right: 16 units, left: 9 units, **Fig. 22b**) compared to different windows (left-right: 5 units, right-left: 3 units, **Fig. 22b**).

Together, this could indicate that the units in the sensory epoch only and in the sensory and test epoch code for a specific touchscreen window rather than the choice of the mouse. Similar results were found by Takeda et al. (2002), who showed that most neurons responsive to a sample location in the oculomotor delayed response task in monkeys were tuned to the same location in the response epoch.

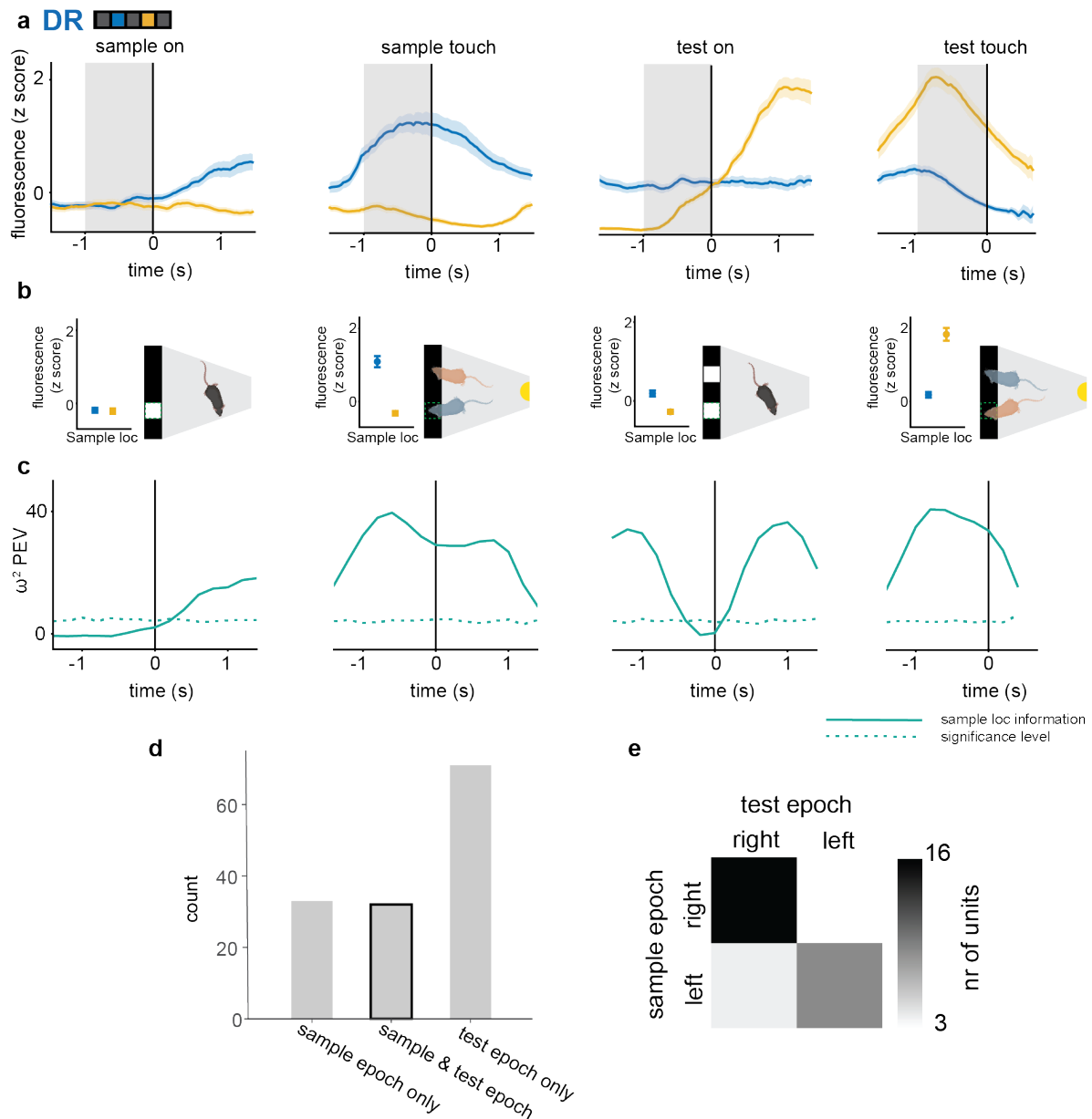


**Figure 22 | DR task units tuned to the same location in sample and test epoch**

**a** Average fluorescence (z scored) and standard error of the mean (SEM) of one example unit tuned to a location within the arena (green dotted line square in **b**) aligned to sample onset, sample touch, test onset and test touch (left to right) in the DR task. Trials are divided by sample location (blue: mid-left window, yellow: mid-right window). **b** The graph on the left shows the average fluorescence and SEM for the shaded areas in **a** for each alignment. The diagram on the right shows an exemplary mouse location at the alignment point. Blue and yellow mice indicate the differing locations in the two sample locations. The location when the unit in **a** is most responsive is indicated with a green dotted square. **c** Percentage explained variance ( $\omega^2$ ) for each alignment of the unit in **a**. The significance level is the 99<sup>th</sup> percentile of the data shuffled 1000 times. **d** Number of units significantly tuned to sample location 1000 ms before sample touch or test touch (grey shaded area in **a**), separated by units tuned in sample epoch only, test epoch only and sample and test epoch. ANOVA,  $p < 0.01$ . **e** All units significantly tuned

## Neuronal results

to both sample and test epoch (highlighted bar in **d**), split by if they are tuned to the left (blue) or the (yellow) side of the touchscreen during the sample epoch and the test epoch.

In the WM task, the differentiation between sample location and choice side is possible, enabling the investigation of sample and choice tuning progression throughout the trial. An example unit encoding a specific response window is shown in **Fig. 23a**. The unit was tuned monotonically to the right side of the touchscreen (red). This tuning pattern can be seen in the sensory epoch (**Fig. 23a/b**, aligned to sample touch) and during the test epoch (**Fig. 23a/b**, aligned to test touch), where the condition with the correct test stimulus at the right corner window has the highest firing rate (**Fig. 23b**, yellow, triangle pointing right). This unit is comparable to the unit shown in **Fig. 22a-c**, where the location of a specific touchscreen window causes the highest firing of the unit. In contrast to the unit shown in **Fig. 22a-c**, however, the information about the sample location is maintained throughout the entire delay into the test epoch without dipping around the test presentation (**Fig. 23c**).

The example unit in **Fig. 23d-f** was also monotonically tuned to the right corner touchscreen window during the sensory epoch (red). During the test epoch, however, this unit codes for choice (**Fig. 23d-f**). The information about the sample location increased during the sensory epoch. However, it was not maintained during the delay, whereas the information about the choice side increased shortly before the test presentation. The increase seems to be earliest in trials where the sample location is the left corner touchscreen window (purple), followed by the middle left (blue), middle (green) and middle right (yellow). In the trials with the sample location in the left corner (purple), the mouse can predict that the correct test will be to the right of the sample stimulus. In contrast, in the other conditions, even though it cannot know the correct test location, it might predict it to be on the right side of the touchscreen if the sample is on the left side of the screen. In summary, there are different ways in which units in the prefrontal cortex encode sample information and choice, with some encoding sample location during the sample and test presentation and others maintaining sample location information throughout the delay.

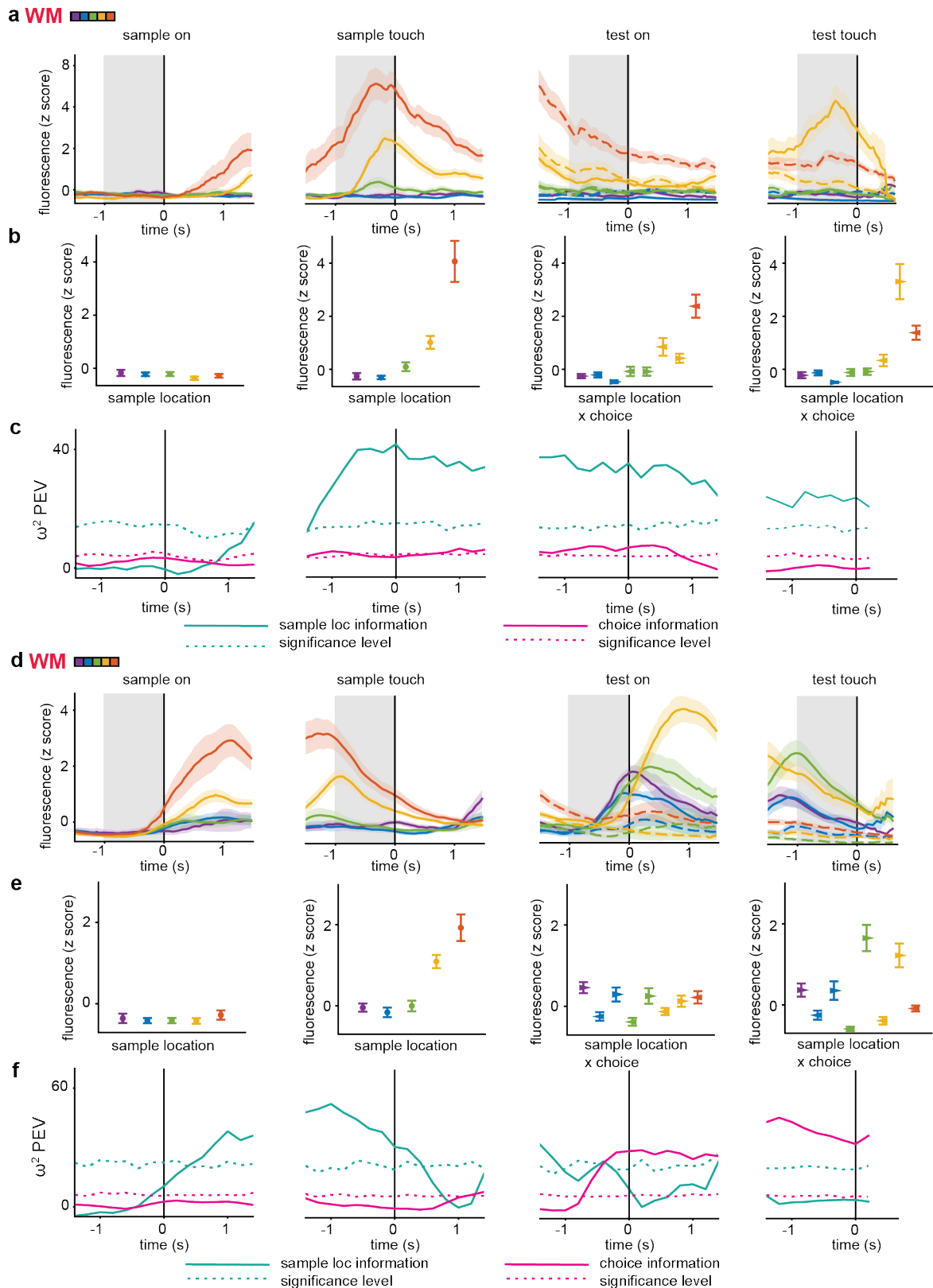


**Figure 23 | Example units tuned to sample location and choice side in WM task**

**a** Average z scores and standard error of the mean (SEM) for one example unit aligned to four trial alignments (sample onset, sample touch, test onset, test touch). Colours indicate sample location and dotted and solid line indicate the side of the correct test stimulus side, i.e. left or right. **b** Average z score

## Neuronal results

and SEM for the shaded area in **a**. **c** Percentage explained variance ( $\omega^2$ ) for the same unit as in **a**, aligned to the four trial alignments, calculated for a 400 ms time window moved stepwise by 200 ms. The significance level shows the 99<sup>th</sup> percentile of the shuffled signal (dotted line). **d-f** The same layout for a different unit in the WM task with a different firing pattern.

### *Prefrontal encoding of sample location and choice in individual units*

It has been shown that units responsive to multiple task parameters, called mixed selectivity units, pose a computational advantage when explaining cognitive processes (Rigotti et al., 2013; Tye et al., 2024). Mixed selectivity units are determined by their tuning to multiple task parameters, such as different features of the sample, e.g. colour, motion, grating, choice location and context (Mante et al., 2013; Mansouri et al., 2006; Parthasarathy et al., 2017). These have also been identified here (**Fig. 23d-f**) and in other mouse studies (Reinert et al., 2021).

Therefore, I investigated the individual units encoding the sample location and choice side during the task further. The percentage explained variances (PEV,  $\omega^2$ ) for the sample location during the sensory epoch was compared to the choice side encoding during the delay epoch for each unit (**Fig. 25a-c**). Units encoding the sample location during the sensory epoch (DR: 72 units, DR/WM: 38 units, WM: 58 units) and the choice during the delay (DR: 134 units, DR/WM: 81 units, WM: 49 units) were found in all three task types, with a small number of units encoding both (DR: 36 units, DR/WM: 12 units, WM: 13 units). However, most units in all three task types show either information coding for the sample location or the choice side. Notably, there were more units encoding the choice during the delay epoch in the DR task (**Fig. 25a**) compared to the WM task, with more units encoding the sample location (**Fig. 25c**). This is in line with the hypothesis that in the DR task choice information is encoded in the delay, which is not possible in WM conditions. In summary, low numbers of units with mixed selectivity were found in the prefrontal cortex during all three task types.

Next, I determined if units strongly encoded sample location, also strongly encoded choice or if they were encoded by non-overlapping, sparse populations. Units were defined as strong coders if their PEV ( $\omega^2$ ) was above two standard deviations of the population (Lin et al., 2023). In the DR task, 13 units strongly encoded sample location (**Fig. 25d**, left), of which 7 units also encoded choice. Furthermore, 19 units encoded

choice strongly (**Fig. 25d**, right), of which 10 units also encoded the choice. Similar numbers of units strongly encoding sample location were observed for DR/WM (**Fig. 25e**, left, 8 units) and WM tasks (**Fig. 25f**, right, 13 units), of which 3 and 7 units, respectively, also encoded choice during the delay. Units strongly encoding choice in the DR/WM (**Fig. 25e**, right, 9 units) and WM (**Fig. 25f**, right, 6 units), of which 1 and 2 units, respectively, were also encoding sample location. Fewer units strongly encoded the choice during delay in the DR/WM and WM tasks, reflecting the animal's inability to predict the correct test location in most conditions. Overall, less than 4% of all detected units strongly encode the sample location (DR: 3.10%, DR/WM: 1.89%, WM: 2.91%), and less than 5% strongly encode the choice (DR: 4.52%, DR/WM: 2.13%, WM: 1.35%). Sparsity is an efficient approach to encode information (Levy and Baxter, 1996) and has been shown to be involved in sensory processing in sensory (Gauld et al., 2024; Newsome et al., 1989) as well as prefrontal cortices (Lin et al., 2023).

## Neuronal results

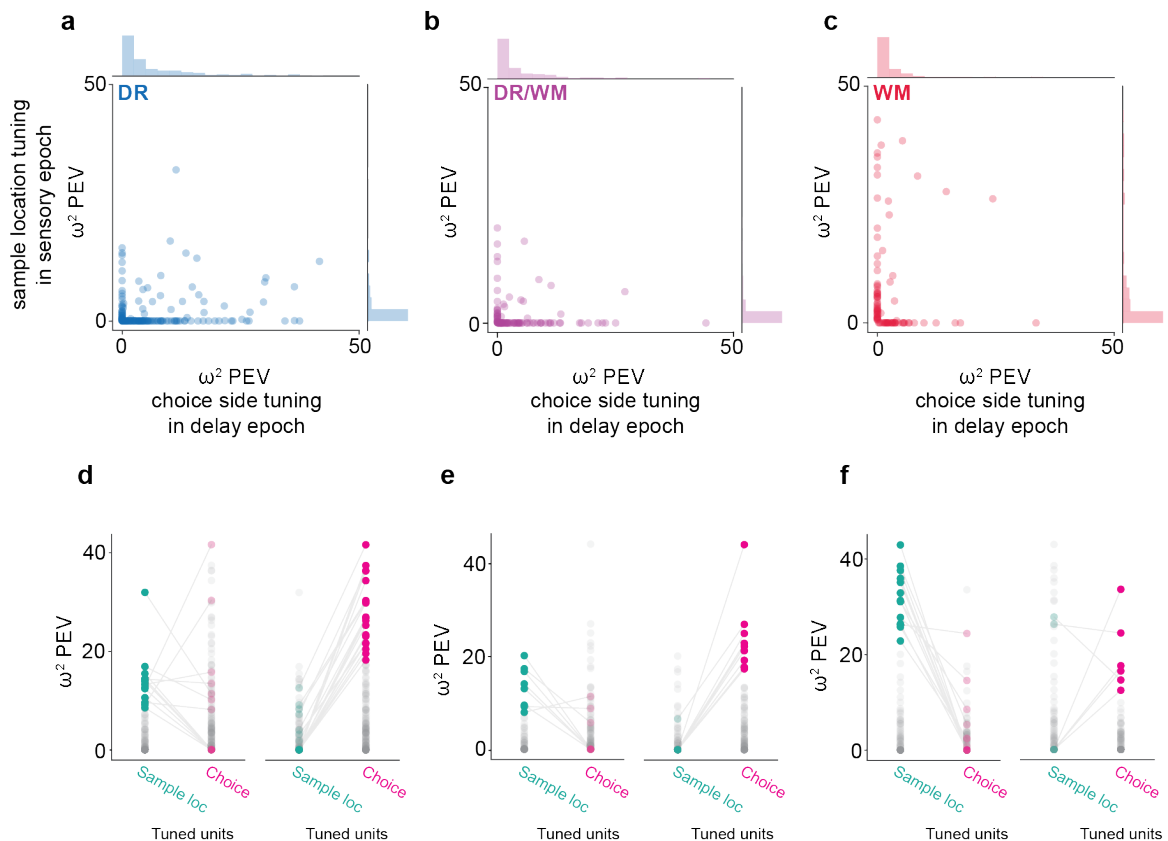


**Figure 24 | Units are tuned to either sample location or choice side**

**a-c** Average percentage explained variance ( $\omega^2$ ) to choice side in the 1 s time window after test onset (x-axis) plotted against sample location in the 1 s time window before sample touch (y-axis) for each unit in the DR (**a**), the DR/WM (**b**) and the WM (**c**) task. **d** Percentage explained variance ( $\omega^2$ ) plotted for each unit separately for sample location and choice side tuning. Strongly tuned units defined as above two standard deviations over the mean for sample location are coloured with their corresponding choice side value (left graph) and for choice side with their corresponding sample location value (right graph) in the DR task. **e** The same layout as in **d**, but for the DR/WM task. **f** The same layout as in **d**, but for the WM task.

### *Temporal dynamics of population coding*

Principal component analysis (PCA) was used to determine how sample locations, choice sides and trial outcomes were represented in the neuronal population throughout the trial. Due to the variable length of individual trials and trial epochs, a PCA was performed for each alignment in each of the three task types. However, this approach comparing of the principal components between alignments difficult, as they are in different coordinate systems and cannot be directly compared.

The trajectories for the sample location in the DR task (**Fig. 25a**) were parallel to each other during sample presentation until the sample touch (**Fig. 25a**, block dot, first two graphs), from where the separation continuously grew during the delay epoch (**Fig. 25a**, third graph). This separation was not observed in the alignment to test touch (**Fig. 25a**, fourth graph). The first three PCs explained most of the variance across all four alignments (sample on: 73%, sample touch: 59%, test on: 62%, test touch: 78%). During the DR/WM and WM task (**Fig. 25b-c**), trajectories were arranged in the order of the response windows. Here, the first three PCs explained a lower percentage of the variance (DR/WM: sample on: 64%, sample touch: 55%, test on: 56%, test touch: 65%; WM: sample on: 49%, sample touch: 43%, test on: 47%, test touch: 58%). These results confirm that locations close to each other on the touchscreen were encoded with more similar neuronal representations.

## Neuronal results

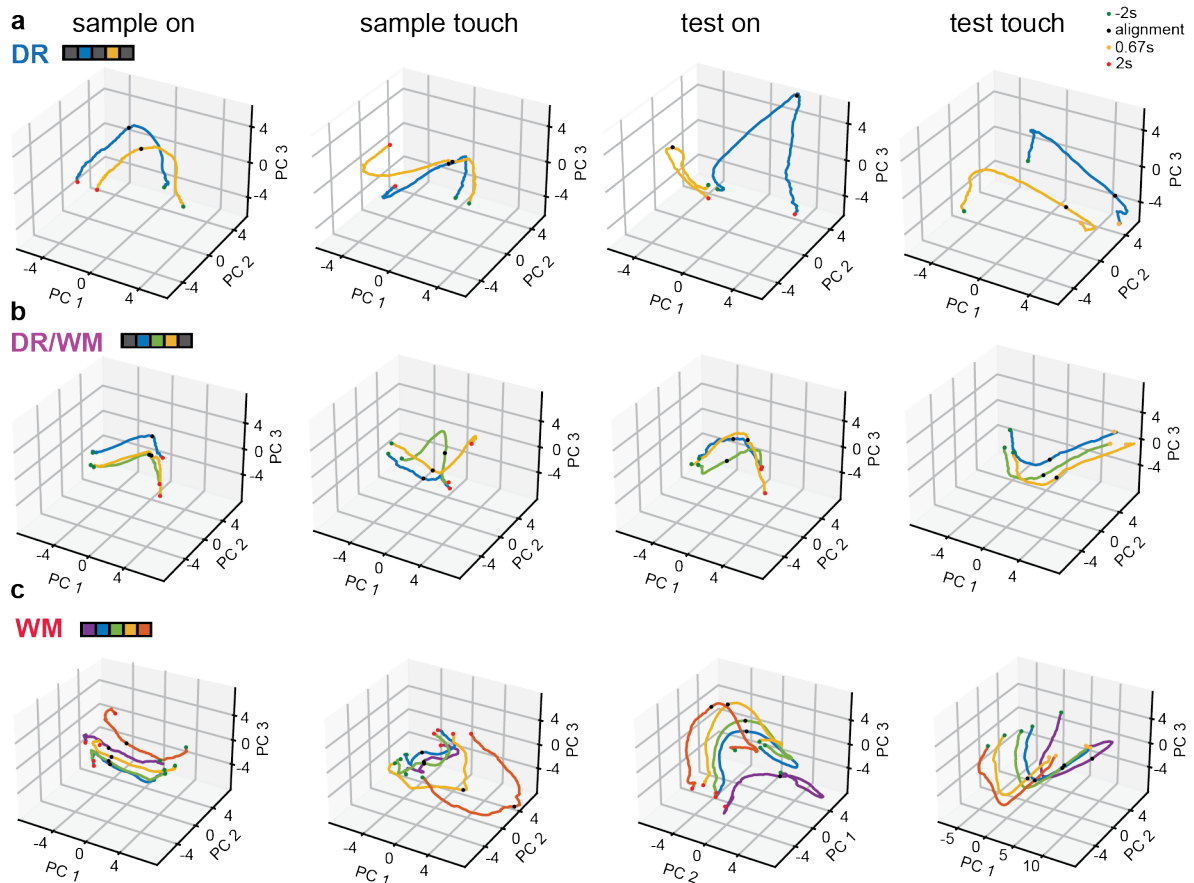


**Figure 25 | Neuronal population trajectories for sample location in different task types**

**a** Principal component analysis (PCA) describing neuronal population activity by sample location (colours) in the DR task. The first three principal components are plotted for each trial alignment (sample onset, sample touch, test onset, test touch). The alignment time point is indicated with a black dot. The start and ending points of the curve are the time points 2 s before and after the alignment (green and red). In the case of the alignment to the test touch, the endpoint is 0.67 s after the alignment (orange). The sample plots are shown for the DR/WM (**b**) and WM (**c**) task.

PCA was also performed for the choice side. In the DR task, the trajectories for choice side (**Fig. 26a**) are equivalent to the trajectories for the sample location seen in **Fig. 25a**. In the DR/WM and WM task (**Fig. 26b/c**), this effect is less pronounced. Here, the first three PCs explained most of the variance (DR/WM: sample on: 75%, sample touch: 70%, test on: 71%, test touch: 75%; WM: sample on: 72%, sample touch: 61%, test on: 70%, test touch: 74%).

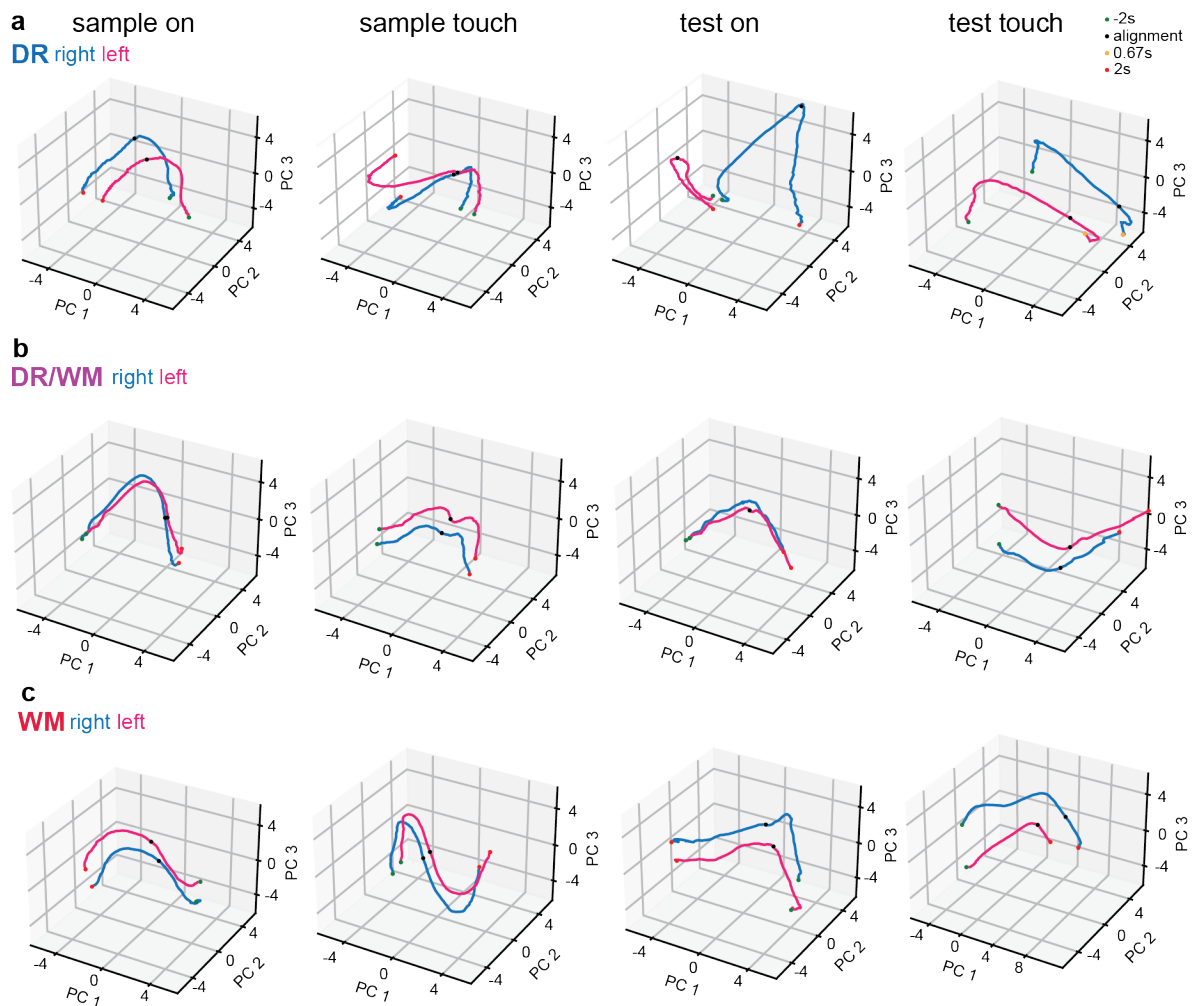


**Figure 26 | Neuronal population trajectories for choice side in different task types**

**a** Principal component analysis (PCA) describing neuronal population activity by choice side (right: blue, left: pink) in the DR task. The first three principal components are plotted for each trial alignment (sample onset, sample touch, test onset, test touch). The alignment time point is indicated with a black dot. The start and ending points of the curve are the time points 2 s before and after the alignment (green and red). In the case of the alignment to the test touch, the endpoint is 0.67 s after the alignment (orange). The sample plots are shown for the DR/WM (**b**) and WM (**c**) task.

Finally, PCA was also performed for trial outcome by including error trials (**Fig. 27**). Trajectories were close in state space for most alignments prior to test touch, but also progressively more separated in space. These results could be interpreted as the encoding of information in correct trials differing from the encoding in error trials, which could have been the reason while the mouse failed to make the correct choice. The first three PCs explained most of the variance for each alignment (DR: sample on: 69%, sample touch: 62%, test on: 64%, test touch: 72%; DR/WM: sample on: 76%,

## Neuronal results

sample touch: 62%, test on: 69%, test touch: 79%; WM: sample on: 74%, sample touch: 67%, test on: 69%, test touch: 79%).

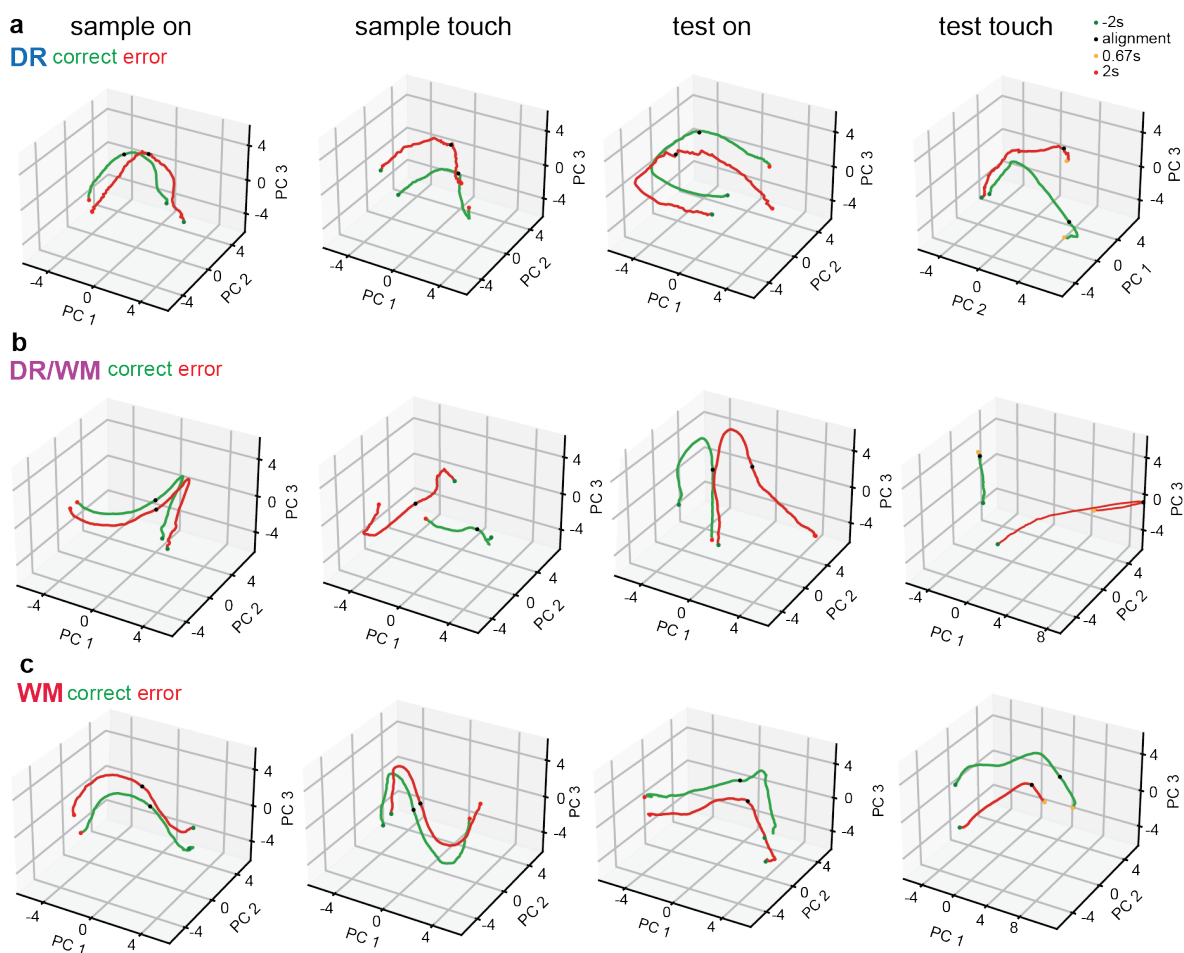


**Figure 27 | Neuronal population trajectories for trial outcome of different task types**

**a** Principal component analysis (PCA) describing neuronal population activity by trial outcome (correct: green, error: red) in the DR task. The first three principal components are plotted for each trial alignment (sample onset, sample touch, test onset, test touch). The alignment time point is indicated with a black dot. The start and ending points of the curve are the time points 2 s before and after the alignment (green and red). In the case of the alignment to the test touch, the endpoint is 0.67 s after the alignment (orange). The sample plots are shown for the DR/WM (**b**) and WM (**c**) task.

In summary, the neuronal analyses showed that a variety of neurons encoding sample location could be found in the prefrontal cortex of the mouse. The sample location was maintained throughout a delay, although at differing levels in the different task types. Specifically, a substantially higher percentage of units encode sample location in the WM task, and the information content of these units is also higher. These results are in line with the proposed hypothesis, arguing that the sample information in the WM must be maintained throughout the delay epoch, as the correct test stimulus location could not be predicted. Most importantly, this confirmed that behavioural differences observed in DR compared to WM tasks are reflected in the underlying neuronal activity of the prefrontal cortex

# Discussion

## Summary of the study

Working memory has been defined as the short-term maintenance of information for a behavioural output to achieve a goal (Fuster, 2015; Baddeley, 1987). Research studies into the behavioural and neuronal underpinnings of working memory have been adapted to a range of model organisms and, thus, vary widely in task design and behavioural and neuronal measurement methodologies. Here, I argue that working memory studies can be divided into two task types, which were defined as delayed response and working memory tasks. The distinction can be made based on the possibility of pre-planning the behavioural output in the delayed response task and the demand for sample information maintenance in the working memory task. Behavioural touchscreen chambers offer a great opportunity to test cognitively challenging tasks in a standardised manner, increasing comparability between different studies and labs (Bennett et al., 2023). The setups are also easily scalable, allowing studies with larger numbers of animals, which increases reproducibility for individual studies. The trial-unique non-matching to location (TUNL) task, especially, enables testing of two different short-term memory tasks within the same cohort of animals, enabling direct comparisons and observations of the diverging behavioural signatures of delayed response and working memory tasks.

In this thesis, it has been shown that in a delayed non-match to location tasks, human subjects will react faster in delayed response conditions compared to working memory conditions (**Fig. 9c/d**) and that the task type influences the amplitude of small eye movements called microsaccades (**Fig. 10g/h**), which have been related to working memory content (de Vries and van Ede, 2024; Liu et al., 2023; Liu et al. 2022). Several studies (Linde-Domingo and Spitzer, 2023; de Vries and van Ede, 2023) have shown that working memory content, especially location, can be decoded from microsaccade direction. Furthermore, microsaccades have been shown to reflect information about the sample location when it had to be maintained during a delay and shift towards planned actions when the correct test location was cued (Liu et al., 2023). A more in-depth analysis of the direction of the microsaccades throughout the trial could reveal,

if the sample location can be decoded from microsaccade direction, as here they were only separated into left and right.

Furthermore, these behavioural differences can also be determined in an equivalent non-match to location task using a touchscreen setup with freely moving mice. The learning speed and performance differed widely between task types, with mice learning the delayed response task significantly faster and generally performing better in delayed response conditions (**Fig. 11**). Over the course of training, mice became more efficient in their movement trajectories (**Fig. 12**). The initial exploration of the task and later refinement to a targeted response, makes evolutionary sense, as it conserves energy when the task is understood. Similar progressions to a more targeted response when the animal is allowed more free movements have been shown in Mosberger et al. (2024), where mice refine reaching movements and Baeg et al. (2003) for the movement trajectories through a figure-eight maze.

Differences were also observed in the strategies the mice used to solve the task based on the animals' movement trajectory through the arena. Here it was shown that animals had to shift from a pre-planning strategy (**Fig. 13**) that maximised the efficiency of the path towards the correct test stimulus towards a less distance-efficient strategy (**Fig. 14**) that allowed them to view the screen, and thus the test stimuli locations, first, before deciding on their motor trajectory. This change in strategy could also be observed by determining the Fréchet distance throughout the trial, with the path of the working memory conditions of the delayed response/working memory task staying closer together until the mouse can see the screen and then diverging (**Fig. 15**). Notably, two animals did not use the pre-planning strategy during the delayed response task. They turned in the same direction in each trial, illustrating that the delayed response task can also be solved by maintaining the sample location during the delay epoch and comparing it to the test stimuli. Regardless, this strategy is less efficient, as the mouse has to run further in half of the trials to receive the reward.

These distinct behavioural signatures related to the differing task types were mirrored by the underlying neuronal activation patterns observed in the lateral prefrontal cortex (prelimbic area) of trained mice. Chronic microendoscopic imaging of calcium transients in pyramidal neurons shows that individual neurons were tuned to different task parameters, such as sample location during the sensory (**Fig. 17**) and delay epoch (**Fig. 18**) and the choice side (**Fig. 19**). Furthermore, single units were found to

## Discussion

use monotonic as well as labelled line tuning to encode the sample location, which has both been described in the PFC before (Funahashi et al., 1989; Takeda et al., 2002; Nieder and Merten, 2007).

The fraction of units significantly tuned to the sample location throughout the trial differed between the three task types (**Fig. 20**). Specifically, more units were tuned to the sample location earlier in the sensory epoch in the working memory task. Furthermore, more units were tuned to the sample location during the delay epoch in the working memory compared to the delayed response task, actively maintaining the sample location.

The fraction of tuned units in the delayed response task was comparable to findings in other delayed response tasks (Horst and Laubach, 2012). Interestingly, even passive viewing of stimuli led to approximately 15% of units being tuned in the delay epoch in the prefrontal cortex of monkeys (Riley et al. 2016), compared to the 30-40% units tuned to the same sample stimuli in the delay epoch when they were being used in a working memory task (Qi and Constantinidis, 2013; Meyer et al., 2011).

Additionally, here I show that the information carried by those units was higher in the working memory compared to the delayed response task, increasing earlier and more strongly in the sensory epoch and being maintained at a higher level during the delay epoch (**Fig. 21**). These results confirm the initial hypothesis that the encoding of the sample location during the delay is higher, as the choice cannot be planned yet. However, alternative explanations, such as increased neuronal activity due to months of behavioural training and a higher number of sample locations, should be addressed with adequate control groups in future experiments.

Units with mixed selectivity, encoding both the sample location in the sensory epoch and the choice in the delay epoch (**Fig. 23**), were found in all three task types (**Fig. 24**). Mixed selectivity has been shown to have a computational advantage when explaining cognitive processes (Rigotti et al., 2013; Tye et al., 2024). Mixed selectivity? Furthermore, the populations encoding the sample location and choice side were found to be largely non-overlapping and sparse (**Fig. 24**). Sparsity has been described in the context of working memory functioning in the prefrontal cortex (Lundqvist, 2018; Quintana et al., 1988). Finally, when analysing the temporal dynamics of the neuronal population, sample locations were found to be organised in state space, with physically close response window locations represented by more similar neuronal population activation (**Fig. 25-27**), which confirms that locations close to each other on the

touchscreen, were encoded with more similar neuronal representations. Similar neuronal activations for sequential objects are also apparent for other parameters in the prefrontal cortex, for example numerosities in monkey research (Jacob and Nieder, 2014).

Thus, this study expands studies describing differences between delayed response and working memory tasks behaviourally and neuronally (Honig and Wasserman, 1981; Bennett et al., 2022; Pontecorvo et al., 1996; Quintana et al., 1988; Bastos et al., 2018) by reporting additional differences in the underlying neuronal activation patterns in mice.

### **Behavioural & neuronal signatures of delayed response and working memory**

The trial-unique non-matching to location task is one of the few reported working memory tasks that mice can successfully learn; others involving multiple sensory dimensions, such as vision and sound (Rikhye et al. 2018) or a non-match to sample task using olfactory cues (Liu et al. 2014). The task used here has the added advantage to allow direct comparison between delayed response and working memory approaches within animals, which few other studies have addressed before (Honig and Wasserman, 1981; Quintana et al., 1988). It has also been shown to be robustly reproducible across different laboratories (Bennett et al., 2022). It takes mice about four months to habituate, progress through pretraining and acquire the final working memory task. However, this is comparable to other working memory tasks in rodents (Nakagawa, 1993), which have a similar training time. In addition, this also illuminates a potential challenge to behavioural tasks capitalising on innate exploratory behaviours, such as the forced alternation task in t-, plus- or radial mazes, as natural exploration and novelty seeking might have a different, more evolutionary efficient underlying neuronal activity than the cognitively challenging working memory.

The cellular basis of the maintenance of information during working memory tasks is not fully understood yet. However, activity during the delay epoch was reported early on. Delay activity has been shown in delayed response tasks in monkeys (Funahashi et al., 1989; Takeda et al., 2002) and rodents (Vogel et al., 2022). However, Vogel et al. (2022) found that many other task parameters, such as location in the maze and time progression, explained the neuronal activation during the delay more

## Discussion

than the sample or choice location. Maintenance of sample information in working memory tasks has also been shown (Miller and Desimone, 1994). The information is maintained in both task types; however, the task type does seem to affect how strongly the information is present in individual prefrontal pyramidal neurons. Here, I directly compare neuronal activity in the delay epoch of delayed response and working memory task types and find that there is a higher number of units tuned to sample location in working memory compared to delayed response tasks (**Fig. 20**) and that these units carry more information (**Fig. 21**). One explanation for this could be that the mice need to maintain the sample information throughout the delay in the working memory task, but not in the delayed response task, thus the fraction of tuned units is higher in the working memory task. However, there might also be different explanations. The number of potential sample locations increases from two in the delayed response task, to three in the delayed response/working memory task to five in the working memory task. This could mean that neurons tuned to the sample location in the delayed response task might also be tuned to that location in the working memory task, but additional neurons are needed to encode the other three sample locations. Another reason could be that mice have to be trained consecutively on the three task types, as they learn the trial structure during the delayed response task. Animals were only imaged in expert sessions of the three task types, which took place several weeks apart (Fig. 10). Continuous training could lead to a gradual increase of recruited neurons over time (Meyer et al., 2011; Qi and Constantinidis, 2013), which could have the same effect, however, studies with complex cognitive tasks, which mice only learned over months of training the number of selective neurons even after a rule-switch remained stable (Reinert et al., 2021). Furthermore, an increase in tuned units before the test stimuli presentation was observed in all three task types. In the delayed response task, this could be explained by the mouse planning the motor output, and, indeed, we see units in the delayed response task being tuned to a specific location in space, indicating the neurons for a particular location start firing when the mouse plans its behavioural output. In the delayed response/working memory and working memory task, this ramping towards the end of the delay epoch is also observed, although at a lower level. Because all task types include at least some delayed response conditions (delayed response 100%, delayed response/working memory 50%, working memory 25%), this might be due to trials where the animal can predict the outcome of the task before the test stimuli

presentation. It should be determined if the increase persists when delayed response conditions are removed from the analysis of the working memory task. However, this ramping activity has also been reported in other studies of delayed response and working memory tasks (Shafi et al., 2007; Markowitz et al., 2015; Watanabe and Funahashi, 2007). In addition, it could be argued that this ramp is due to preparatory mechanisms of the animal (Lundqvist et al., 2018; Stokes, 2015) or the effect could also be due to the animal making a prediction in WM trials, where the sample stimulus is on the left side of the touchscreen, for the test stimulus to more likely be on the right side, even though the task design is balanced, and the animals cannot make this prediction accurately (Bennett et al., 2023).

## Limitations

A limitation of the task is that the sample location and choice are difficult to separate, especially in the delayed response task. Task designs with binary options often pose this challenge, but it is impossible in the smallest separation level of the delayed response task, where only two conditions are used and, thus, in the analysis, sample locations and choice side separate the trials into the same two groups. Adding conditions to the last separation level of the delayed response task or having a final testing session including all separation levels used in the behavioural training, during which the neuronal signal is recorded, could improve the analysis by enabling the separation between the sample location and choice side. This additional imaging session is especially interesting in the delayed response task, as a shift from sample location to choice side information in the neuronal population is expected during the delay epoch. In addition, this would increase the number of sample locations used from two to four, which, if the neuronal signal stays the same, would indicate that the observed increase in tuned units in the WM task is not due to an increase in the number of sample locations.

The training procedure of the task takes about four months in total for each mouse. Each mouse is habituated to the touchscreen chamber, pretrained to touch the lit-up window, and then is trained on the DR task, followed by the DR/WM and WM tasks. Unfortunately, the DR task is integral for the mice to learn the trial structure, which they

## Discussion

can then adapt to the more difficult working memory conditions. Therefore, the order of the task types cannot be changed in mice. Sentence here

Furthermore, it cannot be directly ruled out that the increase in tuned units is due to the length of training of the animals. Studies comparing the percentage of units significantly tuned during the delay epoch in a working memory task in the monkey prefrontal cortex found an increase from around 10% before training the animal to about 35-40% after behavioural training (Meyer et al., 2011; Qi and Constantinidis, 2013). However, in other studies, the size of neuronal populations after switch rules has been shown to be stable (Reinert et al., 2022), which could indicate that the neuronal population, tuned to a specific sample location, increases in size throughout training as the animal learns the three task types, however, in expert animals, it remains stable. Adding a control group that is solely and continuously trained on the delayed response task for a comparable timespan and imaged at similar intervals could illuminate if the increase in the fraction of tuned units is affected by the length of training. In addition, adding imaging sessions throughout the learning phase for all animals, for example, at a novice and intermediate training state, could also determine if the increase happens during learning but stays stable in the expert animal.

Furthermore, mice have been shown to be able to generalise task rules across different visual stimuli (Reinert et al., 2022). However, we cannot determine if the mouse truly learned the rule of touching the non-matching stimulus or if it learned each condition separately. Although in the working memory task, that would mean, that the mice would maintain eight different rules simultaneously. The consistently high performance in the delayed response conditions across task types confirms at least in part that the mice achieve a generalisation between conditions.

The time to learn the task illuminates one of the biggest differences between the human and the mouse version of the non-matching to location task. Humans understand the task rule within the first two trials of the DR block. Interestingly, both participants choose the matching stimulus in the first trial. The participants immediately, abstracted the rule that they must touch the non-matching stimulus, and performance was close to 100% for each block, regardless of task type, for the rest of the session. It could be argued that the simplicity of the task might mean that humans do not consciously pre-plan where they have to saccade to. Indeed, one of the participants did not report the differences of blocks when asked for observations about

the task after the session was completed. Moreover, the significantly faster response saccades and differences in the amplitude of microsaccades in the delayed response block could be due to the block being the first one to be shown to the participants and them tiring throughout the session. These effects could also be further tested by changing the order of the task blocks.

### **Updating the definition of working memory**

The current definition of working memory based on models from Atkinson and Shiffrin (1968) and later Baddeley and Hitch (1974), described working memory as the short-term information storage space that is needed for a prospective behavioural output and is malleable by further internal or external input (Fuster, 2015). In many studies, this has been interpreted as the maintenance of sample information in prefrontal neurons during a delay epoch and task designs were adapted accordingly. However, delayed response task designs, where the behavioural output can be preplanned, have been shown to elicit differences in behavioural and neuronal responses compared to working memory tasks (Honig and Wasserman, 1981; Bennet et al., 2022; Quintana et al., 1988; Bastos et al., 2018), which may be because, although the tasks are solvable by keeping the sample information in mind, it is also possible to pre-plan the behavioural outputs. Evolutionary, that makes sense as maintaining information costs energy and preparing for a behavioural output that, for example, will be rewarded with food allows swift and economical reactions. The plan of the animal still needs to be maintained throughout the delay, so the argument that information is maintained would still be aligned with the working memory definition. However, as shown here, alongside other studies (Honig and Dodd, 1983; Honig and Wasserman, 1981; Pontecorvo et al., 1996; Bennett et al., 2023; Quintana et al., 1988), it seems to be important to make a distinction if the information is about the sample or the choice. It has been suggested to use “prospective” and “retrospective” working memory to differentiate between the two task types (Bennett et al., 2022; Pontecorvo et al., 1995). However, this may be confusing as working memory is generally defined as a prospective cognitive function, as it involves a future behavioural output (Fuster, 2015). The terminology used in this dissertation reserves the term working memory for tasks, where the sample information must be

## Discussion

maintained, and no preplanning can take place, as it is the essential part of working memory to maintain behaviourally relevant information throughout a delay, whereas preplanning can occur without working memory. However, in many studies, the term “working memory” has been used to describe delayed response tasks, and it could be argued that information about the choice, i.e. the plan, must be maintained throughout a delay. The original definition is not clear enough. It could be adapted to add “sensory information”, in which case only tasks where the sample information must be maintained can be called “working memory tasks”, while delayed response tasks are testing for other closely related cognitive resources. Nevertheless, regardless of the definition, the task design of each study should be cautiously evaluated to determine if the task requires short-term maintenance of sensory information or allows active planning of the behavioural output when comparing across different studies and, especially across species.

## Outlook

This study has shown distinct behavioural and neuronal signatures of delayed response and working memory tasks in mice and man. However, many questions about the properties of the neuronal information remain to be answered.

Firstly, based on the observation that a significant difference in the fraction of units tuned to sample location across the three task types was found and that the two non-overlapping sparse populations encoded sample location and choice. It would be interesting to see how these populations develop throughout the behavioural training. Especially if the populations encoding sample location and choice side in the delayed response task are the same in the delayed response/working memory and working memory tasks. It could be hypothesised that the neurons encoding a specific sample location stay the same but change their activation throughout a trial from being only active during the sensory and early delay period in the delayed response task to extending their activation throughout the late delay period in the delayed response/working memory and working memory task, until a different population takes over as soon as the choice side becomes known. In addition, investigating how these populations emerge during initial learning of the three different task types and how they adapt when switching to a new task type could help understand the cellular basis

of rule learning. As described above, one advantage of chronic endoscopic fluorescence microscopy over electrophysiology is that single neurons can be identified and followed across weeks of behavioural training. In the experiments described above, due to technical issues impeding the consistent focusing of the V3 UCLA Miniscopes, the multi-session registration was below acceptable quality standards. However, this issue can be avoided using the newer V4 UCLA Miniscopes, which have a software-guided focus that allows a stable focal plane across several imaging sessions, even if they are weeks or months apart. In addition, dental cement hardened with ultraviolet light should be used to ensure consistent volume of the implant. The next experiment in this study will be to run a batch of mice using V4 UCLA Miniscopes to allow multi-session registration and track neurons throughout the entire behavioural training procedure.

Furthermore, the prefrontal cortex is highly connected with other areas of the brain (Ährlund-Richter et al., 2019; Chafee and Goldman-Rakic, 2000; Bolkan et al., 2017) and their involvement in processing sensory information, internal representation and generating a choice is important to understand the entire circuit of working memory. Novel methods, such as meso-scale calcium imaging of the entire dorsal cortex, described in MacDowell et al. (2024), allow us to visualise multiple areas simultaneously and determine functional connectivity and individual area's involvement in cognitive processes.

Secondly, any behavioural study, however controlled the design is, will show some variability. Here, this was briefly alluded to in **Fig. 13**, where two animals used a different, potentially non-preplanning strategy to solve the delayed response task (**Fig. 13b**). In this case, it clearly illustrated the possibility of using both a preplanning strategy and memorising the sample location of the delayed response task. The freely moving task design in the touchscreen chamber that does not enforce trial progression enhances behavioural differences as it allows the mice to exhibit any behaviour they want and proceed with the task in their own time. In addition, it has been shown that, for example, behavioural differences could be related to differences in spatiotemporal motifs of neuronal activation via functional connectivity (MacDowell et al., 2024). Indeed, relating individual behaviour and neuronal activation, rather than averaging across animals, could allow the determination of specific neuronal activations for idiosyncratic strategies and potentially improve translation to a highly variable human

## Discussion

population. Sentence This becomes especially important when using rodent studies to test disease models or potential drugs to recover the symptoms.

Finally, the experiments with human subjects showed that a simple delayed non-match to location task also elicited behavioural differences between delayed response and working memory blocks in humans compared to mice, validating the task design and translating the results across species. The mouse experiments then allowed the visualisation and analysis of neuronal signals in the prefrontal cortex to determine that neuronally, the two tasks also show distinct signatures. The last step to close the circle would be to acquire neuronal signals with single-unit resolution in humans and determine if the neuronal differences between delayed response and working memory tasks persist across species. These experiments would not only validate the neuronal data of the mouse model and task design of the non-matching to location tasks in touchscreen setups, but it would also support the proposal that delayed response and working memory tasks should not be equated, which is an important factor to be considered in biomedical research and translation to clinical studies. Single-unit resolution in human research, however, is still challenging to achieve, yet with the advent of more mature recording technologies using intracortically implanted microelectrode arrays or linear probes in human patients (Eisenkolb et al., 2023; Leonard et al., 2024; Coughlin et al., 2023; Paulk et al., 2022), a whole new window into the human brain will be opened.

*Conclusion*

Working memory research has made great progress since the first definitions and models were proposed in the 1960s and 70s (Atkinson and Shiffrin, 1968; Baddeley and Hitch, 1974). Many studies have shown that the prefrontal cortex plays an essential role in maintaining information across a delay, where information about sensory inputs as well as motor plans can be decoded from its neurons. The proposal of a distinction of sample information and choice in working memory tasks is made here, based on observed differences in behavioural and neuronal signatures of delayed response and working memory tasks. The distinction between experimental paradigms could improve the comparability across studies and species in the future. This is especially important in studies researching the underlying mechanisms of disorders where working memory is impaired and testing the feasibility of potential treatments.

## References

- Ährlund-Richter, S., Xuan, Y., van Lunteren, J.A., Kim, H., Ortiz, C., Pollak Dorocic, I., Meletis, K., and Carlén, M. (2019). A whole-brain atlas of monosynaptic input targeting four different cell types in the medial prefrontal cortex of the mouse. *Nature Neuroscience*, 22, 657 – 668, DOI:10.1038/s41593-019-0354-y
- Alexander, G. E., and Fuster, J. M. (1973). Effects of cooling prefrontal cortex on cell firing in the nucleus medialis dorsalis. *Brain research*, 61, 93–105, DOI:10.1016/0006-8993(73)90518-0
- Andrews, J., and Jansen, J. (1996). Matching to sample in rats using projected visual stimuli. *Neuroscience Research Communications*, 18(2),115-124
- Atkinson, R.C. and Shiffrin, R.M (1968). Human Memory: A proposed System and its Control Process. *Psychology of Learning and Motivation*, Vol. 2, pp. 89-195, New York: Academic Press
- Baeg, E.H., Kim, Y., Huh, K., Mook-Jung, I., Kim, H.T. and Jung, M.W. (2003). Dynamics of Population Code for Working Memory in the Prefrontal Cortex. *Neuron*, 40, 177-188, DOI:10.1016/S0896-6273(03)00597-X
- Baddeley, A.D. and Hitch, G. (1974). Working Memory, In *The psychology of learning and motivation*. Vol. 8, pp. 47-90, New York: Academic Press
- Baddeley, A.D. (1983). Working Memory. *Philosophical Transactions of the Royal Society of London. B, Biological Sciences*. 302(1110). pp.311-324.
- Bähner, F., Demanuele, C., Schweiger, J., Gerchen, M.F., Zamoscik, V., Ueltzhöffer, K., Hahn, T., Meyer, P., Flor, H., Durstewitz, D., Tost, H., Kirsch, P., Plichta, M.M., Meyer-Lindenberg, A. (2015). Hippocampal-Dorsolateral Prefrontal Coupling as a Species-Conserved Cognitive Mechanism: A Human

- Translational Imaging Study. *Neuropsychopharmacology*, 40, 1674-1681, DOI:10.1038/npp.2015.13
- Bastos, A.M., Loonis, R., Kornblith, S., Lundqvist, M., and Miller, E.K. (2018). Laminar recordings in frontal cortex suggest distinct layers for maintenance and control of working memory. *Proceedings of the National Academy of Sciences of the United States of America*, 115, 1117 – 1122, DOI:10.1073/pnas.1710323115
- Bauer, R.H., and Fuster, J.M. (1976). Delayed-matching and delayed-response deficit from cooling dorsolateral prefrontal cortex in monkeys. *Journal of comparative and physiological psychology*, 90(3), 293-302, DOI:10.1037/H0087996
- Bennett, D., Nakamura, J.P., Vinnakota, C., Sokolenko, E., Nithianantharajah, J., van den Buuse, M., Jones, N.C., Sundram, S., & Hill, R.A. (2022). Mouse Behavior on the Trial-Unique Nonmatching-to-Location (TUNL) Touchscreen Task Reflects a Mixture of Distinct Working Memory Codes and Response Biases. *The Journal of Neuroscience*, 43, 5693 – 5709, DOI:10.1101/2022.10.30.514444
- Bolkan, S.S., Stujenske, J.M., Parnaudeau, S., Spellman, T.J., Rauffenbart, C., Abbas, A.I., Harris, A.Z., Gordon, J.A., and Kellendonk, C. (2017). Thalamic projections sustain prefrontal activity during working memory maintenance. *Nature neuroscience*, 20, 987 – 996, DOI:10.1038/nn.4568
- Buschman, T.J., Siegel, M., Roy, J.E., Miller, E.K. (2011). Neural substrates of cognitive capacity limitations. *Proceedings of the National Academy of Sciences*, 108, 11252-1255, DOI: 10.1073/pnas.1104666108
- Bussey, T.J., Holmes, A., Lyon, L., Mar, A.C., McAllister, K.A., Nithianantharajah, J., Oomen, C.A., and Saksida, L.M. (2012). New translational assays for preclinical modelling of cognition in schizophrenia: The touchscreen testing

## References

- method for mice and rats. *Neuropharmacology*, 62, 1191-1203,  
DOI:10.1016/j.neuropharm.2011.04.011
- Chafee, M. V., and Goldman-Rakic, P. S. (2000). Inactivation of parietal and prefrontal cortex reveals interdependence of neural activity during memory-guided saccades. *Journal of Neurophysiology*, 83(3), 1550–1566,  
DOI:10.1152/jn.2000.83.3.1550
- Carlén, M. (2017). What constitutes the prefrontal cortex?. *Science*, 358, 478-482,  
DOI:10.1126/science.aan8868
- Chen, T., Wardill, T.J., Sun, Y., Pulver, S.R., Renninger, S.L., Baohan, A., Schreiter, E.R., Kerr, R.A., Orger, M.B., Jayaraman, V., Looger, L.L., Svoboda, K., Kim, D.S. (2013). Ultra-sensitive fluorescent proteins for imaging neuronal activity. *Nature*, 499(7458), 295-300
- Constantinidis, C., Funahashi, S., Daeyeol, L., Murray, J.D., Qi, X., Wang, M., Arnsten, A.F.T. (2018). Persistent Spiking Activity Underlies Working Memory. *The Journal of Neuroscience*, 38(32), 7020-7028,  
DOI:10.1523/JNEUROSCI.2486-17.2018
- Coughlin, B., Muñoz, W., Kfir, Y., Young, M.J., Meszéna, D., Jamali, M., Caprara, I., Hardstone, R., Khanna, A.R., Moustroph, M.L., Trautmann, E.M., Windolf, C., Varol, E., Soper, D.J., Stavisky, S.D., Welkenhuysen, M., Dutta, B., Shenoy, K.V., Hochberg, L.R., Mark Richardson, R., Williams, Z.M., Cash, S.S., & Paulk, A.C. (2023). Modified Neuropixels probes for recording human neurophysiology in the operating room. *Nature Protocols*, 18, 2927 – 2953,  
DOI: :10.1038/s41596-023-00871-2
- Chudasama, Y., and Muir, J.L. (1997). A behavioural analysis of the delayed non-matching to position task: the effects of scopolamine, lesions of the fornix and of the prelimbic region on mediating behaviours by rats. *Psychopharmacology*, 134, 73-82, DOI:10.1007/s002130050427

- Danziger, Z. (2024). Discrete Frechet Distance (<https://www.mathworks.com/matlabcentral/fileexchange/31922-discrete-frechet-distance>), MATLAB Central File Exchange. Retrieved April 21, 2024.
- de Vries, E. and van Ede, F. (2024). Microsaccades Track Location-Based Object Rehearsal in Visual Working Memory. *eNeuro*, 11, DOI:10.1523/ENEURO.0276-23.2023
- Dexter, T.D., Palmer, D., Hashad, A.M., Saksida, L.M., and Bussey, T.J. (2022). Decision Making in Mice During an Optimized Touchscreen Spatial Working Memory Task Sensitive to Medial Prefrontal Cortex Inactivation and NMDA Receptor Hypofunction. *Frontiers in Neuroscience*, 16, DOI:10.3389/fnins.2022.905736
- Duvarci, S., Simpson, E.H., Schneider, G., Kandel, E.R., Roeper, J., and Sigurdsson, T. (2018). Impaired recruitment of dopamine neurons during working memory in mice with striatal D2 receptor overexpression. *Nature Communications*, 9, DOI:10.1038/s41467-018-05214-4
- Eisenkolb, V.M., Held, L.M., Utzschmid, A., Lin, X., Krieg, S.M., Meyer, B., Gempt, J., and Jacob, S.N. (2023). Human acute microelectrode array recordings with broad cortical access, single-unit resolution, and parallel behavioral monitoring. *Cell Reports*, 42, DOI:10.1016/j.celrep.2023.112467
- Engbert, R., Kliegl, R. (2003). Microsaccades uncover the orientation of covert attention. *Vision Research*, 43, 1035-1045, DOI:10.1016/S0042-6989(03)00084-1
- Funahashi, S., Bruce, C.J., and Goldman-Rakic, P.S. (1989). Mnemonic coding of visual space in the monkey's dorsolateral prefrontal cortex. *Journal of Neurophysiology*, 61(2), 331-349, DOI:10.1152/JN.1989.61.2.331

## References

- Funahashi, S., Bruce, C.J., Goldman-Rakic, P.S. (1990). Visuospatial coding in primate prefrontal neurons revealed by oculomotor paradigms. *Journal of Neurophysiology*, 63(4), 814-831, DOI:10.1152/JN.1990.63.4.814
- Fuster, J.M. (2015) *The Prefrontal Cortex*, Fifth Edition, Academic Press
- Fuster, J.M., and Alexander, G.E. (1971). Neuron Activity Related to Short-Term Memory. *Science*, 173, 652 – 654, DOI:10.1126/science.173.3997.652
- Gauld, O.M., Packer, A., Russell, L.E., Dalgleish, H., Iuga, M., Sacadura, F., Roth, A., Clark, B.A., and Häusser, M. (2024). A latent pool of neurons silenced by sensory-evoked inhibition can be recruited to enhance perception. *Neuron*, 112, 1-18, <https://doi.org/10.1016/j.neuron.2024.04.015>
- Gaunt, J.T., and Bridgeman, B. (2012) Microsaccades and Visual-Spatial Working Memory. *Journal of Eye Movement Research*, 5(5), 1-16, DOI:10.16910/jemr.5.5.3
- Ghosh, K.K., Burns, L.D., Cocker, E.D., Nimmerjahn, A., Ziv, Y., Gamal, A.E., & Schnitzer, M.J. (2011). Miniaturized integration of a fluorescence microscope. *Nature methods*, 8, 871 – 878, DOI: 10.1038/nmeth.1694
- Gioannucci, A., Friedrich, J., Gunn, P., Kalfon, J., Brown, B.L., Koay, S.A., Taxidis, J., Najafi, F., Gauthier, J.L., Zhou, P., Khakh, B.S., Tank, D.W., Chklovskii, D.B., Pnevmatikakis, E.A. (2019) CalmAn an open source tool for scalable calcium imaging data analysis. *eLife*, 8, DOI:10.7554/eLife.38173
- Gold, J.M., Hahn, B., Zhang, W., Robinson, B.M., Kappenman, E.S., Beck, V.M., and Luck, S.J. (2010). Reduced capacity but spared precision and maintenance of working memory representations in schizophrenia. *Archives of general psychiatry*, 67(6), 570-577. DOI:10.1001/archgenpsychiatry.2010.65
- Goldman-Rakic, P.S. (1995). Cellular basis of working memory. *Neuron*, 14, 477-485. DOI:10.1016/0896-6273(95)90304-6

- Guo, C., Blair, G.J., Sehgal, M., Sangiuliano Jimka, F.N., Bellafard, A., Silva, A.J., Golshani, P., Basso, M.A., Blair, H.T., and Aharoni, D. (2021). Miniscope-LFOV: A large-field-of-view, single-cell-resolution, miniature microscope for wired and wire-free imaging of neural dynamics in freely behaving animals. *Science Advances*, 9, DOI:10.1126/sciadv.adg3918
- Hafed, Z.M., Clark, J.J. (2002). Microsaccades as an overt measure of covert attention shifts. *Vision Research*, 42, 2533-2545, DOI:10.1016/S0042-6989(02)00263-8
- Harris, C.R., Millman, K.J., van der Walt, S.J. et al. Array programming with NumPy. *Nature* 585, 357–362 (2020). DOI: 10.1038/s41586-020-2649-2.
- Hwang, J., Mitz, A.R., Murray, E.A. (2019). NIMH MonkeyLogic: Behavioral control and data acquisition in MATLAB. *Journal of Neuroscience Methods*, 323, 13-21, DOI:10.1016/j.jneumeth.2019.05.002
- Honig, W.K. and Dodd, P.W.D (1983). Delayed discrimination in the pigeon: The role of within-trial location of conditional cues. *Animal Learning and Behavior*, 11(1), 1-9, DOI:10.3758/BF03212300
- Honig, W.K., & Wasserman, E.A. (1981). Performance of pigeons on delayed simple and conditional discriminations under equivalent training procedures. *Learning and Motivation*, 12, 149-170, DOI:10.1016/0023-9690(81)90016-3
- Horst, N.K., and Laubach, M. (2012). Working with memory: evidence for a role for the medial prefrontal cortex in performance monitoring during spatial delayed alternation. *Journal of Neurophysiology*, 108(12), 3276-88, DOI:10.1152/jn.01192.2011
- Hubel D. H., and Wiesel, T. N. (1962). Receptive fields, binocular interaction and functional architecture in the cat's visual cortex. *The Journal of Physiology*, 160(1), 106–154, DOI:10.1113/jphysiol.1962.sp006837

## References

- Hunter, J.D. (2007). Matplotlib: A 2D Graphics Environment, *Computing in Science and Engineering*, vol. 9, no. 3, pp.90-95
- Hunter, W.S. (1914). The Delayed Reaction in Animals and Children, [Doctoral dissertation at the University of Chicago], published at Henry Holt & Company, New York
- Hussar, C.R., and Pasternak, T. (2012). Memory-Guided Sensory Comparisons in the Prefrontal Cortex: Contribution of Putative Pyramidal Cells and Interneurons. *The Journal of Neuroscience*, 32, 2747 – 2761, DOI:10.1523/JNEUROSCI.5135-11.2012
- Jackman, S.L., Chen, C.H., Chettih, S.N., Neufeld, S.Q., Drew, I.R., Agba, C.K., Flaquer, I., Stefano, A.N., Kennedy, T.J., Belinsky, J.E., Roberston, K., Beron, C.C., Sabatini, B.L., Harvey, C.D., Regehr, W.G. (2018). Silk Fibroin Films Facilitate Single-Step Targeted Expression of Optogenetic Proteins. *Cell Reports*, 22, 12, 3351-3361, DOI: 10.1016/j.celrep.2018.02.081
- Jackson, A.D., Cohen, J.L., Phensy, A.J., Chang, E.F., Dawes, H.E., Sohal, V.S. (2024). Amygdala-hippocampus somatostatin interneuron beta-synchrony underlies a cross-species biomarker of emotional state. *Neuron*, 112, 1-14, DOI:10.1016/j.neuron.2023.12.017
- Jacob, S.N., Nieder, A. (2014). Complementary Roles for Primate Frontal and Parietal Cortex in Guarding Working Memory from Distractor Stimuli. *Neuron*, 83, 226-237, DOI:10.1016/j.neuron.2014.05.009
- Kim, C.H., Romberg, C., Hvoslef-Eide, M., Oomen, C.A., Mar, A.C., Heath, C.J., Berthiaume, A., Bussey, T.J., Saksida, L.M. (2015). Trial-unique, delayed nonmatching-to-location (TUNL) touchscreen testing for mice: sensitivity to dorsal hippocampal dysfunction. *Psychopharmacology*, 232, 3935-3945, DOI:10.1007/s00213-015-4017-8

- Kofler, M.J., Sarver, D.E., Harmon, S.L., Moltisanti, A.J., Aduen, P.A., Soto, E.F., and Ferretti, N. (2018). Working memory and organizational skills problems in ADHD. *Journal of Child Psychology and Psychiatry*, 59, 57–67, DOI:10.1111/jcpp.12773
- Le Merre, P., Ährlund-Richter, S., Carlén, M. (2021) The mouse prefrontal cortex: Unity in diversity. *Neuron*, 109, 1925-1944, DOI:10.1016/j.neuron.2021.03.035
- Leonard, M.K., Gwilliams, L., Sellers, K.K., Chung, J.E., Xu, D., Mischler, G., Mesgarani, N., Welkenhuysen, M., Dutta, B., & Chang, E.F. (2023). Large-scale single-neuron speech sound encoding across the depth of human cortex. *Nature*, 626, 593 - 602. DOI: 10.1038/s41586-023-06839-2
- Levy, W. B., and Baxter, R. A. (1996). Energy efficient neural codes. *Neural computation*, 8(3), 531–543, DOI:10.1162/neco.1996.8.3.531
- Lin, X., Nieder, A., and Jacob, S.N. (2023). The neuronal implementation of representational geometry in primate prefrontal cortex. *Science Advances*, 9(50), DOI: 10.1126/sciadv.adh8685
- Linde-Domingo, J. and Spitzer, B., (2023). Geometry of visuospatial working memory information in miniature gaze patterns. *Nature Human Behaviour*, 8, 336-348, DOI:10.1038/s41562-023-01737-z
- Liu, B., Alexopoulou, Z., van Ede, F., (2023). Jointly looking to the past and the future in visual working memory, *eLife*, 12, DOI:10.7554/eLife.90874
- Liu, B., Nobre, A.C., van Ede, F., (2022). Functional but not obligatory link between microsaccades and neural modulation by covert spatial attention. *nature communications*, 13, DOI:10.1038/s41467-022-31217-3
- Liu, D., Gu, X., Zhu, X., Zhang, X., Han, Z., Yan, W., Cheng, Q., Hao, J., Fan, H., Hou, R., Chen, Z., Chen, Y., Li, C.T. (2014). Medial prefrontal activity during

## References

- delay period contributes to learning of a working memory task. *Science*, 346, 458-463, DOI:10.1126/science.1256573
- Lowet, E., Gomes, B., Srinivasan, K., Zhou, H., Schafer, R.J., & Desimone, R. (2018). Enhanced Neural Processing by Covert Attention only during Microsaccades Directed toward the Attended Stimulus. *Neuron*, 99, 207-214.e3. DOI:10.1016/j.neuron.2018.05.041
- Lundqvist, M., Herman, P., Miller, E.K. (2018). Working Memory: Delay Activity, Yes! Persistent Activity? Maybe Not. *The Journal of Neuroscience*, 38(32), 7013-7019, DOI:10.1523/JNEUROSCI.2485-17.2018
- MacDowell, C. J., Briones, B. A., Lenzi, M. J., Gustison, M. L., and Buschman, T. J. (2024). Differences in the expression of cortex-wide neural dynamics are related to behavioral phenotype. *Current biology*, 34(6), 1333–1340.e6. DOI: 10.1016/j.cub.2024.02.004
- Mansouri, F.A., Matsumoto, K., and Tanaka, K. (2006). Prefrontal Cell Activities Related to Monkeys' Success and Failure in Adapting to Rule Changes in a Wisconsin Card Sorting Test Analog. *The Journal of Neuroscience*, 26, 2745 – 2756, DOI:10.1523/JNEUROSCI.5238-05.2006
- Mante, V., Sussillo, D., Shenoy, K.V., Newsome, W.T. (2013). Context-dependent computation by recurrent dynamics in prefrontal cortex. *Nature*, 503, 78-84, DOI:10.1038/nature12742
- Mathis, A., Mamidanna, P., Cury, K.M., Abe, T., Murthy, V.N., Mathis, M.W., Bethge M (2018). DeepLabCut: markerless pose estimation of user-defined body parts with deep learning. *Nature Neuroscience*, 21, 1281-1288, DOI:10.1038/s41593-018-0209-y
- Meyer, T., Qi, X., Stanford, T.R., and Constantinidis, C. (2011). Stimulus Selectivity in Dorsal and Ventral Prefrontal Cortex after Training in Working Memory Tasks.

- The Journal of Neuroscience*, 31, 6266 – 6276,  
DOI:10.1523/JNEUROSCI.6798-10.2011
- Miller, E.K. and Desimone, R., (1994). Parallel neuronal mechanisms for short-term memory. *Science*, 263(5146), 520-522, DOI:10.1126/SCIENCE.8290960
- Miller, E.K., Erickson, C.A., and Desimone, R. (1996). Neural Mechanisms of Visual Working Memory in Prefrontal Cortex of the Macaque. *The Journal of Neuroscience*, 16, 5154 – 5167, DOI:10.1523/JNEUROSCI.16-16-05154.1996
- Miyawaki, A., Llopis, J., Heim, R., McCaffery, J.M., Adams, J.A., Ikura, M., Tsien, R.Y. (1997). Fluorescent indicators for Ca<sup>2+</sup> based on green fluorescent proteins and calmodulin. *Nature* 388, 882–887, DOI:10.1038/42264
- Mosberger, A.C., Sibener, L.J., Chen, T.X., Rodrigues, H.F.M., Hormigo, R., Ingram, J.N., Athalye, V.R., Tabachnik, T., Wolpert, D.M., Murray, J.M., Costa, R.M. (2024). Exploration biases forelimb reaching strategies. *Cell Reports*, 43(4), 113958, DOI:10.1016/j.celrep.2024.113958
- Nakagawa, E. (1993). Matching and nonmatching concept in rats. *Psychobiology*, 21(2), 142-150, DOI:10.3758/BF03332041
- Nakai, J., Ohkura, M. and Imoto, K. (2001). A high signal-to-noise Ca<sup>2+</sup> probe composed of a single green fluorescent protein. *Nature Biotechnology*, 19, 137–141, DOI:10.1038/84397
- Nakamura, J.P., Gillespie, B., Gibbons, A., Jaehne, E.J., Du, X., Chan, A., Schroeder, A., van den Buuse, M., Sundram, S., Hill, R.A. (2021). Maternal immune activation targeted to a window of parvalbumin interneuron development improves spatial working memory: Implications for autism. *Brain, Behavior, and Immunity*, 91, 339-349, DOI:10.1016/j.bbi.2020.10.012

## References

- Newsome, W.T., Newsome, W.T., Britten, K.H., Britten, K.H., and Movshon, J.A. (1989). Neuronal correlates of a perceptual decision. *Nature*, 341, 52-54, DOI:10.1038/341052A0
- Nieder, A., and Merten, K., (2007). A Labeled-Line Code for Small and Large Numerosities in the Monkey Prefrontal Cortex. *The Journal of Neuroscience*, 27(22), 5986-5993, DOI:10.1523/JNEUROSCI.1056-07.2007
- Nithianantharajah, J., Komiyama, N.H., McKechnie, A., Johnstone, M., Blackwood, D.H., St Clair, D., Emes, R.D., van de Lagemaat, L.N., Saksida, L.M., Bussey, T.J., Grant, S.G.N. (2013). Synaptic scaffold evolution generated components of vertebrate cognitive complexity. *Nature Neuroscience*, 16(1), 16-24, DOI:10.1038/nn.3276
- Nithianantharajah, J., McKechnie, A., Stewart, T.J., Johnstone, M., Blackwood, D.H., St Clair, D., Grant, S.G.N., Bussey, T.J., Saksida, L.M. (2015). Bridging the translational divide: identical cognitive touchscreen testing in mice and humans carrying mutations in a disease-relevant homologous gene. *Scientific Reports*, 5, DOI:10.1038/srep14613
- Olton, D.S., and Samuelson, R.J. (1976). Remembrance of places passed: Spatial memory in rats. *Journal of Experimental Psychology: Animal Behavior Processes*, 2, 97-116. DOI:10.1037/0097-7403.2.2.97
- Oomen, C.A., Hvoslef-Eide, M., Heath, C.J., Mar, A.C., Horner, A.E., Bussey, T.J., Saksida, L.M. (2013). The touchscreen operant platform for testing working memory and pattern separation in rats and mice. *Nature Protocols*, 8(10), DOI:10.1038/nprot.2013.124
- Parthasarathy, A., Herikstad, R., Bong, J.H., Medina, F.S., Libedinsky, C., and Yen, S.C. (2017). Mixed selectivity morphs population codes in prefrontal cortex. *Nature Neuroscience*, 20, 1770 – 1779, DOI:10.1038/s41593-017-0003-2

- Paulk, A.C., Kfir, Y., Khanna, A.R., Mustroph, M.L., Trautmann, E.M., Soper, D.J., Stavisky, S.D., Welkenhuysen, M., Dutta, B., Shenoy, K.V., Hochberg, L.R., Richardson, R.M., Williams, Z.M., & Cash, S.S. (2022). Large-scale neural recordings with single neuron resolution using Neuropixels probes in human cortex. *Nature Neuroscience*, 25, 252 – 263, DOI:10.1038/s41593-021-00997-0
- Pedregosa, F., Varoquaux, G., Gramfort, A., Michel, V., Thirion, B., Grisel, O., Blondel, M., Louppe, G., Prettenhofer, P., Weiss, R., Weiss, R.J., Vanderplas, J., Passos, A., Cournapeau, D., Brucher, M., Perrot, M., & Duchesnay, E. (2011). Scikit-learn: Machine Learning in Python. *Journal of Machine Learning Research*, 12, 2825-2830, DOI: 10.5555/1953048.2078195
- Pnevmatikakis, E.A., Soudry, D., Gao, Y., Machado, T.A., Merel, J., Pfau, D., Reardon, T., Mu, Y., Lacefield, C., Yang, W., Ahrens, M., Bruno, R., Jessell, T.M., Peterka, D.S., Yuste, R., Paninski, L. (2016). Simultaneous denoising, deconvolution, and demixing of calcium imaging data. *Neuron*, 89, 285–299, DOI:10.1016/j.neuron.2015.11.037
- Pontecorvo, M.J., Sahgal, A., and Steckler, T. (1996). Further developments in the measurement of working memory in rodents. *Brain research. Cognitive brain research*, 3 3-4, 205-213. DOI:10.1016/0926-6410(96)00007-9
- Qi, X., and Constantinidis, C. (2013). Neural changes after training to perform cognitive tasks. *Behavioural Brain Research*, 241, 235-243, DOI:10.1016/j.bbr.2012.12.017
- Quintana, J., Yajeya, J., and Fuster, J.M. (1988). Prefrontal representation of stimulus attributes during delay tasks. I. Unit activity in cross-temporal integration of sensory and sensory-motor information. *Brain Research*, 474, 211-221, DOI:10.1016/0006-8993(88)90436-2

## References

- Reinert, S., Hübener, M., Bonhoeffer, T., Goltstein, P.M. (2021) Mouse prefrontal cortex represents learned rules for categorization. *Nature*, 593, 411-417, DOI:10.1038/s41586-021-03452-z
- Rigotti, M., Barak, O., Warden, M.R., Wang, X., Daw, N.D., Miller, E.K., Fusi, S. (2013). The importance of mixed selectivity in complex cognitive tasks. *Nature*, 497, 585-590, DOI:10.1038/nature12160
- Rikhye, R.V., Gilra, A., Halassa, M.M. (2018). Thalamic regulation of switching between cortical representations enables cognitive flexibility. *Nature Neuroscience*, 21, 1753-1763, DOI:10.1038/s41593-018-0269-z
- Riley, M.R., Qi, X., and Constantinidis, C. (2016). Functional specialization of areas along the anterior–posterior axis of the primate prefrontal cortex. *Cerebral Cortex*, 27, 3683–3697, DOI:10.1093/cercor/bhw190
- Romo, R., Brody, C.D., Hernández, A., & Lemus, L. (1999). Neuronal correlates of parametric working memory in the prefrontal cortex. *Nature*, 399, 470-473, DOI: 10.1038/20939
- Sandberg, M.A. (2011). Cambridge Neuropsychological Testing Automated Battery. In: Kreutzer, J.S., DeLuca, J., Caplan, B. (eds) *Encyclopedia of Clinical Neuropsychology*. Springer, New York, NY. DOI:10.1007/978-0-387-79948-3\_169
- Shafi, M.M., Zhou, Y., Quintana, J., Chow, C.C., Fuster, J.M., and Bodner, M. (2007). Variability in neuronal activity in primate cortex during working memory tasks. *Neuroscience*, 146, 1082-1108, DOI:10.1016/j.neuroscience.2006.12.072
- Shallice, T., and Warrington, E. K. (1970). Independent Functioning of Verbal Memory Stores: A Neuropsychological Study. *Quarterly Journal of Experimental Psychology*, 22(2), 261-273, DOI:10.1080/00335557043000203

- Scoville, W.B. (1968). Amnesia after bilateral mesial temporal-lobe excision: Introduction to case H.M.. *Neuropsychologia*, 6, 211-213, DOI:10.1016/0028-3932(68)90020-1
- Sokolenko, E., Nithianantharajah, J., Jones, N.C. (2020). MK-801 impairs working memory on the Trial-Unique Nonmatch-to-Location test in mice, but this is not exclusively mediated by NMDA receptors on PV1 interneurons or forebrain pyramidal cells. *Neuropharmacology*, 171, 108103, DOI:10.1016/j.neuropharm.2020.108103
- Spellman, T.J., Rigotti, M., Ahmari, S.E., Fusi, S., Gogos, J.A., and Gordon, J.A. (2015). Hippocampal-prefrontal input supports spatial encoding in working memory. *Nature*, 522, 309 – 314, DOI:10.1038/nature14445
- Steele, S., Minshew, N.J., Luna, B., and Sweeney, J.A. (2007). Spatial Working Memory Deficits in Autism. *Journal of Autism and Developmental Disorders*, 37, 605-612. DOI:10.1007/S10803-006-0202-2
- Stokes, M.G. (2015). 'Activity-silent' working memory in prefrontal cortex: a dynamic coding framework. *Trends in Cognitive Sciences*, 19, 394 – 405, DOI:10.1016/j.tics.2015.05.004
- Takeda, K. and Funahashi, S., (2002) Prefrontal Task-Related Activity Representing Visual Cue Location or Saccade Direction in Spatial Working Memory Tasks. *The Journal of Neurophysiology*, 87, 567-588, DOI:10.1152/JN.00249.2001
- Talpos, J.C., McTighe, S.M., Dias, R., Saksida, L.M., and Bussey, T.J. (2010). Trial-unique, delayed nonmatching-to-location (TUNL): A novel, highly hippocampus-dependent automated touchscreen test of location memory and pattern separation. *Neurobiology of Learning and Memory*, 94, 341 – 352, DOI:10.1016/j.nlm.2010.07.006
- Tolman, E.C. (1925). Purpose and cognition: the determiners of animal learning. *Psychological Review*, 32, 285-297, DOI:10.1037/H0072784

## References

- The MathWorks Inc. (2023). MATLAB version: 9.14.0 (R2023a), Natick, Massachusetts: The MathWorks Inc. <https://www.mathworks.com>
- Tye, K.M., Miller, E.K., Taschbach, F.H., Benna, M.K., Rigotti, M., Fusi, S., (2024). Mixed selectivity: Cellular computations for complexity. *Neuron*, 112, DOI:10.1016/j.neuron.2024.04.017
- Verin, M., Partiot, A., Pillon, B., Malapani, C., Agid, Y., Dubois, B. (1993). Delayed response tasks and prefrontal lesions in man – Evidence for self generated patterns of behaviour with poor environmental modulation. *Neuropsychologia*, 31(12), 1379-1396, DOI:10.1016/0028-3932(93)90105-9
- Vogel, P., Hahn, J., Duvarci, S., Sigurdsson, T., (2022). Prefrontal pyramidal neurons are critical for all phases of working memory, *Cell Reports*, 39(2), 110659, DOI:10.2139/ssrn.3869902
- von Ziegler, L.M., Sturman, O., and Bohacek, J. (2020). Big behavior: challenges and opportunities in a new era of deep behavior profiling. *Neuropsychopharmacology*, 46, 33 – 44, DOI:10.1038/s41386-020-0751-7
- Warrington, E.K., & Shallice, T. (1969). The selective impairment of auditory verbal short-term memory. *Brain : a journal of neurology*, 92 4, 885-96, DOI: 10.1093/BRAIN/92.4.885
- Watanabe, K., and Funahashi, S. (2007). Prefrontal delay-period activity reflects the decision process of a saccade direction during a free-choice ODR task. *Cerebral cortex*, 17 Suppl 1, i88-100. DOI:10.1093/CERCOR/BHM102
- Weinreb, C., Osman, M.A., Zhang, L., Lin, S., Pearl, J.E., Annapragada, S., Conlin, E., Gillis, W.F., Jay, M., Ye, S., Mathis, A., Mathis, M.W., Pereira, T.D., Linderman, S.W., and Datta, S.R. (2023). Keypoint-MoSeq: parsing behavior by linking point tracking to pose dynamics. *bioRxiv*, DOI:10.1101/2023.03.16.532307

Wiltschko, A.B., Johnson, M.J., Iurilli, G., Peterson, R.E., Katon, J.M., Pashkovski, S., Abaira, V.E., Adams, R.P., and Datta, S.R. (2015). Mapping Sub-Second Structure in Mouse Behavior. *Neuron*, 88, 1121-1135, DOI:10.1016/j.neuron.2015.11.031

Zangwill, O. L. (1946). Some qualitative observations on verbal memory in cases of cerebral lesion. *The British journal of psychology*. General section, 37(1), 8–19, DOI:10.1111/j.2044-8295.1946.tb01272.

## Acknowledgements

I would like to thank everyone who has been part of my PhD journey over the last years and without whom this dissertation would not have been possible. In particular, I would like to thank my supervisor Prof. Simon Jacob, for his support, guidance, and optimism in the face of challenges throughout the last years. Thank you for providing an environment that has allowed me to fail, try again, and ultimately grow as a researcher. Through your guidance, I've been challenged to think deeper about problems, to be critical of data, and most importantly to never rest until every figure has labelled axes. I would also like to thank my thesis advisory committee members, Prof. Mark Hübener and Prof. Laura Busse, for their useful advice on my project and the Graduate School of Systemic Neurosciences (GSN) for their support.

I would like to thank my parents, who have supported all my ideas during my entire academic journey and my whole life. To my mum for teaching me determination and persistency and to my dad for introducing me to mathematics and scientific experiments at an early age.

I would also like to thank my wonderful friends, Dr. Daniel Hunter, Dr. Andrea Gondová, Els Alsema, Batuhan Ugyar, Peter Whitton, Katrin Buschmann and Anke Pluppins, who have been an invaluable part of my PhD journey, especially in times when visiting friends in person had to be replaced by hourlong phone calls. I am grateful for your support throughout the last years and to have stayed close with all of you, regardless of geographical distance.

Finally, I would like to say thank you to my fellow labmates: Dr. Tobias Bernklau, Dr. Laura Schiffli, Xuanyu Wang, Beatrice Righetti, Richard Demann, Lisa Held, Alexander Utzschmid, Paolo Favero, Hongbiao Chen, Göktug Alkan, Yuyang Huang, Anna Haller, David Haase, Dr. Xiaoxiong Lin, Leonie Mehrke, Ajit Ranganath, Dr. Daniel Hähnke and Dr. Viktor Eisenkolb, for your warm welcome in the lab, support and advice throughout the good and the difficult times, the Pizza Fridays, the rooftop hot-tubs, the Feierabendtours, the bunny-sitting, the weekend training sessions, the Green Beer Thursdays, the boardgame nights, the Chinese dinners, and all the evenings by the Isar.

# Affidavit

Hiermit versichere ich an Eides statt, dass ich die vorliegende Dissertation:

*“Distinct behavioural and neuronal signatures in delayed response and working memory tasks of mice and man”*

selbstständig angefertigt habe, mich außer der angegeben keiner weiteren Hilfsmittel bedient und alle Erkenntnisse, die aus dem Schrifttum ganz oder annähernd übernommen sind als solche kenntlich gemacht und nach ihrer Herkunft unter Bezeichnung der Fundstelle einzeln nachgewiesen habe.

Victoria Hohendorf

München, den 27. Mai 2024